Cronfa
Swansea University's Research Repository

Swansea University
Prifysgol Abertawe

Conditions for biofilm formation in Extraintestinal Pathogenic *E. coli* (ExPEC)

Martynas Basevicius

Submitted to Swansea University in fulfilment of the requirements for the Degree of Master of Science by Research

Swansea University, 2024

Copyright: The Author, Martynas Basevicius, 2025.

Abstract

Sepsis is a complex multi-organ state caused by a dysfunctional immune response to infection. Recent estimates suggest an incidence of around 360 cases per 100,000 population per year, resulting in approximately 20% of all mortality rates. Bacteria cause about 70% of sepsis cases, with extrapathogenic *Escherichia coli* (ExPEC) being a major contributor locally in the Hywel Dda University Health Board (HDUHB). ExPEC utilise various virulence factors (VF) to evade the immune system. Some of these are responsible for producing biofilms, which are aggregates of bacteria, providing protection in diverse environments, but less work has focused on parameters of biofilm formation in ExPEC. This thesis aimed to identify optimal conditions for biofilm formation in ExPEC strains, then use these conditions to implicate phenotypes, genes and visualise structure in the biofilm formation process. Blood culture-positive *E. coli* isolates from HDUHB were used in growth and biofilm assays. Phenotypic, clinical and sequence metadata was used for isolate comparisons, while imaging experiments were performed using confocal laser scanning microscopy (CLSM). The optimal parameters needed for biofilm formation in ExPEC were Luria Bertani, Tryptic Soy Broth+Glucose or Escherichia Coli broth, 24-hour pre-culture and bile salts. Sequence type 73 (ST73) isolates had significantly higher biofilm levels than ST131 isolates. Subsequently, *fimACDFGHI*, *rcsAB* and *acrE* genes were associated with biofilm formation in ExPEC bacteraemia strains. CLSM confirmed live biofilms with significant biomass and thickness in both biofilm-positive and negative isolates. This work demonstrated the requirement of bile salts for biofilm formation in ExPEC, while iron supplementation had no effect. It also identified potential list of biofilm-promoting genes in ExPEC, requiring functional confirmation in knockout mutants and visualisation in live biofilm structures. In conclusion, this work will enhance the understanding of ExPEC pathogenesis and contribute to biomarker identification to predict severe infections using optimised methods for gene identification.

Declarations

This work has not previously been accepted in substance for any degree and is not being concurrently submitted in candidature for any degree.

Signed .[redacted]

Date .....27/06/2025.....

STATEMENT 1

This thesis is the result of my own investigations, except where otherwise stated. Where correction services have been used, the extent and nature of the correction is clearly marked in a footnote(s).

Other sources are acknowledged by footnotes giving explicit references. A bibliography is appended.

Signed .[redacted]

Date .....27/06/2025.....

STATEMENT 2

I hereby give consent for my thesis, if accepted, to be available online in the University's Open Access Repository and for inter-library loan, and for the title and summary to be made available to outside organisations.

Signed ...[redacted]

Date .....27/06/2025.....

Table of contents

Abstract ..... **I**

Declarations ..... **II**

Acknowledgements ..... **VI**

List of abbreviations ..... **VII**

List of figures ..... **XI**

List of tables ..... **XII**

1 Introduction **1**

1.1 Sepsis 1

1.1.1 Definition 1

1.1.2 Global burden 2

1.1.3 Origins of Infection 3

1.1.4 Major causative organisms 3

1.2 *Escherichia coli* 5

1.2.1 *E. coli* phylogroups, and O, K and H antigens 6

1.2.2 ExPEC 6

1.2.3 *E. coli* bacteraemia 7

1.3 *E. coli* Virulence factors 8

1.3.1 Adhesins 9

1.3.2 Invasins 9

1.3.3 Iron uptake factors 10

1.3.4 Protectins 11

1.3.5 Toxins 11

1.4 Biofilm 12

1.4.1 General 12

1.4.2 Biofilm formation and life cycle 14

1.4.3 *E. coli* Biofilm 17

1.4.4 *E. coli* biofilm methods 20

1.5 Gaps in the literature 20

1.6 Aims and objectives 21

2 Materials and methods **22**

2.1 Media 22

2.1.1 Luria Bertani (Lennox) Broth (LB) 22

2.1.2 Bacto Tryptic Soy Broth with dextrose (TSB+G) 22

2.1.3 Bacto Tryptic Soy Broth without Dextrose (TSB-G) 22
2.1.4 Escherichia coli (EC) Broth 22
2.1.5 Columbia Agar with Horse Blood 22
2.2 Minimal media 23
2.2.1 Phosphate Buffered Saline (PBS) + LB (90/10 %) 23
2.2.2 Gibco Leibovitz's L-15 Medium, no phenol red 23
2.2.3 M9 Minimal Medium 23
2.3 Stock solutions 23
2.3.1 Crystal violet 23
2.3.2 Glycerol 23
2.3.3 Phosphate Buffered Saline (PBS) 24
2.3.4 Specpure Iron 1000 µg/ml, AAS standard solution 24
2.3.5 Bile Salts No. 3 24
2.4 Reagents 24
2.4.1 Healthy volunteer blood serum 24
2.5 Microbiology 24
2.5.1 *E. coli* strains from Hywel Dda University Health Board (HDUHB) 24
2.5.2 Biofilm and *E. coli* control strains 26
2.5.3 Physiological and mechanical parameters used for biofilm assay 26
2.5.4 Routine Culture and storage of microorganisms 27
2.5.5 *S. epidermidis* pre-culture 27
2.5.6 Growth Assay 27
2.5.7 Biofilm Assay 28
2.5.7.1 Biofilm assay with different media 28
2.5.7.2 Biofilm Assay with Linear shaking 28
2.5.7.3 Biofilm Assay with Orbital shaking 29
2.5.7.4 Biofilm Assay with Circular shaking 29
2.5.7.5 Biofilm Assay with incubation at 30°C 29
2.5.7.6 Biofilm Assay with short pre-culture 29
2.5.7.7 Biofilm Assay with extended (48/72 hour) incubation time 29
2.5.7.8 Biofilm Assay with blood serum 29
2.5.7.9 Biofilm Assay with Bile Salts 29
2.5.7.10 Biofilm Assay with Iron 29
2.5.7.11 Biofilm Assay with Bile Salts and Iron 30
2.6 Data analysis 30

2.6.1 Gene analysis 30
2.6.2 Biofilm visualisation and Confocal Laser Scanning Microscopy (CLSM) data analysis 30
2.6.2.1 Sample preparation for CLSM 30
2.6.2.2 CLSM imaging and analysis 31
2.7 Statistical comparisons and analysis 31
3 Results 32
3.1 *E. coli* growth in defined media 32
3.2 Screening of conditions for *E. coli* biofilm deposition and formation 33
3.3 Biofilm formation in *E. coli* bacterial isolates using bile salts 36
3.4 The effect of iron on *E. coli* biofilm formation 38
3.5 The effect of *E. coli* sequence type and origin of infection on biofilm formation 39
3.6 The effect of bile salts biofilm formation and growth of individual *E. coli* isolates 41
3.7 The effect of using bile salts with iron supplementation on *E. coli* biofilm formation 44
3.8 The effects of bile salts and iron on biofilm formation and growth of individual *E. coli* isolates 46
3.9 Genetic analysis of biofilm and bile salt resistance associated genes 49
3.10 CLSM biofilm visualization and data analysis 55
4 Discussion 57
4.1 Growth and biofilm formation utilising different physiological and mechanical parameters 57
4.2 Biofilm formation in *E. coli* and other pathogens, the bile salts effect, and the influence of iron 58
4.3 *E. coli* genes important for biofilm formation 60
4.4 Differences in methods to study biofilm formation 60
4.5 Physiological and clinical relevance, biofilm formation on pathogenesis and host-pathogen interactions 62
4.6 Limitations 63
4.7 Future Perspectives 63
5 Conclusion 65
6 References 66
7 Appendices 86

Acknowledgements

This work would not have come to fruition without the guidance of my supervisor, Professor Thomas Wilkinson. Thank you for your constant encouragement and support throughout all stages of the project. Your infectious (pun intended) excitement and passion for science kept me motivated even at my lowest points, and I will cherish that forever. I am also grateful to Dr Llinos Harris for her valuable insights and tips during group meetings and in the lab, and to Dr Lydia Powell for sharing fascinating topics about biofilms and imaging. Special thanks to Megan and Liam for patiently showing me the ropes in the lab and never once complaining about my mistakes. I would also like to thank Dr Heather Chick, Dr Michelle Hardman, the rest of the MID group, and everyone on the fifth floor for the moments of laughter, thought-provoking discussions, and enjoyable time I had in Swansea over the last two years.

I would also like to express my heartfelt gratitude to my incredible wife, Agnė, for her unwavering support, constant motivation, and encouragement to always strive for greater achievements.

Lastly, I would like to thank my parents and my family. Their emotional support and unwavering pride in my accomplishments have been a constant source of motivation and strength throughout this journey.

List of abbreviations

Afa	Afimbrial adhesin
acr	Acriflavine resistance efflux pump gene
adk	Adenylate kinase gene
Ag43	Antigen 43
AHL	N-acyl-Homoserine Lactone
APEC	Avian Pathogenic *E. coli*
Bcl-xL	B-cell lymphoma-extra large anti-apoptotic protein
bcs	Bacterial Cellulose Synthesis
bsh	Bile salt hydrolase gene
BSI	Bloodstream Infections
C4B	Complement component 4B
CA	Colonic Acid
CBD	Calgary Biofilm Device
CDC42	Cell division control protein 42
c-di-GMP	Cyclic-diguanylic acid-Guanosine Monophosphate
CLSM	Confocal Laser Scanning Microscopy
cnf1	Cytotoxic necrotising factor 1 gene
CNF1	Cytotoxic necrotising factor 1
csg	Curli-specific gene
CV	Crystal Violet
DAMP	Damage Associated Molecular Pattern
DNA	Deoxyribonucleic Acid
dra	Dr fimbriae operon
EC Broth	Escherichia coli Broth
emrAB	Multidrug efflux pump components EmrA and EmrB
EPS	Extracellular Polymeric Substance
ExPEC	Extrapathogenic *E. coli*
fad	Fatty acid degradation gene
FeoAB	Ferrous iron transport system components A and B
fim	Type 1 fimbriae regulatory operon
flh	Flagellar master regulator
fliA	Sigma factor F gene
FliG	flagellar protein FliG

flu	Gene encoding antigen 43
foc	F1C fimbriae operon
fumC	Fumarate hydratase class II (Fumarase C) gene
GTP	Guanosine Triphosphate
GTPase	Guanosine Triphosphate
gyrB	DNA gyrase subunit B gene
HAI	Healthcare-Associated Infection
HBMEC	Human Brain Microvascular Endothelial Cell
HDUHB	Hywel Dda University Health Board
hfq	Host factor for RNA phage replication
hha	Hemolysin expression-modulator
hly	Haemolysin encoding operon
ibe	Invasion of brain endothelium protein gene
icd	Isocitrate dehydrogenase gene
ICU	Intensive Care Unit
IPC	Infection Prevention and Control
IPEC	Intestinal Pathogenic *E. coli*
iro	Salmochelin siderophore system operon
iut	Aerobactin siderophore receptor
kpsMTII	Group 2 capsular polysaccharide
lacZ	Beta-galactosidase gene
LB	Luria Bertani (Lennox) Broth
LMIC	Low-to-Middle-Income Country
LOS	Length Of Stay
LPS	Lipopolysaccharide
luxR	Transcriptional regulator of *luxR* family proteins
macAB	Macrolide-specific efflux genes
mar	Multiple antibiotic resistance operon
mdh	Malate dehydrogenase gene
mdt	Multidrug transporter gene
MIP	Macrophage Inflammatory Protein
MLEE	Multi-Locus Enzyme Electrophoresis
MLST	Multi Locus Sequence Typing
MotA	Motility protein A
NMEC	Neonatal Meningitis *E. coli*

OD	Optical Density
OEP	Outer membrane Efflux Protein
OMP	Outer Membrane Protein
OmpA	Outer membrane protein A
PAI	Pathogenicity Island
PAMP	pathogen associated molecular pattern
pap	Pyelonephritis-associated pili operon
PapG(I,II,III)	Pap glycosylation island (I, II, III)
PBS	Phosphate Buffered Saline
PGA	Poly-β-1,6-N-acetyl-D-glucosamine
pic	Protease involved in colonisation gene
PIC	Protease Involved in Colonisation
PRR	Pattern Recognition Receptors
purA	Adenylosuccinate synthetase gene
qse	Quorum sensing regulatory system
qSOFA	quick Sequential Organ Failure Assessment
Rac1	Ras-related C3 botulinum toxin substrate 1
rapA	RNA polymerase-associated protein A gene
rcs	Regulator of capsule synthesis
recA	Recombinase A gene
RhoA	Ras homologue A
rpm	Revolutions Per Minute
rpoS	RNA polymerase sigma factor S gene
RT-PCR	Real-Time Polymerase Chain Reaction
SAT	Secreted Autotransporter Toxin
sat	Secreted autotransporter toxin gene
SEPEC	Septicaemia-Associated *E. coli*
sfa	S fimbrial adhesin gene
SIRS	Systemic Inflammatory Response Syndrome
SitABCD	Iron/manganese transport system SitABCD
SOFA	Sequential Organ Failure Assessment
SPATE	Serine Proteases Autotransporters of Enterobacteriaceae
ST	Sequence Type
TB	Tube Method
TNF	Tumour Necrosis Factor

tolC	Outer membrane channel
TSB+G	Tryptic Soy Broth with dextrose
TSB-G	Tryptic Soy Broth without dextrose
UpaG	Uropathogenic *E. coli* autotransporter G
UPEC	Uropathogenic *E. coli*
UTI	Urinary Tract Infections
vat	Vacuolating autotransporter protein gene
VAT	Vacuolating Autotransporter Protein
VF	Virulence Factor
yafQ	YafQ-DinJ toxin-antitoxin system gene
YCgR	c-di-GMP-binding protein YcgR
yojI	Putative efflux transporter gene

List of figures

Figure 1.1 – The first line treatment and clinical management of sepsis. 2
Figure 1.2 – Different *E. coli* pathotypes. 5
Figure 1.3 – Biofilm formation divided into four main phases: Adhesion (Reversible and irreversible), Aggregation, Maturation and Dispersion. 14
Figure 3.1 – Bacterial growth in defined media. 33
Figure 3.2 – Biofilm deposition of *E. coli* isolates under different physiological and mechanical conditions. 34
Figure 3.3 – Growth and biofilm Formation in LB Medium Supplemented with bile salts. 36
Figure 3.4 – Growth and biofilm formation in TSB+G medium supplemented with bile salts. 37
Figure 3.5 – Growth and biofilm formation in LB medium supplemented with iron. 38
Figure 3.6 – Growth and biofilm formation in TSB+G medium supplemented with iron. 39
Figure 3.7 – *E. coli* isolate growth and biofilm formation comparison between sequence type (a) and origin of infection (b). 40
Figure 3.8 – Individual strain growth and biofilm formation with bile supplementation. 43
Figure 3.9 – Growth and biofilm formation with bile salts and iron. 44
Figure 3.10 – *E. coli* growth and biofilm formation in ST73 and ST131 with bile salt and iron supplementation. 45
Figure 3.11 – *E. coli* isolate growth and biofilm formation comparison between gut and urinary origin of infection, with bile salt and iron supplementation. 46
Figure 3.12 – Individual strain growth and biofilm formation with bile salt and iron supplementation. 48
Figure 3.13 – Live biofilm formation and comparison between biofilm positive and biofilm negative isolates. 56

List of tables

Table 1.1 – Top species causing bacteraemia in Wales 2023-2024. 4
Table 1.2 – Direct & indirect genes associated with biofilm formation in *E. coli* 19
Table 2.1 – List of *E. coli* isolates obtained from Hywel Dda University Health Board. 25
Table 2.2 – List of biofilm and *E. coli* control strains. 26
Table 2.3 – Physiological and mechanical conditions tested during Biofilm Assay. 26
Table 3.1 – Biofilm formation of individual *E. coli* isolates with bile salt supplementation. ... 42
Table 3.2 – Biofilm formation of individual *E. coli* isolates with bile salt and iron supplementation. 47
Table 3.3 – The selected direct and indirect biofilm and bile salt resistance gene list. 50
Table 3.4 – Biofilm positive and biofilm negative isolate gene profile comparison. 52
Table 3.5 – ST73 versus ST131 biofilm related and bile resistance gene comparison. 54
Table 3.6 – Isolates for CLSM biofilm visualisation and analysis. 55

1 Introduction

1.1 Sepsis

1.1.1 Definition

Sepsis, also known as blood poisoning, is a complex, multi-organ state that manifests as a dysfunctional immune response to infection. It is a life-threatening condition associated with exaggerated inflammation, metabolic and catabolic changes, disruption in coagulation and complement cascades and immune suppression (1, 2). A common infection associated with sepsis is bacteraemia (presence of bacteria in the blood), which is present in approximately 38-69% of the cases, having developed from localised infection (e.g. gut, urinary tract) (3, 4). The definition of sepsis has evolved over the last 2000 years, from early references in Homer's poems to Sir William Osler's observation that the body's immune response could "kill itself" rather than succumbing directly to infection (5). The first international conference on sepsis in 1991 defined it as a systemic inflammatory response syndrome (SIRS) (6). In addition, the increased severity of the disease and organ dysfunction termed 'severe sepsis' and 'septic shock' was described as 'sepsis with refractory hypotension' (7). More recently, during the third international sepsis consensus in 2016, sepsis was redefined as "life-threatening organ dysfunction caused by a dysregulated host response to infection." Septic shock was further specified as "a subset of sepsis associated with greater mortality, characterised by profound circulatory, cellular, and metabolic abnormalities," and the term 'severe sepsis' was removed. For detecting organ dysfunction, the task force recommended using Sequential [Sepsis-related] Organ Failure Assessment (SOFA), with a score increase of two points or more, and the quickSOFA (qSOFA) for use in out-of-hospital or resource-limited settings (1, 8).

Sepsis is not only complex and associated with a poor prognosis but is also a medical emergency. Time to treatment has been outlined as a primary factor contributing to success of sepsis treatment, which recommends antibiotic administration, fluid resuscitation and vasoactive agent usage within 1 hour of patient admission (9, 10). Each hour delay of antibiotic administration has been linked with a significant reduction in survival when septic shock is present (11-13). In addition, failure to provide sufficient crystalloid fluids for the patient within 3 hours has been found to increase in-hospital mortality, delayed stabilisation of hypotension and prolonged length of stay (LoS) in the intensive care unit (ICU) (14). Subsequently, timely

administered vasoactive agents have been shown to improve outcomes by shortening the LoS and reducing mortality risk (10, 15, 16).

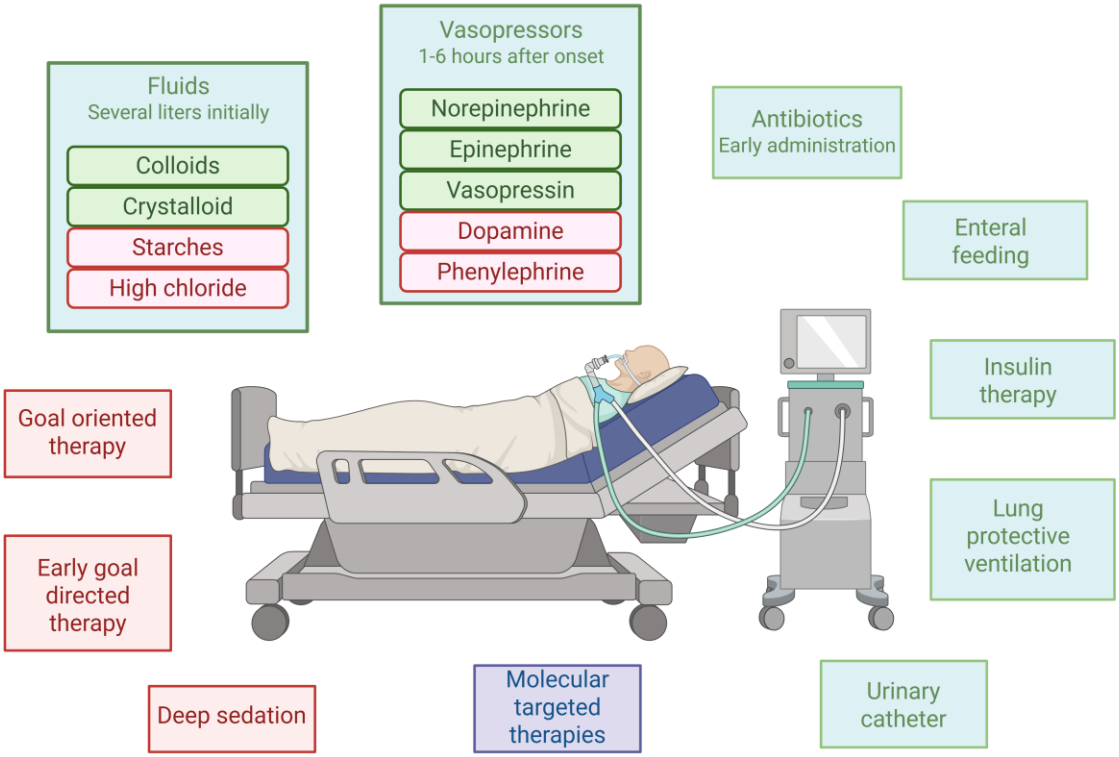

Figure 1.1 – The first line treatment and clinical management of sepsis.
Green text and squares indicate the recommended treatment options. Red text and squares indicate treatment options that should be avoided. Blue text and a square indicate a treatment option that is lacking clinical significance. Adapted from (11) created in (17).

1.1.2 Global burden

Sepsis is regarded as a leading cause of mortality and morbidity worldwide and in 2017, according to Kristina Rudd and colleagues, there were 48.9 million cases, resulting in 11 million deaths (18). In the same year, sepsis accounted for 19.7% of global deaths and estimates suggest it is increasing due to 85% of death records coming from low-to-middle-income countries (LMICs) (18, 19). A meta-analysis from 2016 found sepsis as a leading cause of hospital associated infections in children, accounting for 22 cases of childhood sepsis per 100,000 patient-years (1% to 20% mortality in severe cases) and 2202 cases of neonatal sepsis per 100,000 live births (11% to 19% mortality), totalling up to 1.2 million childhood sepsis and up to 3 million neonate sepsis cases per year worldwide (20, 21). Intensive care units (ICUs) are also a strong contributor to sepsis cases. It has been reported, that 29.5% of ICU patients are affected by sepsis (22) and, in the US, 54.7% of patients who developed sepsis were

treated in ICU (23), showcasing the importance and critical treatment sepsis requires. In the UK, sepsis accounts for at least 200,000 and potentially up to 918,000 cases per year (24-26). The death rate reaches 40,000 to 48,000 deaths per year, while 80,000 patients are left with post-sepsis cognitive or physical complications (27-29). Comparatively, sepsis in the UK is responsible for more deaths annually than bowel, breast and prostate cancer combined (30). Locally, in Wales, sepsis cases account for around 5.5% of hospital in-patients (31-33). The recorded 30-day mortality rates vary between 18.3% and 22.9%, while the 90-day mortality rates are 25.3% to 31.3% of cases in Wales (28, 31, 32, 34). Apart from the high impact on global death rates, sepsis is also associated with high direct and societal costs for healthcare systems. In 2011, sepsis accounted for $20 billion of all hospital costs (5.2%) in the US and in 2017 it was found that the average hospital-wide cost of sepsis was more than $32,000 per patient in high-income countries (35, 36). While in the UK, sepsis is estimated to cost directly £2.5 billion and up to £15.6 billion in societal costs, putting a significant burden on the NHS (37). In Wales, deaths have been estimated to reach 1800 cases yearly, with the costs at approximately £125 million (28, 33)

1.1.3 Origins of Infection

Sepsis is commonly preceded by a localised infection, often restricted to one body compartment. Specifically, the most common are respiratory (31.1 – 37.2%), abdominal (26.3 – 29.3%), urinary tract (10.7 – 18.4%), bone/soft tissue (7.2 – 13.3%) and cardiovascular infections (3.2%) (12, 38). In addition, 70% of primary infections of sepsis were reported to be community-acquired (39). While the majority of healthcare-associated infections (HAIs) are preventable by implementing infection prevention and control (IPC) measures (40, 41), 5.7% to 19.1% of worldwide infections were HAIs and some of them were associated with sepsis (42). Moreover, organisms such as Gram-positive bacteria were predominantly identified in bone/soft tissue (55.7%) or cardiovascular infections (52.6%), whereas Gram-negative bacteria were associated with urinary (72%) and abdominal (38.4%) infections (38, 43, 44).

1.1.4 Major causative organisms

The causative organism plays a critical role in primary infection, as specific pathogens often thrive in the distinct local niches of organ systems, leading to organ-specific infections. Sepsis can be caused by a virus, fungus or bacterium, but approximately 70% of all cases are

attributed to bacterial infection (45, 46). Over the last few decades, the aetiology of Gram-positive (35.4 – 59.8%) and Gram-negative (40.2 – 62.2%) bacteraemia has shifted but the prevalence is region- and economy-dependent (45, 47, 48). Gram-positive and negative bacterial infections can overlap due to polymicrobial sepsis, meaning more than one bacterial species is present in the blood culture. The major causative organisms have remained relatively constant throughout the decades, with *Staphylococcus spp.* and *Streptococcus pneumoniae* being the most common Gram-positive bacteria, while *Escherichia coli*, *Klebsiella spp*. and *Pseudomonas aeruginosa* are the most prevalent Gram-negative bacteria (38, 45, 47, 49). These species account for about 80% of all bacterial sepsis, with >50% being attributed to the top 3: *E. coli*, *S. epidermidis* and *S. aureus* (38, 49). In Wales, *E. coli* has been the most common cause of bacteraemia for over a decade (50). Notably, data from the Hywel Dda Health Board reveal a sharp rise in *E. coli* sepsis cases among the elderly (>65 years), increasing from 40 to 100 cases per 100,000 population, emphasising the organism's importance for study in this region (Table 1.1) (51).

Table 1.1 – Top species causing bacteraemia in Wales 2023-2024. Data from Public Health Wales (52).

Organism	Rate per 100,000 population in Wales
Escherichia coli	72.61
Clostridium difficile	38.89
Methicillin-susceptible Staphylococcus aureus	25.67
Klebsiella spp.	23.53
Pseudomonas aeruginosa	4.66
Methicillin-resistant Staphylococcus aureus	1.82

1.2 *Escherichia coli*

Escherichia coli, a member of the *Enterobacteriaceae* family, is a Gram-negative, rod-shaped bacterial species highly adapted to its ecological niche worldwide (53). *E. coli* is best known as a commensal organism in humans, warm-blooded animals and reptiles, being able to colonise an infant's gut within the first hours after birth, establishing a symbiotic relationship with the host. *E. coli* provides numerous benefits for the host, specifically in humans, as it participates in digestion, synthesises certain vitamins and protects the gut from pathogenic *Enterobacteriaceae* colonisation (54). Under normal circumstances, *E. coli* helps its host to develop and thrive, but if the host becomes immunocompromised or the gut barrier has been breached, the commensal strains can become opportunistic pathogens bringing dysbiosis to the gut and imbalance to the host (54, 55).

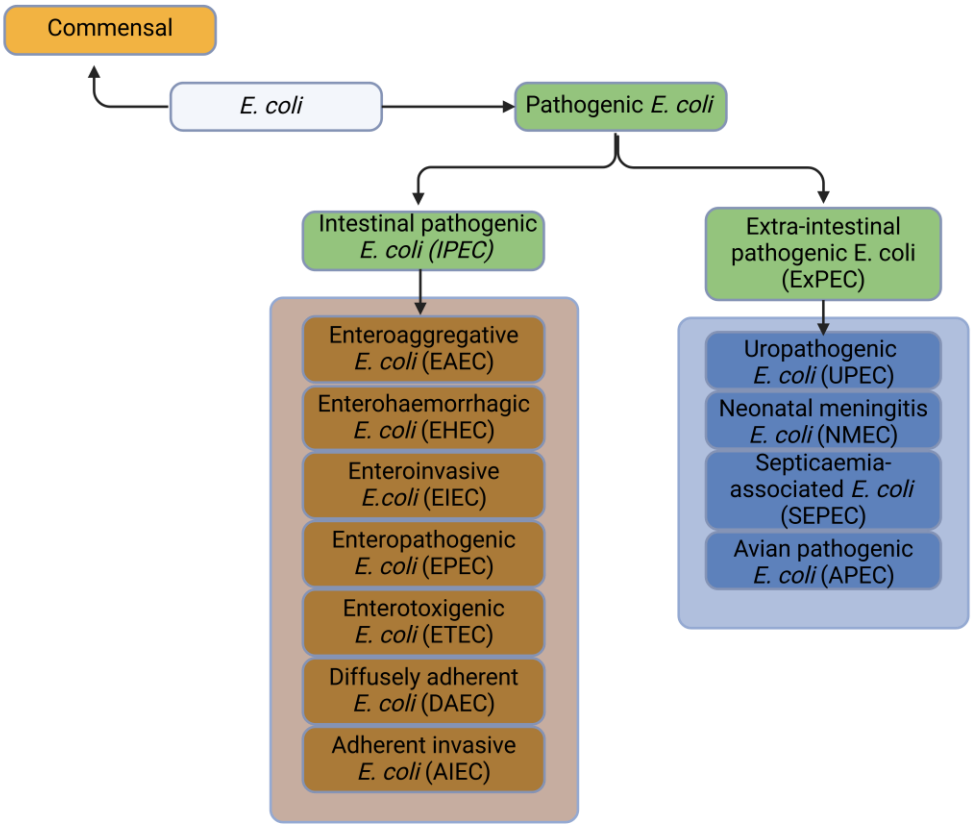

Figure 1.2 – Different *E. coli* pathotypes.
E. coli can be commensal or pathogenic, where pathogenic strains are defined by the site of infection as intestinal pathogenic *E. coli* (IPEC) and extraintestinal pathogenic *E. coli* (ExPEC). Adapted from (55).

Escherichia coli is usually divided into commensal and pathogenic strains (Figure 1.2). Pathogenic *E. coli* can be subsequently divided into intestinal pathogenic *E. coli* (IPEC) and

extraintestinal pathogenic *E. coli* (ExPEC), based on their site of infection. Intestinal pathogenic *E. coli* are usually associated with food poisoning, local enteric and diarrheagenic infections while ExPEC are related to urinary tract infections (UTI), bloodstream, spinal fluid and respiratory tract infections (56, 57).

1.2.1 *E. coli* phylogroups, and O, K and H antigens

In 1984 Ochman and Selander established the ECOR strain collection of *E. coli* based on results from multi-locus enzyme electrophoresis (MLEE). This collection included 72 isolates from humans and 16 isolates of *E. coli* from mammals and showcased the genetic diversity of *E. coli* species (58). Originally, it was classified into 5 major phylogenetic lineages named A, B1, B2, D and E. Over time it was expanded and today it is generally regarded that there are 9 phylogroups: A, B1, B2, C, D, E, F, G, and H (59, 60). There is some connection between the phylogroups and the pathotypes as commensal *E. coli* are mostly associated with A and B1, while IPEC and ExPEC are more linked with B2, D, E and F (where F is related to B2 and E is related to D) phylogroups (56, 61). Another way to classify *E. coli* isolates is by identifying specific antigens present on their surface, which are known as polysaccharide (somatic) (O), flagellar (H) and capsular (K) antigens. It is estimated that *E. coli* has over 80 K antigens, 171–186 O antigens, and 53–55 H antigens, yielding hundreds of thousands of possible serotype combinations and highlighting the extensive diversity of the species (61-63). Furthermore, due to the development of molecular biology techniques, such as Multi Locus sequence typing (MLST) or whole-genome sequencing, the ExPEC strains have been analysed and segregated into sequence types (STs). Sequence typing is based on analysing the sequences of internal fragments of several house-keeping genes (64-66) and depending on their combination of alleles at these loci, defines a specific sequence type (67).

1.2.2 ExPEC

Initially, extraintestinal pathogenic *E. coli* were considered part of the healthy gut microbiota, but once they translocate the gut wall, they are likely to colonise other niches and cause disease in the host (56, 68). Due to their distinct pathogenic capabilities to cause disease at multiple anatomical locations, ExPEC are further categorized into pathotypes, which include uropathogenic *E. coli* (UPEC), neonatal meningitis *E. coli* (NMEC), septicaemia-associated *E. coli* (SEPEC), and avian pathogenic *E. coli* (APEC) (Figure 1.2) (55, 61). Uropathogenic *E. coli* are

the predominant species causing UTIs worldwide, which impact more than 150 million people annually (69, 70). In addition, UPEC account for up to 95% of uncomplicated UTIs and up to 50% of complicated UTI cases which can further develop into urosepsis (61, 71, 72). Avian pathogenic *E. coli* are mostly associated with disease in poultry but can cause multiple organ dysfunction and sepsis (73). However, there are APEC strains that possess ExPEC virulence factors associated with humans, although clinical illness could not be confirmed (74). Neonatal meningitis-associated *E. coli* contribute to mortality (10%) and morbidity (30%) rates in newborn infants. Furthermore, NMEC is the second leading cause of bacterial meningitis in neonates and other life-threatening conditions, such as sepsis (75-77). Sepsis–associated *E. coli* strains are mostly involved with infection leading to sepsis. Recent studies show that SEPEC was the major contributor to preterm sepsis in newborns among ICU patients in Saudi Arabia (78, 79). In addition, sepsis-associated *E. coli* usually shares many virulence factors with NMEC and UPEC that they utilise to infect the host and initiate inflammatory responses (72, 80).

1.2.3 *E. coli* bacteraemia

Globally, *E. coli* has been the most frequent cause of bloodstream infections (BSIs), with one in three cases progressing into sepsis or septic shock (60, 81, 82). The major origins of bloodstream infections associated with *E. coli* are the urinary tract and intra-abdominal sites. This is consistent with the large diversity of the *E. coli* species, being either benign strains that are frequent colonisers of the gastrointestinal tract that are able to become pathogenic outside of the gut or pathogenic strains that remain in the gut or invade extraintestinal tissues (38, 55, 61). In the UK, *E. coli* is a major cause of bacteraemia, with an incidence rate of 50.7 cases/100,00 patients (79, 83). In the EU, a recent study identified 224 *E. coli* bacteraemia isolates from 22 hospitals in Spain, where 52% (n=116) of cases were urinary infections, 33% (n=73) intra-abdominal and 7% (n=15) respiratory as the clinically defined source of bacteraemia. The most common strains were from phylogroup B2 (n=127, 57%) and D (n=32, 14%), where sequence types ST131 (n=38, 17%), ST73 (n=25, 11%), ST69 (n=23, 10%) and ST95 (n=12, 5%) accounted for 44% of all isolates. Globally, ST131 is regarded as the predominant ExPEC clone, with ST73 and ST69 identified as high-risk types (84, 85). The median age of patients was 75 years and the co-morbidities were neoplasia (n=60, 27%), diabetes (n=58, 26%), chronic pulmonary disease (n=32, 14%) and liver disease (n=28, 13%), which is

consistent with other studies (38, 60). Furthermore, 54% (n=121) were community-acquired bacteraemia infections, which was again consistent with the literature (39 – 70%) (39, 86, 87). Overall, *E. coli* was reported to have a 30-day mortality rate of 31%, which is on the higher side of average mortality rates worldwide (13.1 – 32%) (45, 47, 60, 88).

1.3 *E. coli* Virulence factors

Genetics plays a vital role in *E. coli* pathogenicity and survival, extending the organism's capabilities in an environmental niche (61, 89). *E. coli* genomes can be organised into 'core genome' and 'accessory genome'. The core genome is generally responsible for essential processes, like replication, transcription and translation, whereas accessory genes provide diverse phenotypes and advantages in specific environmental conditions often encoding multiple virulence / survival factors (VFs) (55). Accessory genes are usually acquired by bacterial strains through horizontal gene transfer or homologous recombination and expressed on plasmids, pathogenicity islands (PAIs), or other mobile elements. This genetic plasticity underpins *E. coli*'s adaptability and success in the bacterial world (55, 90). Genetic flexibility has also been observed in commensal *E. coli*, obtaining virulence factors and pathogenic capabilities (91). This further highlights the concerns that ExPEC cannot be easily distinguished from commensals as many factors responsible for pathogenesis are equally useful for the colonisation of commensals (55, 56). Interestingly, the literature suggests that some VFs are essential for commensal *E. coli* to survive, while other factors help solidify their presence in the gut (55, 92, 93). For instance, commensal *E. coli* were found to have VF genes such as *adk*, *fumC*, *gyrB*, *icd*, *mdh*, *purA*, *recA* and a plasmid that share 81% similar genes with the plasmid found in UPEC UTI89 strain (55, 93). In ExPEC strains, there is strong evidence for the expression of various virulence factors that facilitate colonisation, survival, proliferation, and immune evasion. These VFs are broadly classified into five groups: adhesins, invasins, iron uptake factors, protectins, and toxins (61, 89).

E. coli strains are generally classified as ExPEC if they are positive for 2 or more of five key virulence factors (94, 95). These virulence factors consist of *papA* and *papC* (P fimbriae structural subunit and assembly), *sfa/foc* (S and F1C fimbriae), *afa/dra* (Dr-binding adhesins), *iutA* (aerobactin receptor), and *kpsM* II (group 2 capsules) (95-99).

1.3.1 Adhesins

Adhesins are protein molecules found on the surface of the bacteria that contribute to specific adhesion and colonisation to host structures. The main types of adhesins are fimbriae, afimbrial adhesins (Afa), and outer membrane proteins (OMPs) (61, 100). Expression of the surface adhesins increases the virulence of ExPEC by facilitating the attachment to host surface structures such as epithelial cells of the gut, respiratory system, urinary tract and other organs. Fimbriae adhesins have affinity for mannose residues on the host and are assembled into hair-like fibres (101). Type 1 fimbriae are the most prevalent surface attachment factor, encoded by the *fim* gene cluster. Almost all UPEC strains express type 1 fimbriae which ensure binding to bladder epithelial cells and increases colonisation of the urinary tract (102-104). Type 2 fimbriae, which do not have affinity to mannose (P, S, Dr fimbriae), are abundant in UPEC, NMEC and SEPEC strains, being found in all strains causing meningitis and sepsis (105). F-type fimbriae, expressed from *pap* gene cluster, have 3 molecular adhesins variants: PapGI, PapGII, PapGIII, where PapGII is associated with human bacteraemia (61). Afimbrial adhesins (Afa) are structured as coil-like adhesive sheaths encoded by the *afa* gene cluster. They are primarily found in UPEC strains with 20-36% prevalence from UTI patient samples (106, 107). In addition, UpaG, a member of the auto-transporter family of adhesins, promotes the adhesion of urinary pathogenic *E. coli* to bladder epithelium and biofilm formation on plastics, such as urological catheters (108). Due to catheter contamination from biofilm, UPEC can cause bacteraemia in such patients (109, 110). Subsequently, type 1 fimbriae and antigen43 (ag43) have been linked with ExPEC biofilm formation implicating adhesion and aggregation as pivotal processes in *E. coli* biofilm formation (111).

1.3.2 Invasins

Invasins are a group of molecules that support ExPEC entry into host cells by modulating host cytoskeleton proteins. RhoA, Rac1, and CDC42 are small guanosine triphosphate (GTPase) molecules that regulate host cytoskeleton organisation, which bacteria are able to exploit to enter the host cells (112, 113). Host actin cytoskeleton rearrangements were also observed in a K antigen variant K1 which was deemed as essential for bacterial invasion of human brain microvascular endothelial cells (HBMECs), although the process is not fully understood (114,

115). ExPEC strains associated with K1 antigen expression have been linked with meningitis and neonatal sepsis (116). IbeA is another invasin that has been linked with HBMECs through Rac1 activation. In NMEC and APEC strains, inactivation of *ibeA* inhibited invasion of brain microvascular endothelial cells *in vivo* and *in vitro* (117-119).

1.3.3 Iron uptake factors

Iron is critical for life and optimal functioning for almost all living organisms, but especially in bacteria (120-123). For instance, iron plays a key role in energy metabolism, respiration, lipid metabolism and DNA replication (120). Due to the functional importance of iron, the ability of the host to deprive it from pathogenic bacteria is the major contributor to the concept of nutritional immunity by storing iron molecules as ferritin, transferrin and lactoferrin (120, 124). In response, ExPEC uses a wide variety of mechanisms to combat the sequestration of iron in the environment. These include membrane pumps, iron transporters and siderophores (123, 125). Siderophores are secondary metabolites that sequestrate iron from ferritin, transferrin and lactoferrin molecules due to their extremely high avidity for iron. They can be divided into five groups: catecholates, phenolates, hydroxamic acids, α-hydroxycarboxylates, and a mixed type containing different siderophores (125, 126). ExPEC possesses a diverse set of siderophores that increase their virulence; enterobactin and salmochelin (catecholate siderophores), aerobactin (a mixed-type siderophore), and yersiniabactin (phenolate siderophore). Enterobactins promote salmochelin generation by undergoing glycosylation from *iroB*, enabling ExPEC to evade the host immune system and acquire iron (127). Salmochelins are considered to be a characteristic virulence factor for the ExPEC pathotype (128). They can be converted into cyclic salmochelins by IroB glycosyltransferase, and they also can generate different forms through the action of IroD, IroE, and Fes esterases, leading to the expression of ferric chelators (129, 130). Aerobactin is another type of low molecular weight organic chelator, which has been shown to increase virulence in UTI in *vivo* models and influence APEC strain infection in chickens (131, 132). In addition, literature suggests that aerobactins are more efficient than enterobactins, as they sequestrate more iron from host transferrin and have more potent bacterial growth promoting effects (89, 133, 134). Yersiniabactin is a major contributor to UPEC pathogenicity in urinary tract infections, by facilitating iron uptake, establishing biofilm formation at the bladder level and protecting bacterial cells against the immune response (131, 135, 136). In addition, yersiniabactin has

been associated with reduction of reactive oxygen species from polymorphonuclear leukocytes, monocytes and macrophages by scavenging iron and preventing the Haber–Weiss reactions (127, 137). Finally, the FeoAB pump and SitABCD transporter have been found in commensal and pathogenic *E. coli* as iron uptake enablers, where they provide an additional method to obtain iron besides siderophore molecules (138, 139).

1.3.4 Protectins

Protectins are proteins found on the surface of ExPEC that provide serum resistance (e.g., Trat, OmpA and capsular antigen K). Trat is an outer membrane protein, providing bacterial cell protection against lytic action of complement by inhibiting correct assembly or functioning of terminal membrane attack complex of complement (140). In addition, the Trat protein has been linked with attenuating phagocytosis by mouse peritoneal macrophages in wild-type *E. coli* (89, 141). Outer membrane protein A (OmpA) is a member of the OMP lipoprotein family responsible for membrane structure and stability, active and passive ion transfer, signal transduction and catalysis (142). Through OmpA, ExPEC have the ability to evade host serum proteins and antibodies by binding the complement regulated protein C4B (143, 144). Furthermore, OmpA help ExPEC induce the antiapoptotic factor Bcl-xL that blocks cytochrome C release and prevents macrophage apoptosis, securing intracellular bacteria and macrophage survival (89, 145). The bacterial capsule is an extensive protective layer surrounding bacteria and is deemed to be a key mechanism used by Gram-negative bacteria to evade phagocytosis (146, 147). From all known (80+) different capsular (K) antigens, K1 and K2 are regarded as major contributors to ExPEC's ability to resist serum (148, 149), while the degree of resistance to serum in K+ strains is determined by the amount of capsular material and variation of K antigen type (150-152). The presence of polysaccharide capsules produced by UPEC strains allows bacteria to inhibit binding of antibodies and prevent opsonisation from complement, making the immune system recognition mechanism ineffective (153-155). In addition, numerous studies found that capsular K antigens increase ExPEC host immune evasion *in vitro* and *in vivo* through serum resistance (156-158).

1.3.5 Toxins

Bacterial toxins are secreted elements that are toxic to cells (cytotoxins), regarded as a key mechanism in discriminating pathogenic from commensal bacteria (159). The most prevalent

types of toxins in ExPEC are α-hemolysin (*hlyA*, *hlyD*, *hlyF*), cytotoxic necrotising factor 1 (*cnf1*), secreted autotransporter toxin (*sat*), protease involved in colonisation (*pic*) and vacuolating autotransporter protein (*vat*) (65, 160, 161). Alpha-hemolysins are cytotoxic proteins, secreted extracellularly by type I secretion complexes, which are involved in membrane pore formation, subsequently initiating cell lysis. Studies suggest that introducing hemolysins to erythrocytes leads to pore formation and partial lysis, which triggers the creation of host-mediated pannexin pores, ultimately leading to complete cell lysis (162, 163). Cytotoxic Necrotizing Factor 1 is a catalytic protein, that activates the GTPases, RhoA, Cdc42, and Rac1 leading to cytoskeleton-rearrangements, interruption of cell-signalling and cell cycle arrest (164-166). In UPEC strains, CNF1 is associated with complicated UTIs as 48% of isolates from patients with pyelonephritis were *cnf1* positive. In addition, in ExPEC CNF1 induces neutrophil dysfunction and epithelial cell invasion (167, 168). The secreted autotransporter toxin (SAT) belongs to the serine proteases autotransporters of Enterobacteriaceae (SPATE) family. SAT is a potent cytotoxin that causes cell lysis, cell cycle arrest and proteolysis of host proteins (169). *In vivo* and *in vitro* studies show that *sat* positive UPEC strains were able to cause alterations to cell cytoskeleton, vacuolation and lesions to the kidney (170). The two other SPATE protein family members, VAT and PIC, are also common in UPEC and APEC strains. These proteases are involved in colonisation and are associated with targeting human leukocyte adhesion proteins, such as CD43 and CD45, resulting in the inhibition of leukocyte trafficking, migration, and inflammation (171). Vacuolating autotransporter protein as the name suggests is known for inducing the formation of vacuoles, which have been linked with cell death during cystitis and pyelonephritis (172).

1.4 Biofilm

1.4.1 General

Biofilm formation is a bacterial survival mechanism that is ubiquitous in nature. Biofilms allow bacteria to adhere to solid surfaces forming a 'slimy' coat termed extracellular polymeric substance (EPS) which acts as a shield from environmental stressors (173). The original observations of biofilms date back to 1683 when Antoni van Leeuwenhoek described biofilms on the surface of his teeth using his microscope (174). The influence of biofilms in bacterial infections and diseases was overlooked until the 1970s when Nils Høiby investigated a link

between the aetiology of persistent infection and aggregates of bacteria in cystic fibrosis patients (174, 175), which revolutionised the importance of biofilm involvement in the medical setting (174, 176). Throughout the 1980s and 1990s, further observations described; i) the structural composition of biofilms including different bacterial species having specific methods for attachment to abiotic surfaces; ii) the clinical importance of biofilms, such as the coaggregation of different bacterial species in the mouth and its association with foreign body infections following introduction of biomaterials in human patients (total joint replacement, artificial organ devices) (173, 177, 178). Today, about 80% of all human body infections are biofilm-related (179), which increases mortality and morbidity rates and transforms existing infections into chronic diseases (180-182). Biofilm infections are particularly diverse and have the ability to form all over the body including; chronic infections such as otitis media and chronic sinusitis, endocarditis, cystic fibrosis, urinary tract infections (UTIs), osteomyelitis, or chronic wound infections (182-184).

Biofilms can be defined as surface-attached aggregates of cells surrounded by self-produced extracellular polymeric substances adherent to an inert or living surface (173, 185-187). Biofilm structures contain bacterial communities within an organised network, where channels specific for nutrient circulation allow cells in different regions of the biofilm to differentially express different gene profiles, which has led to the analogy that biofilms resemble tissues of higher organisms (173, 188). Biofilms are a response to external stress or stimuli such as changes in pH, temperature, oxygen and availability of nutrients (187, 189, 190). Bacteria within the biofilm are protected from several challenges such as UV exposure, host defence mechanisms and antimicrobial therapies, which makes biofilm formation an essential mechanism to understand and study for their impact on the environment, industry, and medicine (187, 191-193).

1.4.2 Biofilm formation and life cycle

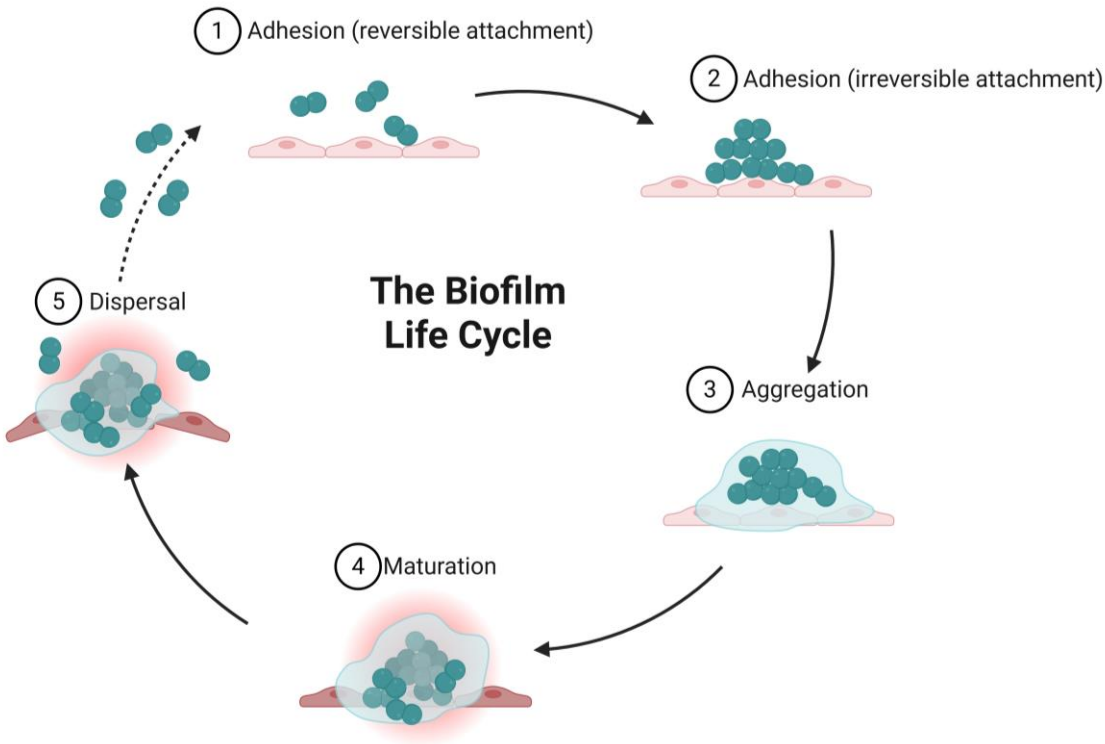

Figure 1.3 – Biofilm formation divided into four main phases: Adhesion (Reversible and irreversible), Aggregation, Maturation and Dispersion.
Adapted from (173) created in (17).

Biofilm development can be divided into four main phases – Adhesion (reversible and irreversible attachment), aggregation (early biofilm structure), maturation (matrix production) and dispersion (detachment) (Figure 1.3) (173, 178, 194-196). The initial adhesion can occur through at least three mechanisms; i) redistribution of attached cells by surface motility; ii) division into daughter cells from the attached cells, and iii) recruitment of cells from the bulk fluid to the developing biofilm (195, 197-200). The specific method used by bacteria depends on species/strain, the nature of the colonised surface, and the environment's physical and chemical conditions (195, 200). During this period, the cells are not fully “committed” to the differentiation process for biofilm formation and a large portion may leave, using pilus-mediated independent movement of twitching or gliding (201, 202), to continue planktonic growth (195, 203). In addition, during the reversible adhesion stage, many bacteria exhibit species-specific behaviours, such as rolling, creeping and “windrow” formation (195, 198). The biofilm structure is then supported by EPS which are composed of

varying proportions of polysaccharides, proteins, nucleic acids and lipids (204). Furthermore, the gene regulation and adaptation to support biofilm formation have been described in previous studies (195, 205). *P. aeruginosa* has been observed to change expression levels in 11 genes during the attachment, while *E. coli* K12 was associated with changes in 38% (out of 446 clones) of attachment-related genes using *lacZ* gene fusions (206, 207). Additionally, *Pseudomonas putida* has shown changes in 40 genes and 45 proteins during the first 6h period of attachment (208). More recent transcriptomic and proteomic studies showcase changes in 339 transcripts and 560 proteins when compared planktonic and biofilm *Desulfovibrio vulgaris* bacteria (209), while *P. aeruginosa* study investigating 77 clinical isolates found 143 gene changes related to biofilm formation (210).

After the initial adhesion, bacteria must remain in contact with the surface to continue biofilm growth and water channel "architecture" is also developed during this stage, which marks the second phase of aggregation (early biofilm structure). This transition is usually defined by thick EPS formation and synthesis of type IV polar pili. *P. aeruginosa* uses type IV pili as a twitching motility mode of locomotion, which helps push or pull bacteria across the surface to form microcolonies (195, 208), as bacteria become more sessile during this phase. As an alternative, *S. epidermidis* has been shown to utilise polysaccharide intercellular adhesin, which bonds cells into microcolonies to promote biofilm growth (211). Type 1 and curli fimbriae also play a major role in irreversible attachment for *E. coli* by strengthening the attachment to the surfaces, facilitating cell-to-cell communication and binding to EPS compounds, such as fibronectin, laminin and plasminogen (212, 213)"cementing" their presence on the surface (214, 215).

The next phase of biofilm formation, maturation, results in the generation of complex 3D matrix, channels, pores and aggregation through cell-to-cell interactions (196, 216). At this stage, many studies have identified a complete shift in bacterial gene profiles compared to planktonic bacteria; increased expression levels in metabolic genes, phospholipid and Lipopolysaccharides (LPS) -biosynthesis, membrane transport and secretion, as well as adaptation and protective mechanisms (196, 217-219). An important mechanism that initiates during the maturation phase is autotransporter molecule formation (196, 215). Autotransporters are the protein molecules that do not require the help of accessory proteins for their translocation to the outer membrane. One of the major autotransporters in *E. coli* is

antigen 43 (Ag43), which promotes cell-to-cell adhesion, therefore facilitating auto-aggregation and three-dimensional development (196, 215). The formation of a chemical-signalling system, which promotes cell-to-cell signalling of autoinducers or quormons is called quorum signalling. This is one of the major components which is initialised in biofilms during the maturation phase (173, 195, 196, 220). These autoinducers are specific for bacterial species and can alter gene expression. Specifically, there have been three quorum-sensing types described in Gram-negative bacteria: N-acyl-homoserine lactones (AHL), also known as AI-1, furanosyl borate diester, also known as AI-2, and threonine dehydrogenase (Tdh) analogs known as AI-3. Quorum-sensing enhances biofilm formation, motility and virulence in *E. coli*, while *P. aeruginosa* studies show differentiation into structured, thick and biocide-resistant biofilms (216, 221-223). Additionally, Gram positive bacteria have been using oligopeptides as autoinducers for the same benefits (224). Finally, many bacteria have been associated with stress-resistance gene expression during biofilm maturation. Stress tolerance improves survival for bacteria in hostile environments by being able to resist acid, ethanol, heat and pH changes through induction of stress-resistance genes, such as *hfq*, *yafQ*, or *rapA* which protect the biofilms from environmental stresses. Furthermore, *rpoS* not only encodes the sigma S factor that regulates the stress response, but also controls the expression of curli fimbriae organelle, cellulose, other matrix components and enzymes involved in the synthesis and degradation of biofilm, suggesting a key role in biofilm defence mechanisms (195, 214, 225, 226). However, at the end of the maturation stage, planktonic revertants, formed out of individual microcolonies, may swim or float away from the matrix-enclosed structures, leaving the crevices that become parts of water channels (195).

The final step of biofilm development is dispersion, which is the release of cells or cell colonies from a biofilm. Active detachment can be due to starvation or deprivation of oxygen by external forces, the quorum-sensing molecules accumulate and release polymer-degrading enzymes, which break the biofilm and release planktonic state bacteria, which can form new biofilms in a distant area, such as *E. coli* or *Streptococcus mutans* (189, 195, 217, 227-229). Additionally, overexpression of alginate lyase can cause alginate degradation and become ineffective in *P. aeruginosa*, while homoserine lactones have been negatively correlated with *Rhodobacter sphaeroides* and *P. fluorescens* biofilms, causing a reduction of biofilm structure (227, 230). Passive detachment can be observed from external factors such as fluid shear

forces or human disturbance (231). Due to dispersed cells having similar gene expression profiles with planktonic cells rather than mature biofilm cells, this marks a full life cycle of bacteria through biofilm development (194, 217).

1.4.3 *E. coli* Biofilm

E. coli is one of the most prevalent biofilm-related microorganisms, causing relapses or chronic infections (182). Many ExPEC strains utilise biofilm formation as a virulence factor, as the process enhances bacterial colonisation, host defence evasion and resistance to antibiotic treatments (182, 232, 233). *E. coli* uses a plethora of genes to initiate and form biofilms under stress conditions effectively. According to the literature, these genes can be classified as direct and indirect based on their role in the biofilm formation process (Table 1.2)(182, 196, 214, 234-248). During the irreversible attachment phase, *E. coli* uses *csgBAC* and *csgDEFG* operons for curli fimbriae expression and *fimAICDFGH* operon for type 1 fimbriae to transition from planktonic to the biofilm state (182, 236). Cyclic-diguanylic acid (c-di-GMP), synthesised from two guanosine triphosphate (GTP) molecules by diguanylate cyclases (DGCs), is a bacterial second messenger that plays an essential role in biofilm synthesis (237). C-di-GMP is associated with curli fimbriae synthesis and the shift from planktonic to sessile state through activation of YCgR which blocks flagellar protein FliG, making bacteria immobile and more prone to forming biofilms (238). In addition, the RcsCDB regulator is another *E. coli* protein involved in biofilm development. The three regulators, RcsC, RcsB, and RcsD, are important in regulation of outer membrane production, such as capsule synthesis, colonic acid (CA) synthesis, and flagella as well as adhesion properties such as curli fimbriae and Ag43 (182, 239, 240) production. CA provides biofilm stability through covalent bonds and is one of the three main polysaccharides involved in biofilm development during the maturation phase (241).

Another major polysaccharide is cellulose, which is synthesised by *bcsABZC* and *bcsEFG* operons, and CsgD regulator (242, 243). Interestingly, the genes encoding cellulose are present in both commensal and pathogenic *E. coli* and over-production can negatively impact biofilm formation and bacterial aggregation (215, 244). Poly-β-1,6-N-acetyl-D-glucosamine (PGA) is the third major exopolysaccharide responsible for cell-to-cell adhesion, stabilisation of biofilms and surface attachment (182, 196, 236). The *pgaABCD* operon encodes proteins related to synthesis (PgaC, PgaD), transport and outer membrane localisation (PgaA, PgaB) of

the PGA polymer, while c-di-GMP is associated with post-translational activation of PGA (196, 215, 236, 245). Stress-response genes, such as *tolC*, also contribute to biofilm synthesis during the maturation phase (182, 246). It is an outer membrane efflux protein (OEP) that maintains structure of the membrane and helps resist antibiotics, but also has been linked to aggregative fimbriae, impacting biofilm formation and adhesion (182, 246, 247). Quorum-sensing in *E. coli* is also pivotal for successful biofilm formation. The *qseBC* operon is responsible for the activation of the master regulon, *flhDC* (which stimulates *motA* and *fliA* production) which subsequently increases biofilm formation and controls motility of bacteria (196, 236). In addition, *luxS* encodes one of the main enzymes producing autoinducers (AI-2) during quorum-sensing, which are required for biofilm formation and maturation (182, 196, 248).

Table 1.2 – Direct & indirect genes associated with biofilm formation in *E. coli*

Biofilm genes	Encoded proteins	Function	Location & Mass (in Daltons)	References
DIRECT				
fimAICDFGH	Type 1 fimbriae regulatory proteins	Type 1 Fimbriae (also called pili) synthesis, enable bacteria to colonize the epithelium of specific host organs	Cytoplasm; 17,317 - 96,482	(182, 196, 225, 235, 236, 244, 255)
pgaABCD	Poly-β-1,6-N-acetyl-D-glucosamine	Synthesis of PGA polymers that helps in biofilm adhesion	Cell inner membrane, Multipass membrane protein; 16,082 - 92,207	(182, 196, 235, 236, 244)
hha	Haemolysin expression modulating protein Hha	Repress the transcription of fimbrial genes thereby decreasing biofilm formation	Cytoplasm; 8628	(196, 225)
bcsABZC and *bcsEFG* operons	Cellulose synthase catalytic subunit	Catalyses the formation of cellulose which is an extracellular component for mechanical and chemical protection of the cell	Cell inner membrane, Multipass membrane protein; 41,700 - 127,724	(182, 196, 244)
kpsMTII	ABC transporter permease	Encodes proteins conducting the polymer translocation to the cell surface; capsular polysaccharide synthesis K1	ATP-binding cassette (ABC) transporter complex; 9,874	(244, 260)
afa	Afimbrial adhesin AFA-I	These adhesins bind to the Dr blood group antigen and also agglutinate human erythrocytes in the presence of D-mannose (mannose-resistant hemagglutination (MRHA))	Fimbrium; 17,184	(235, 244, 255)
csgGFED and *csgBAC* operons	CsgBAC operon transcriptional regulatory protein	Synthesis and assemblence of Curli fimbriae.Involved in cellulose synthesis	Cell inner membrane, Peripheral membrane protein; 11,967 - 30,557	(182, 196, 225, 235, 236, 244)
RcsCDB regulator	the RcsC, RcsB, and RcsD proteins	Synthesis of the capsule, regulate the synthesis of the Colanic Acid and the expression of some genes related to the synthesis of the flagella and adhesion structures such as curli and Ag43	Cell inner membrane; Multi-pass membrane protein, Cytosol; 23,671 - 106,506	(182, 235, 236, 244)
flu	Antigen 43	Adhesin protein that helps in auto-aggregation	Secreted onto cell surface, Cell outer membrane; 106,825	(182, 196, 225, 235, 236, 244)
INDIRECT				
tolC	Outer membrane channel (TolC)	Major channel for drug efflux across the outer membrane of E. coli, involved in the transportation of various types of chemicals, leading to bacterial antimicrobial resistance	Cell-outer membrane, Multi-pass membrane protein; 53,741	(182, 235, 236, 246, 264, 280)
luxS	S-ribosylhomocysteine	Synthesises autoinducer substances (furanosyl borate diester). Stimulates biofilm formation and controls the biofilm architecture	Cytoplasm; 19,416	(182, 196, 225, 235, 236)
qseBC	Transcriptional regulatory protein QseB; Sensor protein QseC	Response regulator in flagella synthesis as it activates transcription of FlhDC and regulates motility; Plays the role of sensor kinase, which is the receptor for autoinducers.	Cytoplasm; Cell inner membrane, Multi-pass membrane protein; 24,678 - 50,282	(182, 196, 225, 235, 236)
flhDC	Flagellar transcriptional regulator FlhD, FlhC	flagellar master operon. Sigma factor that activates the class 3 flagellum operons. Component of Flagellar Motor Complex	Cytolpasm; 13,317 - 21,566	(182, 196, 225, 235, 236)
fliA	RNA polymerase sigma factor FliA	Sigma factor that activates flagella gene transcription	Cytoplasm; 27,521	(182, 196, 225, 235, 236, 285)
motA	Motility Protein A	Flagellor stator which regulates rotation	Cell inner membrane, Multipass membrane protein; 32,011	(182, 196, 225, 235, 236, 285)
rpoS	RNA polymerase Sigma factor RpoS	Regulating genes and structural proteins involved in the synthesis and degradation of biofilm, under stress conditions	Cytoplasm; 37,972	(182, 196, 225, 226, 234-236)
hfq	RNA-binding protein Hfq	Stabilizes to small regulatory RNA in response to stress and stress responses mediated by the sigma factors RpoS	Cytoplasm; 11,166	(196, 225, 244)

1.4.4 *E. coli* biofilm methods

Due to the unique nature of *E. coli* biofilms, there are many methods described that can be used to detect biofilm formation in this species. The traditional crystal violet (CV) assay remains a vital laboratory workhorse and is a standard assay using microtiter plates (236, 249). In this method, transfer of an overnight bacterial pre-culture into the 96-well plate, precedes incubation for 1-4 days, a brief plate wash with PBS, before a staining procedure with crystal violet and measuring the absorbance using 500-600nm wavelengths (250). But similar methods like the tube method (TM), where bacteria are grown in tubes instead of microtiter plates or Congo Red Agar method, where specific media is used and biofilms are evaluated qualitatively are also used (236, 251, 252). The calgary biofilm device (CBD) uses pins attached to 96-well plate and measures the interaction between the pins and the biofilm. But instead of measuring the biofilm forming capabilities, the technique is mostly used for antibiofilm testing (236, 253). Unfortunately, the variety of usable methods also results in potential inconsistencies between the techniques, raising questions about the validity, value and role of each method in biofilm testing (236, 249, 254). The crystal violet assay was selected for this project because the microtiter plate method is the most widely used and is favoured by researchers for its superior reliability compared to other available techniques.

1.5 Gaps in the literature

Despite increasing knowledge of ExPEC using biofilms as a virulence mechanism for pathogenicity, the literature about biofilm formation impact in bacteraemia is very minimal. UPEC have been the only pathotype linked with the majority of genes associated with biofilm formation in *E. coli* (196, 255), while other ExPEC pathotypes have not been studied. Subsequently, the phylogroups B2 and D are well documented as predominant biofilm formers in UPEC, which can be linked with other pathotypes in ExPEC (256-258). In addition, despite ST131 being the most common sequence type among *E. coli* bacteraemia isolates, very little is known about the relationship between *E. coli* biofilm formation and sequence type (259-262), while no information can be found about *E. coli* ST73 in relation to biofilm. The literature does emphasise the importance of *tolC* and *iroN* genes in ExPEC *E. coli* biofilms, but the processes are not fully understood (246, 263, 264). Furthermore, the methods used for *E. coli* biofilm detection are varied and studies are difficult to compare. Even using the

same crystal violet assay with microtiter plates, the methods can vary in pre-culture times, main incubation periods, optimal medias, shaking/static incubation and many crystal violet concentration differences (0.01-1 %) (249, 265-268). There is also inconclusive evidence whether iron supplementation and/or serum can influence biofilm formation in ExPEC strains despite these mechanisms being essential for survival in blood (259, 269, 270). In addition, there have been reports about biofilm forming ExPEC leading to worse clinical outcomes in bacteraemia, compared to non-biofilm forming *E. coli*, suggesting a link between biofilm and the pathogenicity of *E. coli* (271).

1.6 Aims and objectives

Given the gaps in the literature identified above, this thesis aims to explore biofilm formation in ExPEC isolates from bacteraemia patients in a local health board in Southwest Wales. Blood culture positive *E. coli* strains, and relevant controls were collected from three Welsh hospitals in the Hywel Dda University Health Board (HDUHB). *E. coli* isolates were confirmed with associated metadata and included phylogroup, origin of infection and sequence type. The objectives are detailed as follows:

- Investigate the role of physiological parameters on biofilm formation in *E. coli* isolates.
    - Minimal media (PBS+ LB broth (90/10%), Leibovitz's, M9)
    - Temperature
    - Serum coating
    - Iron or other compound supplementation
- Investigate the role of mechanical parameters on biofilm formation in *E. coli* isolates.
    - Shaking methods
    - Static methods
- Investigate the differences in biofilm formation between sequence types and the origin of infection based on clinical and sequence metadata.
- Explore the presence and absence of virulence genes in biofilm positive and negative ExPEC isolates.
- Visualise and image ExPEC biofilm formation and structure and investigate the differences between the isolates.

2 Materials and methods

2.1 Media

Media were prepared using 200-1000 ml distilled water (H_2O) and sterilised by autoclaving at 121°C for 20 minutes.

2.1.1 Luria Bertani (Lennox) Broth (LB)

Luria Bertani (Lennox) Broth medium in tablet form (Sigma-Aldrich; Gillingham, UK), dissolved 1 tablet in 50 ml of H_2O. Once prepared the medium contained; 10 g/L Tryptone, 5 g/L Yeast Extract, 5 g/L NaCl and 2.2 g/L inert binding agents.

2.1.2 Bacto Tryptic Soy Broth with dextrose (TSB+G)

Tryptic Soy Broth with dextrose was purchased in powder form (Thermo Fisher Scientific; Loughborough, UK) and dissolved 3 g per 100 ml in H_2O. Once prepared the medium contained; 17 g/L Pancreatic digest of Casein, 3 g/L Papaic digest of Soybean, 2.5 g/L Dextrose, 5 g/L Sodium chloride, and 2.5 g/L Dipotassium phosphate.

2.1.3 Bacto Tryptic Soy Broth without Dextrose (TSB-G)

Tryptic Soy Broth without Dextrose was purchased in powder form (Thermo Fisher Scientific; Loughborough, UK) and dissolved 2.75 g per 100 ml in H_2O. Once prepared the medium contained; 17 g/L Pancreatic digest of Casein, 3 g/L Papaic digest of Soybean, 5 g/L Sodium chloride and 2.5 g/L Dipotassium phosphate.

2.1.4 Escherichia coli (EC) Broth

EC broth medium was purchased in powder form from Oxoid (Basingstoke, UK) and dissolved 3.7 g per 100 ml in H2O. Once prepared the medium contained; 20 g/L Tryptone, 5 g/L Lactose, 1.5 g/L Bile salts No. 3, 4 g/L Di-potassium phosphate, 1.5 g/L Mono-potassium phosphate, 5 g/L Sodium chloride.

2.1.5 Columbia Agar with Horse Blood

Agar plates were purchased pre-sterilised (Oxoid; Basingstoke, UK).

2.2 Minimal media

Minimal media were prepared using 200-1000 ml distilled water (H_2O) and sterilised by autoclaving at 121°C for 20 minutes or purchased sterilised in liquid form.

2.2.1 Phosphate Buffered Saline (PBS) + LB (90/10 %)

One tablet LB medium was dissolved in 50 ml of H_2O and added to 450 ml of PBS.

2.2.2 Gibco Leibovitz's L-15 Medium, no phenol red

Leibovitz's L-15 minimal medium was purchased in liquid form (Thermo Fisher Scientific; Loughborough, UK).

2.2.3 M9 Minimal Medium

M9 minimal medium was made by weighing chemicals separately, mixed in a beaker and dH_2O was added up to 1000 ml and autoclaved. Once prepared the medium contained; 6 g/L Sodium phosphate dibasic (anhydrous), 3 g/L Potassium phosphate monobasic, 0.5 g/L Sodium chloride, 1 g/L Ammonium chloride. Then 1ml of sterile 1M Magnesium sulfate, 1ml 0.1M calcium chloride and 10ml of 10% (w/v) glucose was added. The solution was filter sterilised through a 0.45µm filter.

2.3 Stock solutions

Stock solutions were prepared using distilled H_2O. Stock solutions used for microbiological work were sterilised by autoclaving.

2.3.1 Crystal violet

>99% crystal violet (0.01% w/v) was purchased in powder form (Sigma Aldrich; Gillingham, UK) and dissolved 0.01 g per 100 ml in H_2O.

2.3.2 Glycerol

>99% Glycerol (Sigma Aldrich; Gillingham, UK) was diluted in dH_2O to a 50% stock solution. Then the solution was autoclaved at 121°C for 20 minutes.

2.3.3 Phosphate Buffered Saline (PBS)

Phosphate buffered saline in tablet form (VWR Life Sciences; Leicestershire, UK) and 1 tablet dissolved per 100 ml dH2O. An equivalent 1000 ml of stock solution was prepared for microbiological work. The final solution contained, 137 mM Sodium chloride, 2.7 mM Potassium chloride and 10 mM phosphate buffer.

2.3.4 Specpure Iron 1000 µg/ml, AAS standard solution

The Specpure Iron >99% (Thermo Fisher Scientific; Loughborough, UK) was diluted in dH_2O to a 100 µM stock solution, by adding 15.74 ml of Iron to 500 ml dH_2O. Subsequently, 0.01 µM, 0.1 µM, 1 µM, 5 µM, and 10 µM were made using 100 µM stock solution diluted into the corresponding medium.

2.3.5 Bile Salts No. 3

A 1.5% w/v stock solution was made from Bile Salts No. 3 powder (Thermo Fisher Scientific; Loughborough, UK) by dissolving 0.15 g in 10 ml in dH_2O. Subsequently, 0.015% w/v, 0.045% w/v, 0.15% w/v, 0.3% w/v, and 0.45% w/v were made using 1.5% w/v stock solution diluted into the corresponding medium.

2.4 Reagents

2.4.1 Healthy volunteer blood serum

Whole blood was collected from healthy volunteers (Ethics:13/WA/0190) in serum separator tubes. Blood was then centrifuged at 2000g for 15 minutes and serum collected and stored at - 20°C.

2.5 Microbiology

2.5.1 *E. coli* strains from Hywel Dda University Health Board (HDUHB)

A set of 41 *E. coli* strains were obtained from the HDUHB (Table 2.1). The sequence typing and phylogroup typing was done by Swansea Genome Center as outlined previously (272)

Table 2.1 – List of *E. coli* isolates obtained from Hywel Dda University Health Board.
This includes isolate ID, hospital ID, source of infection, phylogroup and sequence type.

isolate ID	Hospital ID	Source	Phylogroup	Sequence type
4	B4019	Intra-abdominal	B2	73
14	B17E00 4376	Urinary	B2	73
15	B17E005868	Biliary	B2	73
18	B17E00 4409	Urinary	B2	131
20	17/123	Other	B1	2628
27	3729	Intra-abdominal	B2	73
31	3747	Intra-abdominal	B2	73
33	17/104	Urinary	B2	73
36	17/108	Biliary	B2	131
38	3697	Intra-abdominal	B2	131
39	3701	Biliary	B2	73
45	3690	Urinary	B2	73
47	3731	Urinary	B2	73
58	B17E00 9003	Urinary	B2	131
59	B17E00 9046	Urinary	B2	131
61	1124046948	Abdominal	B2	429
62	1124046825	Urinary	B2	73
63	1124046973	Urinary	B2	131
65	112405550	Urinary	B2	12
66	1124055651	Abdominal	B2	127
67	1124055426	Urinary	B2	429
69	B17A002373	Urinary	B2	7497
76	B18A0000136	Abdominal	None assigned	38
77	B18A000099	Urinary	B2	73
87	B18E000711	Urinary	B2	404
88	B18E000666	Urinary	B2	404
102	B19E006314	Urinary	B2	131
103	B19E006384	Urinary	B2	131
110	B19E006458	Abdominal	B2	131
113	B19E006453	Abdominal	B2	131
118	B19E006615	Abdominal	B2	73
129	B20E000718	Other	B2	131
131	B20E000781	Urinary	B2	131
128.2	B20E000204	Urinary/Abdominal	B2	131
172	B20E000880	Urinary	B2	73
90	E17E505558	Water	B1	4118
91	E17E505761	Water	D	4118
94	E18E500166	Water	B1	1205
ANC2	U20E240114	ANC Urine	B2	None assigned
ANC3	U20E240117	ANC Urine	B2	None assigned
ANC4	U20E282052	ANC Urine	B2	None assigned

2.5.2 Biofilm and *E. coli* control strains

Three additional control strains were used in this study (Table 2.2).

Table 2.2 – List of biofilm and *E. coli* control strains.

Species	Strain	Comments	References
Escherichia coli	K12 (ATCC-29425)	Model laboratory strain Descendent of a strain first isolated in 1922 from a stool sample	(273, 274)
Escherichia coli	CFT073 (ATCC-700928)	Uropathogenic bacterium that was isolated in Baltimore, Maryland, from the blood and urine of a woman with acute pyelonephritis.	(275, 276)
Staphylococcus epidermidis	1457	Cause of central-venous catheter associated disease; Selected as positive biofilm producer	(277)

2.5.3 Physiological and mechanical parameters used for biofilm assay

List of all physiological and mechanical parameters used to determine the biofilm formation in *E. coli* isolates (Table 2.3).

Table 2.3 – Physiological and mechanical conditions tested during Biofilm Assay.

Media	Shaking method	Temperature	Pre-culture time	Incubation time	Other
LB Broth	No Shaking				Blood serum
PBS+LB media				24 h incubation	
		37 °C temperature	20 min pre-culture		
TSB+G Broth	Linear Shaking				Bile salts
TSB-G Broth				48 h incubation	
Leibovitz's media	Circular Shaking				
EC Broth		30 °C temperature	24 hour pre-culture		Iron
				72 h incubation	
M9 Minimal media	Orbital Shaking				

2.5.4 Routine Culture and storage of microorganisms

The forty-one clinical strains of *E. coli* were obtained from the HDUHB on agar slopes. Upon receipt of the strains, bacteria were inoculated onto Columbia Horse Blood Agar and incubated at 37°C overnight (16-18 h). Freezer stocks were created by inoculating Cryobeads (Qiagen) with 2-3 colonies before storage at –80°C.

The three control strains (table 2.2) were obtained from archived collections within the Microbiology and Infectious Diseases' group at Swansea University. Upon receipt of the strains, bacteria were cultured independently by streaking from freezer stocks onto Columbia Horse Blood Agar plates. Plates were incubated for 24 h in a 37°C Genlab Incubator (Cheshire, UK). Following incubation, a single colony from the overnight culture plate was used to inoculate 700 µl of LB (for *E. coli*) or TSB+G (for *S. epidermidis*) broth in a 1.5 ml microcentrifuge tube. Next, 300 µl of 50% glycerol was added to the microcentrifuge tube. The glycerol stock was pulse vortexed on a Genius 3 vortex (IKA®; Oxford, UK) and stored at -80°C (Thermo Fisher Scientific TSX Series Freezer; Loughborough, UK).

2.5.5 *S. epidermidis* pre-culture

S. epidermidis was cultured according to previously developed protocols (278). In brief, *S. epidermidis* 1457 was streaked onto Columbia Horse Blood Agar plates and incubated at 37°C overnight in a Genlab incubator. From the streak plate, one to five colonies were selected and suspended into 3 ml TSB+G broth in a 7 ml Bijou tube. The bacterial suspension was incubated with shaking at 37°C for up to 24 h depending on the protocol, in a Kuhner shaker X incubator (Basel, Switzerland) at 200 rpm. Then, the preculture was used for growth curve assay and biofilm assay as a strong biofilm positive strain.

2.5.6 Growth Assay

Following the culture onto agar (section 2.5.5 for *S. epidermidis*), one colony of each bacterial strain was inoculated in 3ml LB broth in a 7ml Bijou tube. The bacterial suspension was incubated with shaking at 37°C for 24 h (3600 minutes) in a Kuhner shaker X incubator at 200 rpm. Then, the suspension was diluted 1:100 (10 µl bacteria, 990 µl media) with fresh LB broth (or TSB+G *for S. epidermidis*) in a 1.5 ml microcentrifuge tube. Then, 150 µL of each sample was added to a Nunc™ 96-well plate (Thermo Fisher Scientific; Loughborough, UK). The optical

density was measured before (0-hour read) and after (24-hour read) incubation at 600 nm using the FLUOstar Omega plate reader (BMG Labtech, Aylesbury, UK). The plate was incubated for 24 hours in a Kuhner shaker X incubator (Basel, Switzerland) at 20 rpm or statically in a Genlab Incubator.

2.5.7 Biofilm Assay

Following the initial culture in section 2.5.4 (section 2.5.5 for *S. epidermidis*), the bacterial strains were inoculated in 3ml LB broth in a 7ml Bijou tube, streaking 1-5 colonies from Columbia Horse Blood Agar. The bacterial suspension was incubated with shaking at 37°C for 24 hours (3600 minutes) in a Kuhner shaker X incubator at 200 rpm. Then, the suspension was diluted in a 1:100 ratio (10 µl bacteria, 990 µl media) with fresh LB broth (TSB+G for S. epidermidis) in a 1.5 ml microcentrifuge tube. Subsequently, 150 µL of each sample was added to a Nunc™ 96-well plate. The plate was incubated for 24 h at 37°C in a Genlab Incubator statically. After the incubation, the medium was carefully removed from the 96-well plate and the wells were washed three times with 200 µl of PBS before airdrying at room temperature overnight. The next day, bacteria adherent to the wells were stained with 150 µl 0.01% Crystal Violet for 15 min in the dark. The excess stain was removed by flicking the plate. The plate was washed five times with PBS before airdrying at room temperature overnight. The optical density of the biofilms was measured at 570 nm using the FLUOstar Omega plate reader. The biofilm assay included the following variations;

2.5.7.1 Biofilm assay with different media

The protocol follows the same steps as in section 2.5.7, but further assay media are used instead of LB broth. They include; PBS+LB broth, TSB+G broth, TSB-G broth, Leibovitz's medium, EC broth or M9 minimal medium (For *S. epidermidis*, only TSB+G was used).

2.5.7.2 Biofilm Assay with Linear shaking

The protocol follows the same steps as in section 2.5.7, but instead of incubating the 96-well plate statically, it was incubated on a Stuart™ See-Saw Rocker at 20 rpm, at 37°C in a Genlab Incubator.

2.5.7.3 Biofilm Assay with Orbital shaking

The protocol follows the same steps as in section 2.5.7, but instead of incubating the 96-well plate statically, it was incubated on a Stuart™ Gyro rocker (Sigma-Aldrich; Gillingham, UK) at 20 rpm., at 37°C in a Genlab Incubator.

2.5.7.4 Biofilm Assay with Circular shaking

The protocol follows the same steps as in section 2.5.7, but instead of incubating the 96-well plate statically, it was incubated in a Kuhner shaker X incubator at 20 rpm.

2.5.7.5 Biofilm Assay with incubation at 30°C

The protocol follows the same steps as in section 2.5.7, but instead of incubating the 96-well plate at 37°C, it was incubated at 30°C.

2.5.7.6 Biofilm Assay with short pre-culture

The protocol follows the same steps as in section 2.5.7, but instead of the first incubation of suspensions with shaking at 37°C for 24 hours (3600 minutes) in a Kuhner shaker X incubator, they were incubated for 20 minutes.

2.5.7.7 Biofilm Assay with extended (48/72 hour) incubation time

The protocol follows the same steps as in section 2.5.7, but instead of the 96-well plate incubating for 24 h, it was incubated for 48 or 72 h.

2.5.7.8 Biofilm Assay with blood serum

The protocol follows the same steps as in section 2.5.7, but 96-well plates were treated with 100 µL of human blood serum for 1 hour, removed and gently washed with PBS before adding 150 µL of each sample.

2.5.7.9 Biofilm Assay with Bile Salts

The protocol follows the same steps as in section 2.5.7, but media (LB broth or TSB+G broth) were supplemented with 0.015% w/v, 0.045% w/v, 0.15% w/v, 0.3% w/v, and 0.45% w/v concentration of bile salts.

2.5.7.10 Biofilm Assay with Iron

The protocol follows the same steps as in section 2.5.7, but media (LB broth or TSB+G broth) were supplemented with 0.01 µM, 0.1 µM, 1 µM, 5 µM, and 10 µM concentration of iron.

2.5.7.11 Biofilm Assay with Bile Salts and Iron

The protocol follows the same steps as in section 2.5.7, but the medium (LB broth) was supplemented with 0.45% w/v concentration of Bile salts and 0.01 µM, 0.1 µM, 1 µM, 5 µM, and 10 µM concentration of iron.

2.6 Data analysis

2.6.1 Gene analysis

The genomic data were acquired from a previous project, where genome assembly, annotation, pangenome generation, and quality control was done at Swansea Genome Center, as outlined (272). The gene analysis was completed by using a pre-existing gene presence/absence table (272) and re-tabulating for known biofilm and bile resistance genes in Microsoft Excel. The total number of strains possessing a gene of interest was also expressed as a percentage. Heatmaps were drawn using R (version: 4.4.2) and R studio (version: 2024.12.0-467) with packages: ggplot2.

2.6.2 Biofilm visualisation and Confocal Laser Scanning Microscopy (CLSM) data analysis

2.6.2.1 Sample preparation for CLSM

Following the initial culture in section 2.5.4, the bacterial strains were inoculated in 3ml LB broth + 0.45% w/v bile salts in a 7ml Bijou tube, streaking single colony from Columbia Horse Blood Agar. The bacterial suspension was incubated with shaking at 37°C for 24 hours in a Kuhner shaker X incubator at 200 rpm. Then, the suspension was diluted in a 1:100 ratio with fresh LB broth + 0.45% w/v bile salts media in a 1.5 ml microcentrifuge tube. Subsequently, 150 µL of each sample was added to a glass-bottomed 96-well plate (655892, Greiner; Stonehouse, UK). The plate was incubated for 24 hours at 37°C shaking on a Stuart™ See-Saw Rocker at 20 rpm in a Genlab Incubator. After incubation, the supernatant was carefully removed from the 96-well plate and the wells were treated with 0.5% of Baclight™ LIVE/DEAD™ stain (Invitrogen; Paisley, UK) and the plate was covered with foil for 5 minutes. After that, 43 µL of PBS was added into each well and the plate was wrapped in foil prior to imaging. The samples were imaged over the next 6 h.

2.6.2.2 CLSM imaging and analysis

The CLSM imaging was performed using a Zeiss LSM980 CLSM, where Z-stack images were taken using a x63 objective lens under oil immersion. Biofilm formation was quantified with COMSTAT analysis (199) to achieve measurements of bacterial biomass and thickness.

2.7 Statistical comparisons and analysis

Statistical analysis of growth curve and biofilm assay data was performed using GraphPad Prism version 10 (La Jolla, California, USA). Firstly, all data sets were tested for normality using the Shapiro-Wilks normality test. For normally distributed data, parametric T-tests, and one-way ANOVAs were applied. For non-normal data, non-parametric Mann-Whitney tests or Kruskal-Wallis tests with Dunn's multiple comparison tests were applied. Data were presented as box and whisker plots. A p value of <0.05 was considered to be significant. The specified statistical tests used in each experiment are confirmed in each figure legend.

3 Results

An archived collection of blood culture positive *E. coli* (Table 2.1) were investigated for their ability to produce biofilm following exposure to defined conditions; changes in media, temperature, time and shaking parameters. Given that growth is an important pre-requisite for biofilm formation on a macroscopic scale, confirmation that this *E. coli* collection could grow in defined media was the project starting point.

3.1 *E. coli* growth in defined media

Growth assays of the 43 *E. coli* isolates (Section 2.5.6) in different bacterial culture media were carried out (Figure 3.1). M9 is a minimal media widely used for *E. coli* cultivation (279). Leibovitz's L-15 Medium (Leibovitz) is a CO_2 buffer-free cell culture medium which was used as iron-free media. PBS+LB (90% PBS +10% LB) media was used as an alternative to minimal media for a low-nutrient environment.

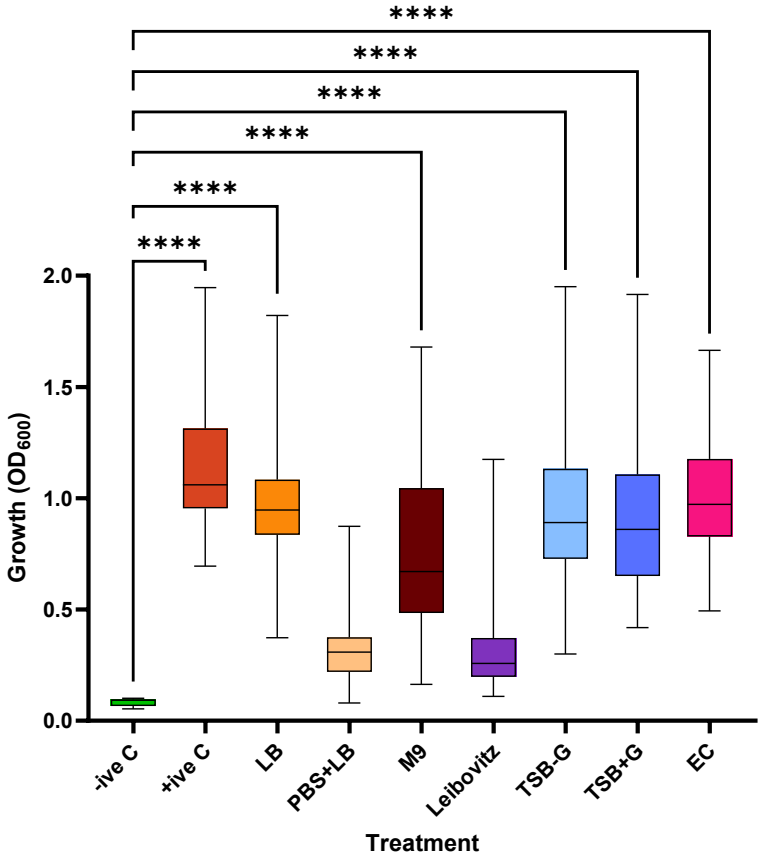

Figure 3.1 – Bacterial growth in defined media.
A total of 43 *E. coli* isolates were incubated in defined media overnight, then grown in 96 well plates for 24 hours. After that, the OD_{600} was determined, and the results were presented as a box and whisker plot. Data is presented as the median with interquartile ranges with whiskers indicating the minimum to maximum values. -ive C = blank media (average of all media, negative control); +ive C = *S. epidermidis* (1457) in TSB (positive control). -/+ G represents media without and with glucose. EC = *E. coli* Broth. Data shown is based on minimum of 3 biological repeats and 2 technical repeats of each isolate. Statistical analyses were performed using Kruskal-Wallis non-parametric tests. Statistical significance is indicated as follows: **** $p < 0.0001$.

Negative and positive controls showed no growth and growth respectively. The growth of *E. coli* strains was media and strain dependent. LB, M9, TSB-G, TSB+G and EC demonstrated significantly higher optical densities than negative control. PBS+LB and Leibovitz media did not show any significant differences compared to negative control.

3.2 Screening of conditions for *E. coli* biofilm deposition and formation

To optimize *E. coli* biofilm formation using the *E. coli* bacteraemia strains, various physiological and mechanical factors were tested (Section 2.5.3, table 2.3). Biofilm assays were conducted as described in the methods (sections 2.5.7 – 2.3.5.8), and the results were compared (Figure

3.2). Throughout the experiments, an OD_{570} value of 0.1 was used as the threshold for biofilm formation.

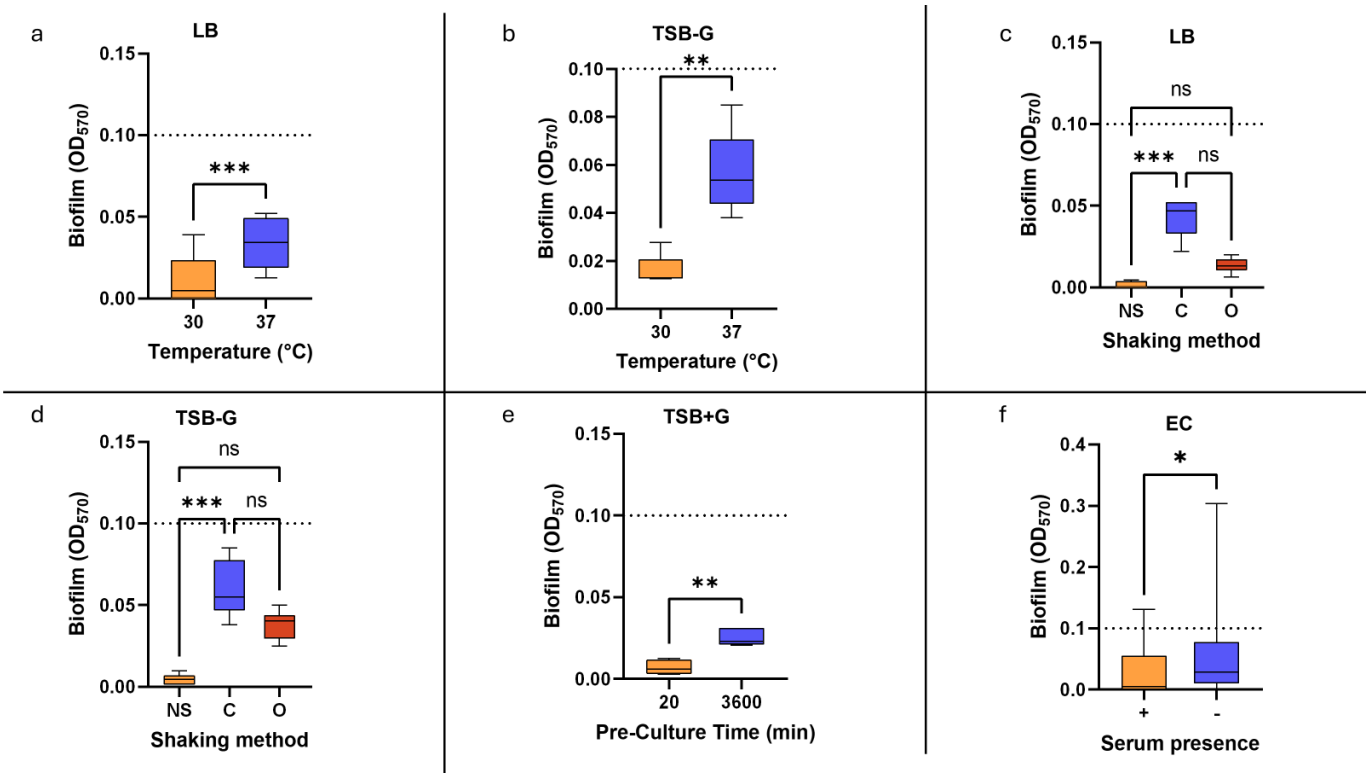

Figure 3.2 – Biofilm deposition of *E. coli* isolates under different physiological and mechanical conditions.
Biofilms were grown on 96 well plates for up to 24 hours. Then, *E. coli* biofilms were washed with PBS, dried overnight, and stained with 0.01% crystal violet. Following staining, the samples were rinsed, and optical density was measured at OD_{570}. The results are presented as box-and-whisker plots, where the boxes represent the median and interquartile ranges, and the whiskers indicate the minimum and maximum values. The dotted line represents the threshold of 0.1 showing a positive biofilm formation. **Panel a**: Biofilm formation at two incubation temperatures (30°C vs. 37°C) in LB. **Panel b**: Biofilm formation at two incubation temperatures (30°C vs. 37°C) in TSB-G. **Panel c:** Comparison of different shaking methods during incubation (C = Circular, O = Orbital, NS = No Shaking) in LB. **Panel d:** Different shaking methods during incubation in TSB-G. **Panel e:** Comparison of different pre-culture times (20 minutes vs. 3600 minutes). **Panel f**: Influence of serum presence (+) or absence (–) on biofilm formation. 5-20 isolates were used with 1 biological repeat and 2 technical repeats of each isolate per experiment. Statistical analyses were performed using Mann-Whitney and Kruskal-Wallis non-parametric tests. Statistical significance is indicated as follows: ns = not significant, * $p < 0.05$, ** $p < 0.01$, *** $p < 0.001$. The positive control (*S. epidermidis* 1457) consistently showed biofilm and growth values within the range of 0.8–1.2. Data values of each graph can be found in Appendix 1.1.

With respect to temperature (Figure 3.2a and b), biofilm deposition at 37°C was significantly greater than at 30°C under circular shaking conditions in both LB (Figure 3.2a) and TSB-G (Figure 3.2b) media. In contrast, at 30°C, biofilm deposition was more pronounced than at 37°C in M9 minimal media, under both circular shaking (P = 0.0079) (Appendix 1.2a) and

orbital shaking conditions (P = 0.0317) (Appendix 1.2b). However, all of the results did not reach the biofilm formation threshold (defined as an absorbance of 0.1).

Circular shaking resulted in significantly higher biofilm deposition compared to no shaking, but no difference to orbital shaking at 37°C in LB (Figure 3.2c) and TSB-G (Figure 3.2d) media. Subsequently, circular shaking was superior in biofilm deposition to orbital shaking with M9 minimal media at both 30°C and 37°C (appendix 1.2c,d). Interestingly, orbital shaking showed a significant advantage over circular shaking at 37°C in TSB+G media (appendix 1.2e).

Biofilm deposition with 3600-minute (24-hour) pre-culture (Figure 3.2e) was significantly greater than a 20-minute pre-culture time in TSB+G media with orbital shaking at 37°C. Additionally, 3600-minute pre-culture was superior at 37°C with orbital shaking in TSB-G media (*P* = 0.0079) (appendix 1.3a), and with circular shaking in both LB (*P* = 0.0317) and TSB-G (*P* = 0.0079) media (appendix 1.3b,c).

The effect of serum on biofilm formation was also investigated. Serum inhibited biofilm deposition at 30°C and under circular shaking conditions, whether cultured in *E. coli* broth (Figure 3.2f) or PBS+LB media (appendix 1.3d). Under the same conditions, biofilm deposition was also significantly higher in the absence of serum when using Leibovitz and M9 minimal media, with *P* values of 0.0101 and 0.0256, respectively (appendix 1.3e,f).

In summary, none of the conditions tested produced a median biofilm formation value exceeding the 0.1 OD_{570} threshold (Figure 3.2). However, some *E. coli* strains cultured in EC broth consistently produced biofilm values above this threshold (Figure 3.2f range values). This observation led to further investigations into the constituents of EC broth.

3.3 Biofilm formation in *E. coli* bacterial isolates using bile salts

The initial screening of conditions conducive for biofilm formation in *E. coli* bacterial isolates implicated EC broth constituents as important. Therefore, the effect of different bile salt concentrations (0.015%-0.45% w/v) on *E. coli* bacterial isolates was investigated (Section 2.5.7.9) and biofilm formation and growth were subsequently measured in LB (Figure 3.3) and TSB with glucose (Figure 3.4).

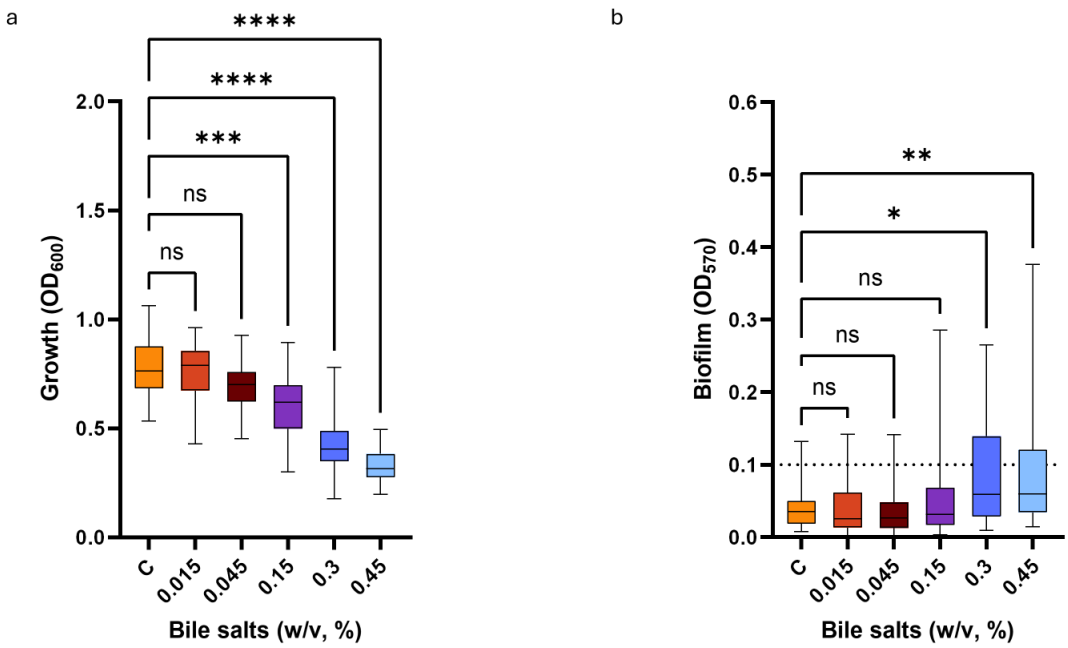

Figure 3.3 – Growth and biofilm formation in LB medium supplemented with bile salts.
E. coli isolates (n=43) were grown in LB with bile salt supplementation over 24 hours. Then, growth was assessed by optical density OD_{600} (a). For biofilm detection the plate was washed with PBS, treated with 0.01% crystal violet and measured at OD_{570} (b). The x-axis indicates increasing bile salt concentrations (weight/volume, %). The results are shown as box-and-whisker plots, where the boxes represent the median and interquartile ranges, and the whiskers indicate the minimum and maximum values. The dotted line represents the threshold of 0.1 showing a significant biofilm formation. "C" denotes the control sample, representing *E. coli* grown in LB without bile salt supplementation. Data shown is based on minimum of 3 biological repeats and 2 technical repeats for each isolate. Statistical analyses were performed using the Kruskal-Wallis non-parametric test. Statistical significance is indicated as follows: ns = not significant, * $p < 0.05$, ** $p < 0.01$, *** $p < 0.001$, **** $p < 0.0001$. The positive control (*S. epidermidis* 1457) consistently showed biofilm and growth values within the range of 0.8–1.2.

In LB media (Figure 3.3), growth was dose dependently inhibited and reached significance (Figure 3.3a) at bile salt concentrations above 0.15% w/v (purple) when compared to the

control. Bile salts showed a dose dependent increase in biofilm formation (Figure 3.3b), reaching significance at 0.3% w/v (blue) and 0.45% w/v (light blue) compared to the control.

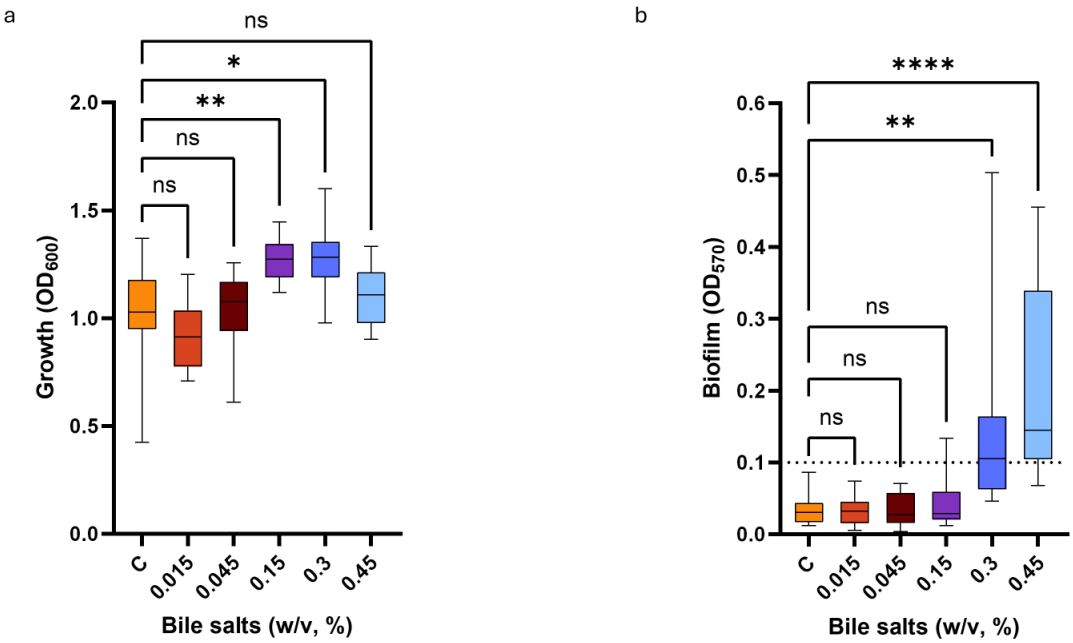

Figure 3.4 – Growth and biofilm formation in TSB+G medium supplemented with bile salts.
E. coli isolates (n=12) were grown in TSB+G with bile salt supplementation over 24 hours. Then, growth was assessed by optical density OD_{600} (a). For biofilm detection the plate was washed with PBS, treated with 0.01% crystal violet and measured at OD_{570} (b). The x-axis indicates increasing bile salt concentrations (weight/volume, %). The results are shown as box-and-whisker plots, where the boxes represent the median and interquartile ranges, and the whiskers indicate the minimum and maximum values. The dotted line represents the threshold of 0.1 showing a significant biofilm formation. "C" denotes the control sample, representing *E. coli* grown in TSB+G without bile salt supplementation. Data shown is based on minimum of 3 biological repeats and 2 technical repeats for each isolate. Statistical analyses were performed using the Kruskal-Wallis non-parametric test. Statistical significance is indicated as follows: ns = not significant, * $p < 0.05$, ** $p < 0.01$, **** $p < 0.0001$. The positive control (*S. epidermidis* 1457) consistently showed biofilm and growth values within the range of 0.8–1.2.

Consistent with this, in TSB+G media (Figure 3.4), a similar trend was observed as bile salts showed a dose dependent increase in biofilm formation (Figure 3.4b) reaching significance at 0.3% w/v (blue) and 0.45% w/v (light blue) compared to untreated control. Growth in TSB+G was increased specifically (Figure 3.4a) at 0.15% w/v and 0.3% w/v bile salt concentration only. These results confirm the importance of bile salts for biofilm formation.

3.4 The effect of iron on *E. coli* biofilm formation

A range of iron concentrations (0.01-10µM) were investigated for their effect on growth and biofilm formation according to methods outlined previously (section 2.5.7.10). Iron influence on *E. coli* biofilm formation and growth was investigated in the LB medium (Figure 3.5) and TSB+G medium (Figure 3.6).

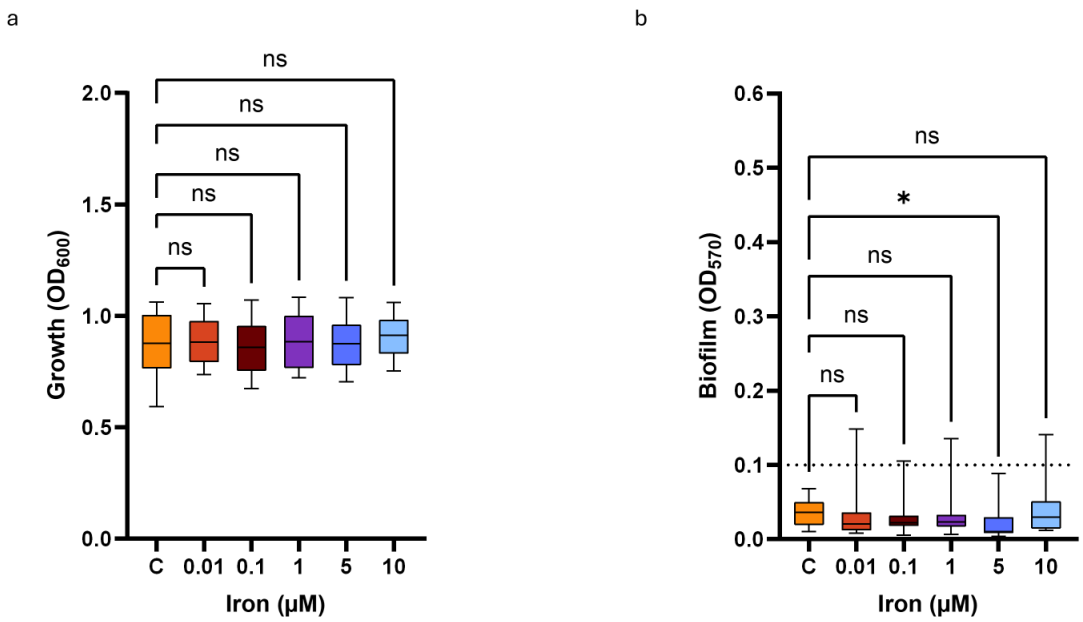

Figure 3.5 – Growth and biofilm formation in LB medium supplemented with iron.
E. coli isolates (n=12) were grown in LB with a range of iron concentrations (0.01-10µM). Then, growth was assessed by optical density OD_{600} (a). For biofilm detection the plate was washed with PBS, treated with 0.01% crystal violet and measured at OD_{570} (b). The x-axis indicates increasing molar concentrations of iron. The results are shown as box-and-whisker plots, where the boxes represent the median and interquartile ranges, and the whiskers indicate the minimum and maximum values. The dotted line represents the threshold of 0.1 showing a significant biofilm formation. "C" denotes the control sample, representing *E. coli* grown in LB without iron supplementation. Data shown is based on minimum of 3 biological repeats and 2 technical repeats for each isolate. Statistical analyses were performed using the Kruskal-Wallis non-parametric test, with significance levels indicated as follows: ns = not significant, * $p < 0.05$. The positive control (*S. epidermidis* 1457) consistently showed biofilm and growth values within the range of 0.8–1.2.

Iron supplementation into LB media (Figure 3.5) had very little effect on growth (Figure 3.5a) and biofilm formation (Figure 3.5b). One condition, at 5 µM iron, reduced biofilm deposition significantly compared to control. Consistent with this, TSB+G media supplemented with iron (Figure 3.6) showed some effect on growth (Figure 3.6a) and very little on biofilm formation

(Figure 3.6b). One condition at 10 µM iron significantly reduced growth compared to the control group and hinted at a dose dependent decrease in growth.

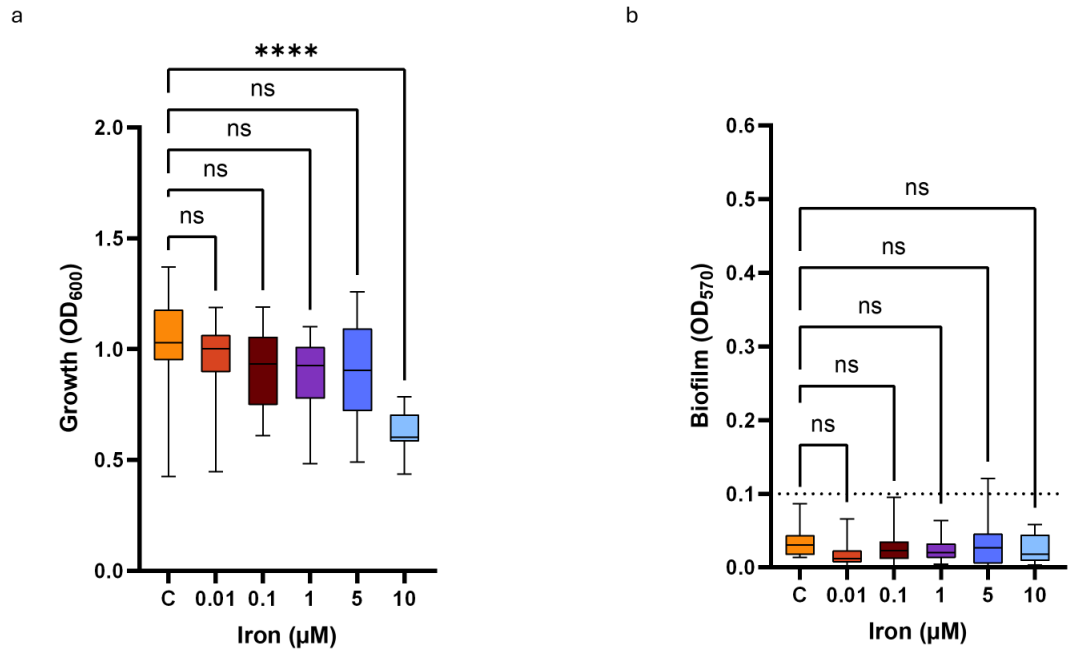

Figure 3.6 – Growth and biofilm formation in TSB+G medium supplemented with iron.
E. coli isolates (n=12) were grown in TSB+G with a range of iron concentrations (0.01-10µM). Then, growth was assessed by optical density OD_{600} (b). For biofilm detection, the plate was washed with PBS, treated with 0.01% crystal violet and measured at OD_{570} (a). The x-axis indicates increasing molar concentrations of iron. The results are shown as box-and-whisker plots, where the boxes represent the median and interquartile ranges, and the whiskers indicate the minimum and maximum values. The dotted line represents the threshold of 0.1 showing a significant biofilm formation. "C" denotes the control sample, representing *E. coli* grown in TSB+G without iron supplementation. Data shown is based on minimum of 3 biological repeats and 2 technical repeats for each isolate. Statistical analyses were performed using the Kruskal-Wallis non-parametric test, with significance levels indicated as follows: ns = not significant, **** $p < 0.0001$. The positive control (*S. epidermidis* 1457) consistently showed biofilm and growth values within the range of 0.8–1.2.

In summary, the effect of iron supplementation on *E. coli* biofilm formation was minimal over the concentrations studied, while growth was significantly reduced when supplemented with 10 µM concentration of additional iron in TSB+G media.

3.5 The effect of *E. coli* sequence type and origin of infection on biofilm formation

Following the initial screening, LB media supplemented with bile salts was selected for further investigations of growth and biofilm formation in 43 *E. coli* bacterial isolates (Table 2.1, 2.2),

including *E. coli*, K12 and CFT073. Next, isolate and clinical meta-data associated with the isolates were used to further understand the optimal conditions for biofilm formation and growth. This analysis used biofilm formation and growth across isolates in 0.45% w/v bile salts and grouped data by sequence type (Figure 3.7a) and origin of infection (Figure 3.7b).

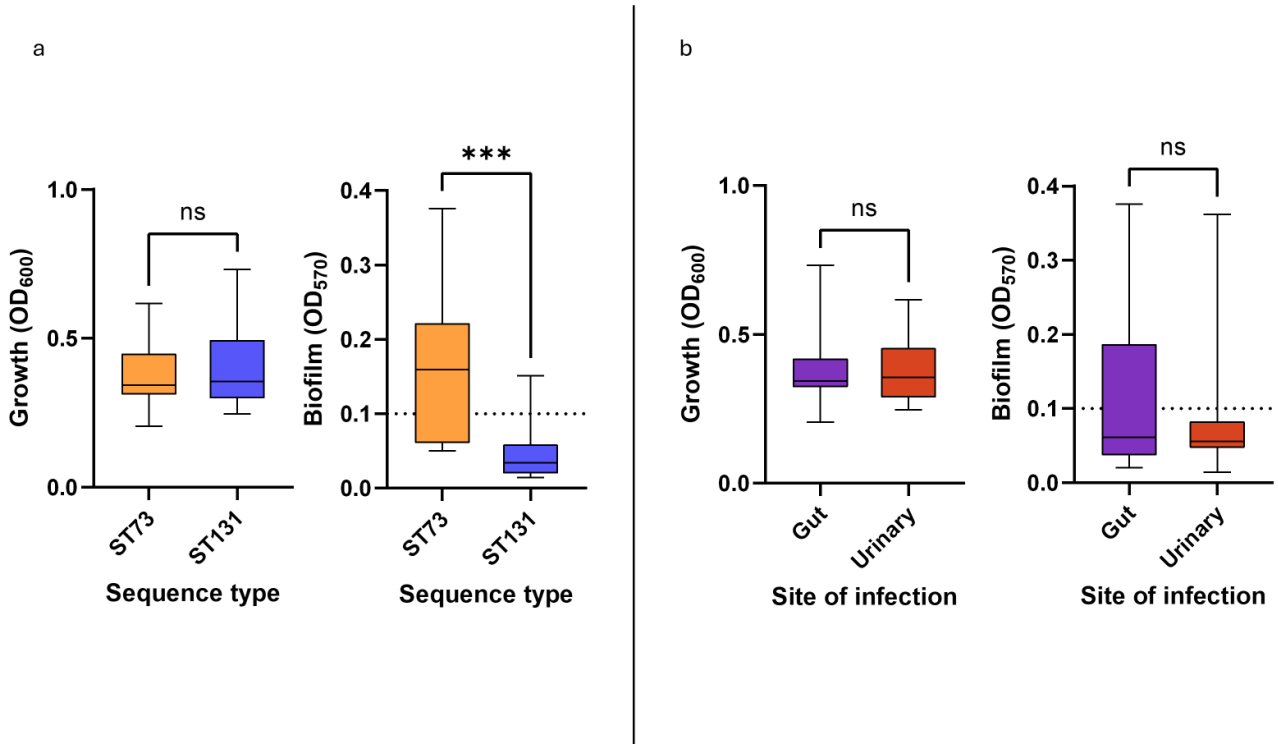

Figure 3.7 – *E. coli* isolate growth and biofilm formation comparison between sequence type (a) and origin of infection (b).
E. coli isolates (n=43) were grown in LB with bile salt supplementation of 0.45% w/v. Then, growth was assessed by optical density OD_{600} (left graphs in panel a and b). For biofilm detection, the plate was washed with PBS, treated with 0.01% crystal violet and measured at OD_{570} (right graphs in panel a and b). The results are depicted as box-and-whisker plots, where the boxes represent the median and interquartile ranges, and the whiskers indicate the minimum and maximum values. The dotted line represents the threshold of 0.1 showing a significant biofilm formation. Data shown is based on minimum of 3 biological repeats and 2 technical repeats for each isolate. Statistical analyses were performed using the Mann-Whitney non-parametric test, with significance levels indicated as follows: ns = not significant, *** $p < 0.001$. The positive control (*S. epidermidis* 1457) consistently showed biofilm and growth values within the range of 0.8–1.2.

ST73 and ST131 were the predominant sequence types identified in the selected bacteraemia isolates. Strikingly, *E. coli* ST73 isolates had significantly higher biofilm formation compared to ST131 isolates (Figure 3.7a, right) with no significant differences in growth (Figure 3.7a, left).

Organising the data by urinary and gut origins of infection did not show any significant differences in growth or biofilm formation (Figure 3.7b).

The striking effect of sequence type on biofilm formation, but not on growth prompted further investigation into individual strain characteristics within the dataset.

3.6 The effect of bile salts biofilm formation and growth of individual *E. coli* isolates

Next, the biofilm formation and growth data for each *E. coli* strain (n=43) was analysed individually (Table 3.1) and their 'best biofilm formation' performance (independent of conditions) was presented in a league table. In this scenario, 15 *E. coli* isolates (35%) were biofilm positive (>0.1 threshold) and 9 of these isolates were significantly increased (*) when bile salts were supplemented. Strikingly, 12 *E. coli* isolates managed to reach a positive biofilm threshold due to exposure to bile salts (purple). The remaining 28 isolates (65%) formed weak biofilm deposits, although 5 isolates showed a significant biofilm deposition increase (') compared to the control.

Out of 15 biofilm positive isolates, 7 of them (47%) were ST73 isolates, while only 2 (13%) were ST131 isolates. This disparity was observed previously (Figure 3.7a), while no difference was observed between gut (6 isolates, 40%) and urinary (5 isolates, 33%) origins of infection. The biofilm negative isolates showed that ST73 was identified for 6 isolates (21%), while ST131 was identified for 11 isolates (39%). Furthermore, the gut origin of infection was identified in 7 isolates (25%) and 14 isolates were identified as urinary (50%).

Table 3.1 – Biofilm formation of individual *E. coli* isolates with bile salt supplementation.
E. coli samples (n=43) were grown in LB with bile salt supplementation over 24 hours. For biofilm detection the plate was washed with PBS, treated with 0.01% crystal violet and measured at OD_{570} (third column). The first column indicates isolate ID. The second column (Concentration) indicates bile salt concentration (weight/volume, %) in LB media. The fourth and fifth columns depict the sequence type and origin of infection, respectively. A threshold absorbance of 0.1 was used to define a biofilm positive phenotype (horizontal double line). Statistical analyses were performed using the Kruskal-Wallis non-parametric test. Statistical significance is indicated as follows: * = biofilm value significantly increased with bile salt supplementation in biofilm positive isolates, ' = biofilm deposition significantly increased with bile salt supplementation in biofilm negative isolates. Purple cells – isolates did not produce positive biofilm before bile salts.

Isolate ID	Bile salt oncentration (weight/volume, %)	CV assay result	Sequence type	Site of infection
4*	0.45	0.376	73	Gut
45*	0.45	0.362	73	Urinary
K12*	0.45	0.299	10	Lab strain
27*	0.15	0.286	73	Gut
ANC3	0.45	0.246	N/A	ANC Urine
20*	0.3	0.240	2628	Other
15	0.45	0.229	73	Gut
39*	0.45	0.215	73	Gut
77*	0.45	0.212	73	Urinary
61	0.3	0.208	429	Gut
38	0.3	0.188	131	Gut
172*	0.45	0.181	73	Urinary
ANC4	0.3	0.148	N/A	ANC Urine
18*	0.3	0.111	131	Urinary
87	0.45	0.103	404	Urinary
62	0.3	0.093	73	Urinary
ANC2	0.45	0.091	N/A	ANC Urine
76	0.045	0.087	38	Gut
33	0.3	0.084	73	Urinary
CFT073	0.45	0.081	73	Control urosepsis isolate
65	0.3	0.078	12	Urinary
59'	0.45	0.075	131	Urinary
63	0.015	0.072	131	Urinary
118	0.3	0.071	73	Gut
47	0.45	0.069	73	Urinary
14'	0.45	0.056	73	Urinary
131	0.45	0.055	131	Urinary
31'	0.45	0.052	73	Gut
67	0	0.050	429	Urinary
58'	0.45	0.049	131	Urinary
88	0.45	0.047	404	Urinary
90	0.015	0.044	4118	Water
66	0.45	0.042	127	Gut
36	0	0.042	131	Gut
94	0	0.038	1205	Water
129'	0.45	0.034	131	Other
128.2	0.45	0.034	131	Urinary/Abdominal
110	0	0.033	131	Gut
103	0	0.032	131	Urinary
113	0.045	0.027	131	Gut
91	0	0.025	4118	Water
102	0	0.025	131	Urinary
69	0.45	0.019	7497	Urinary

Finally, given the paired growth and biofilm data available, an inverse correlation between these parameters was investigated (Figure 3.8). Using the linear regression model, the inverse correlation between growth and biofilm formation was statistically significant (P = 0.0064) over the range studied.

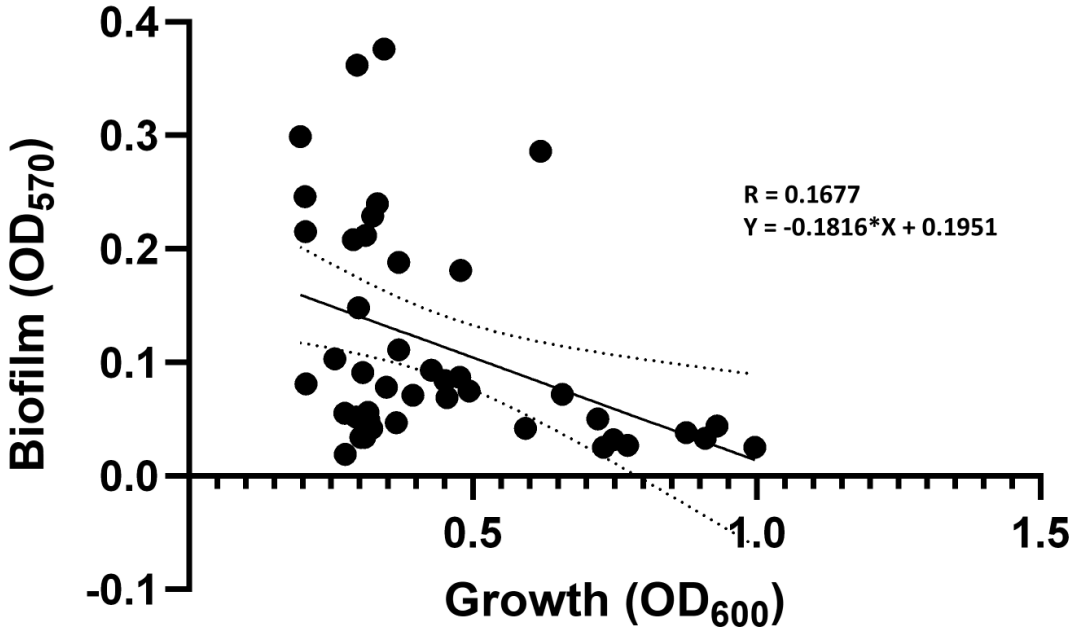

Figure 3.8 – Individual strain growth and biofilm formation with bile supplementation.
E. coli samples (n=43) were grown in LB with bile salt supplementation over 24 hours. Then, growth was assessed by optical density OD_{600} (x-axis). For biofilm detection the plate was washed with PBS, treated with 0.01% crystal violet and measured at OD_{570} (y-axis). The results are depicted as scatter plot where each dot represents individual strain performance. Simple linear regression was applied with 95% confidence intervals (CI) (the dotted lines). The positive control (*S. epidermidis* 1457) consistently showed biofilm and growth values within the range of 0.8–1.2.

3.7 The effect of using bile salts with iron supplementation on *E. coli* biofilm formation

The synergistic effect of iron and bile salts was investigated for 24 *E. coli* isolates. Bile salts at 0.45% w/v were used with varying concentrations of iron supplementation (0.01-10µM) in LB media. Growth and biofilm formation were measured as previously described (section 2.5.6, 2.5.7.11) and presented as box and whisker plots (Figure 3.9).

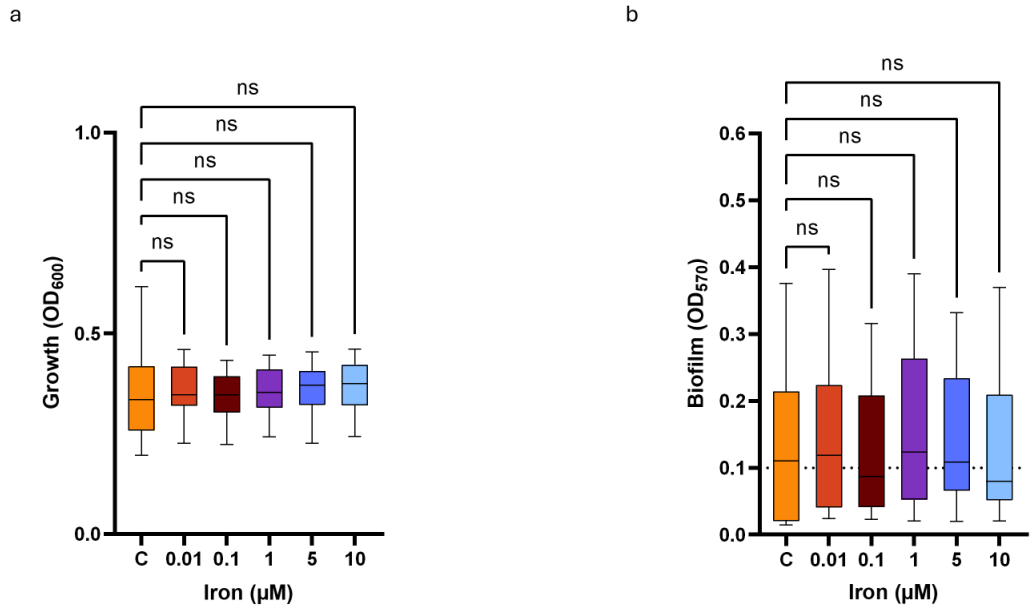

Figure 3.9 – Growth and biofilm formation with bile salts and iron.
E. coli isolates (n=24) were grown in LB with a bile salt supplementation of 0.45% w/v and a range of iron concentrations (0.01-10µM). Then, growth was assessed by optical density OD_{600} (a). For biofilm detection, the plate was washed with PBS, treated with 0.01% crystal violet and measured at OD_{570} (b). The results are depicted as box-and-whisker plots, where the boxes represent the median and interquartile ranges, and the whiskers indicate the minimum and maximum values. The dotted line represents the threshold of 0.1 showing a significant biofilm formation. "C" denotes the control sample, representing *E. coli* grown in LB with bile salts of 0.45% w/v and without iron supplementation. Data shown is based on minimum of 3 biological repeats and 2 technical repeats for each isolate. Statistical analyses were performed using the Kruskal-Wallis non-parametric test, with significance levels indicated as follows: ns = not significant. The positive control (*S. epidermidis* 1457) consistently showed biofilm and growth values within the range of 0.8–1.2.

The bile salt and additional iron combination (Figure 3.9) did not cause any significant changes in growth (Figure 3.9a) and biofilm formation (Figure 3.9b) when compared to the control. Considering the previous dose dependent effects of bile salts on biofilm formation and the importance of sequence type, the synergistic effect of additional iron was investigated

by comparing *E. coli* isolates grouped by sequence type (Figure 3.10) and origin of infection (Figure 3.11).

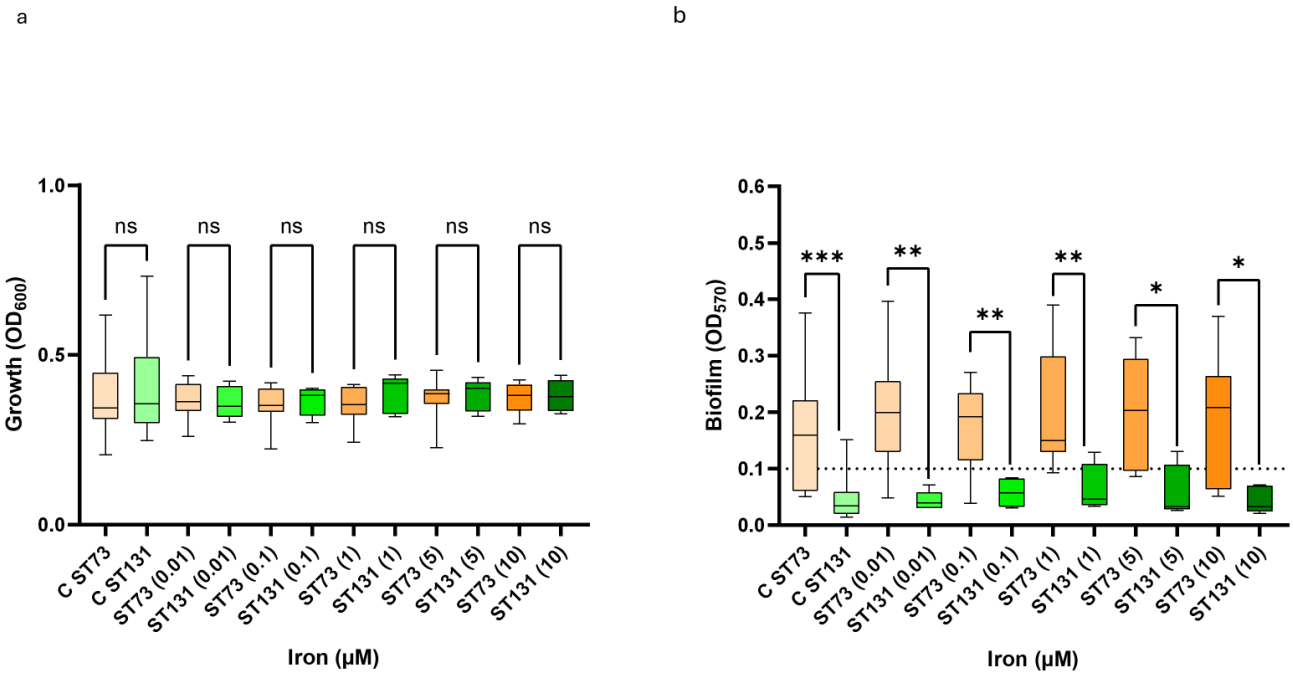

Figure 3.10 – *E. coli* growth and biofilm formation in ST73 and ST131 with bile salt and iron supplementation.
E. coli isolates (n=14) were grown in LB with bile salt supplementation of 0.45% w/v and a range of iron concentrations (0.01-10µM). Then, growth was assessed by optical density OD_{600} (a). For biofilm detection, the plate was washed with PBS, treated with 0.01% crystal violet and measured at OD_{570} (b). The results are depicted as box-and-whisker plots, where the boxes represent the median and interquartile ranges, and the whiskers indicate the minimum and maximum values. The dotted line represents the threshold of 0.1 showing a significant biofilm formation. "C" denotes the control sample, representing *E. coli* grown in LB with bile salts of 0.45% w/v and without iron supplementation. Data shown is based on minimum of 3 biological repeats and 2 technical repeats for each isolate. Statistical analyses were performed using multiple Mann-Whitney non-parametric tests, with significance levels indicated as follows: ns = not significant, * $p < 0.05$, ** $p < 0.01$, *** $p < 0.001$. The positive control (*S. epidermidis* 1457) consistently showed biofilm and growth values within the range of 0.8–1.2.

Sequence type analysis showed that ST73 was significantly superior in biofilm formation (Figure 3.10b) compared to ST131, but the results were independent of additional iron (0.01-10µM). Growth data (Figure 3.10a) also confirm limited effects of supplemented iron.

Furthermore, growth (Figure 3.11a) and biofilm formation (Figure 3.11b) were found to be independent of iron supplementation or the origin of infection.

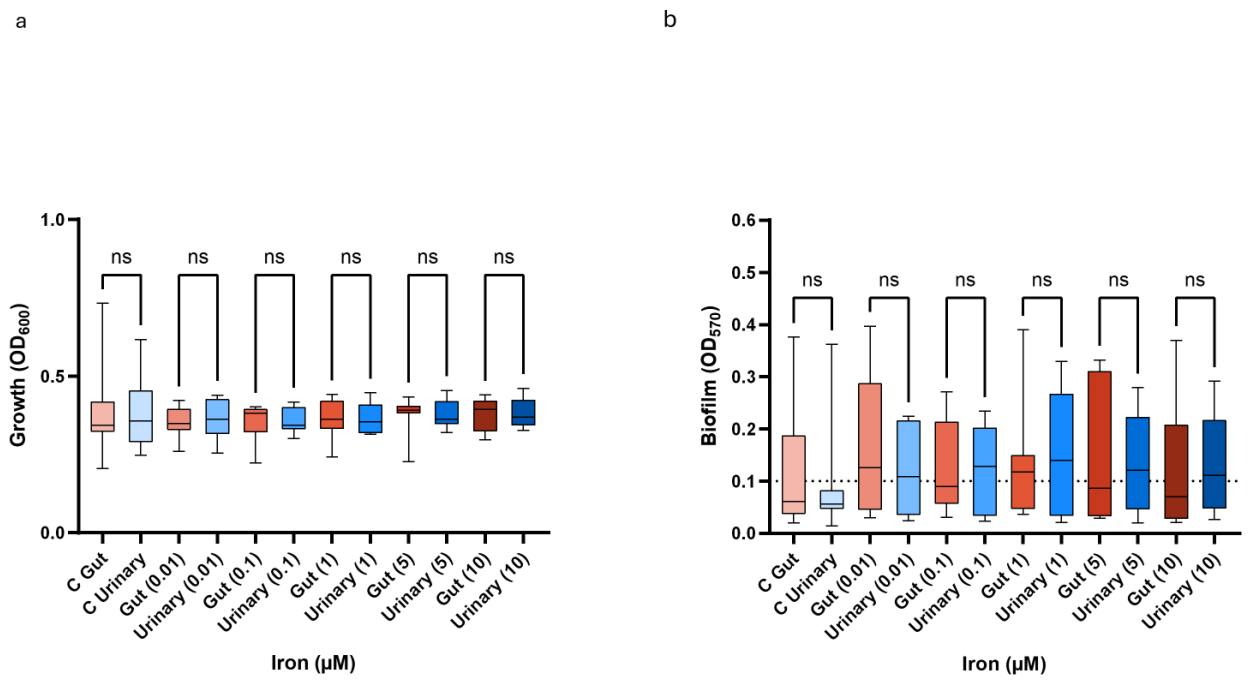

Figure 3.11 – *E. coli* isolate growth and biofilm formation comparison between gut and urinary origin of infection, with bile salt and iron supplementation.
E. coli isolates (n=16) were grown in LB with bile salt supplementation of 0.45% w/v and a range of iron concentrations (0.01-10µM). Then, growth was assessed by optical density OD_{600} (a). For biofilm detection, the plate was washed with PBS, treated with 0.01% crystal violet and measured at OD_{570} (b). The results are depicted as box-and-whisker plots, where the boxes represent the median and interquartile ranges, and the whiskers indicate the minimum and maximum values. The dotted line represents the threshold of 0.1 showing a significant biofilm formation. "C" denotes the control sample, representing *E. coli* grown in LB with bile salts of 0.45% w/v and without iron supplementation. Data shown is based on minimum of 3 biological repeats and 2 technical repeats for each isolate. Statistical analyses were performed using multiple Mann-Whitney non-parametric tests, with significance levels indicated as follows: ns = not significant. The positive control (*S. epidermidis* 1457) consistently showed biofilm and growth values within the range of 0.8–1.2.

3.8 The effects of bile salts and iron on biofilm formation and growth of individual *E. coli* isolates

Bacteraemia isolates treated with bile salts (0.45% w/v) and iron (0.01-10µM, n=24) were also analysed individually (Table 3.2) and their best biofilm formation performance was presented in a league table. Surprisingly, 16 isolates (67%) were biofilm positive (>0.1 threshold) and 4 isolates had significantly increased biofilm formation with iron supplementation (*) compared to control. Negative biofilm was observed in 8 isolates (33%), but 1 isolate demonstrated a

significant biofilm deposition increase (‘) in the presence of iron. In addition, 4 isolates (purple) produced positive biofilm due to iron supplementation (previously were below 0.1 absorbance value in Table 3.1).

Table 3.2 – Biofilm formation of individual *E. coli* isolates with bile salt and iron supplementation. *E. coli* isolates (n=24) were grown in LB with bile salt supplementation of 0.45% w/v and a range of added iron concentrations (0.01-10µM). For biofilm detection the plate was washed with PBS, treated with 0.01% crystal violet and measured at OD_{570} (third column). The first column indicates isolate ID. The second column indicates additional iron concentration (µM) in LB medium. The fourth and fifth columns depict the sequence type and origin of infection, respectively. A threshold absorbance of 0.1 was used to define a biofilm positive phenotype (horizontal double line). Statistical analyses were performed using the Kruskal-Wallis non-parametric test. Statistical significance is indicated as follows: * = biofilm value significantly increased with bile salt supplementation in biofilm positive isolates, ‘ = biofilm deposition significantly increased with bile salt supplementation in biofilm negative isolates. Purple cells – isolates did not produce positive biofilm before iron supplementation.

Isolate ID	Added iron concentration (µM)	CV assay result	Sequence type	Site of infection
4	0.01	0.397	73	Gut
15	1	0.390	73	Gut
K12	0.01	0.354	10	Lab strain
20*	1	0.332	2628	Other
172	1	0.330	73	Urinary
ANC3	0.01	0.311	N/A	ANC Urine
62*	1	0.269	73	Urinary
87*	1	0.267	404	Urinary
77	1	0.253	73	Urinary
45	0.1	0.234	73	Urinary
39	1	0.150	73	Gut
27	0.01	0.134	73	Gut
103*	5	0.131	131	Urinary
94	5	0.113	1205	Water
38	0.01	0.112	131	Gut
47	5	0.106	73	Urinary
CFT073	1	0.088	73	Control urosepsis isolate
ANC4	0.01	0.088	N/A	ANC Urine
91	5	0.064	4118	Water
113	0.1	0.057	131	Gut
69	5	0.053	7497	Urinary
110'	1	0.047	131	Gut
67	0.01	0.037	429	Urinary
102	0.1	0.035	131	Urinary

In summary, of the biofilm positive isolates (n=16), 9 were identified as ST73 (56%), while only 2 isolates (12%) were ST131 isolates. Gut origin of infection was identified in 5 isolates (31%) and urinary in 7 isolates (43%). Biofilm negative isolates (n=8) did not contain a single ST73 bacteraemia isolate, while there were three (38%) ST131 isolates, two gut isolates (25%) and three urinary origin of infection isolates (38%).

Finally, given the paired growth and biofilm data, a relationship between these parameters was investigated (Figure 3.12). The linear regression model showed that it was not statistically significant (P = 0.3745 and R^2 = 0.03601) suggesting that growth was not a significant predictor in biofilm formation with bile salt and iron supplementation.

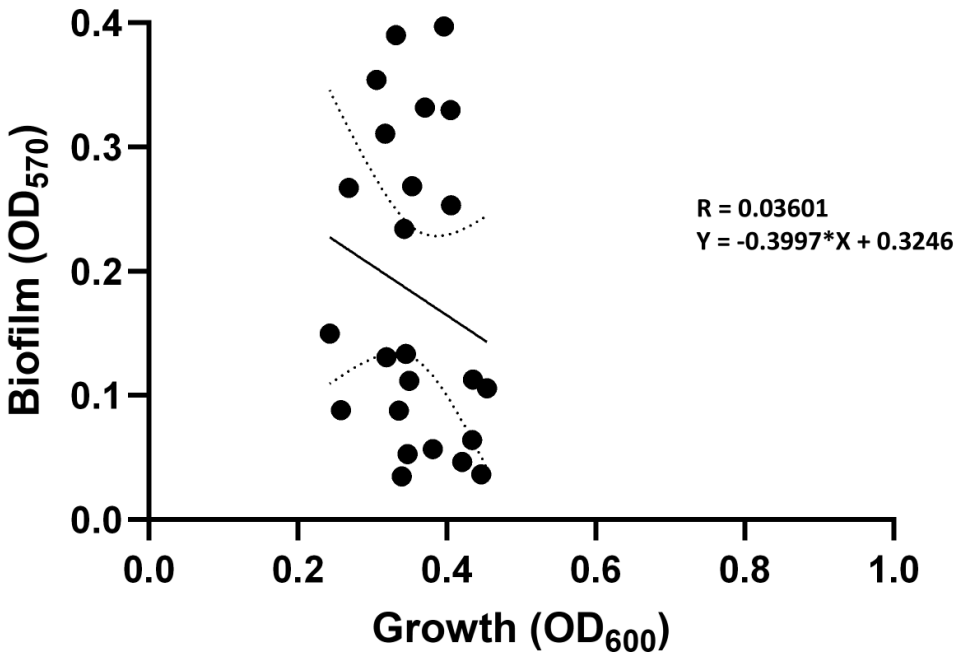

Figure 3.12 – Individual strain growth and biofilm formation with bile salt and iron supplementation. *E. coli* isolates (n=24) were grown in LB with bile salt supplementation of 0.45% w/v and a range of iron concentrations (0.01-10µM). Then, growth was assessed by optical density OD_{600} (x-axis). For biofilm detection, the plate was washed with PBS, treated with 0.01% crystal violet and measured at OD_{570} (y-axis). The results are depicted as a scatter plot where each dot represents individual strain performance. Simple linear regression line was applied with 95% confidence intervals (CI) (the dotted lines). The positive control (S. epidermidis 1457) consistently showed biofilm and growth values within the range of 0.8–1.2.

3.9 Genetic analysis of biofilm and bile salt resistance associated genes

Following biofilm assay analysis, the biofilm formation and bile resistance associated genes were investigated in all *E. coli* bacterial isolates as described previously (Section 2.6.1) using previously acquired annotated genomic data (272). Direct and indirect genes involved in biofilm formation and bile salt resistance were selected (Table 3.3)(280-286). This analysis compares biofilm-positive versus biofilm-negative isolates (Table 3.4) and ST73 versus ST131 isolates (Table 3.5). In addition, the corresponding heatmaps confirm the global presence and absence of genes (appendix 1.4, 1.5).

Table 3.3 – The selected direct and indirect biofilm and bile salt resistance gene list.

Biofilm genes	Encoded proteins	Function	References
DIRECT			
fimAICDFGH	Type 1 fimbriae regulatory proteins	Type 1 Fimbriae (also called pili) synthesis, enable bacteria to colonize the epithelium of specific host organs	(182, 196, 225, 235, 236, 244, 255)
pgaABCD	Poly-β-1,6-N-acetyl-D-glucosamine	Synthesis of PGA polymers that helps in biofilm adhesion	(182, 196, 235, 236, 244)
hha	Haemolysin expression modulating protein Hha	Repress the transcription of fimbrial genes thereby decreasing biofilm formation	(196, 225)
bcsABZC and *bcsEFG* operons	Cellulose synthase catalytic subunit	Catalyses the formation of cellulose which is an extracellular component for mechanical and chemical protection of the cell	(182, 196, 244)
kpsMTII	ABC transporter permease	Encodes proteins conducting the polymer translocation to the cell surface; capsular polysaccharide synthesis K1	(244, 260)
afa	Afimbrial adhesin AFA-I	These adhesins bind to the Dr blood group antigen and also agglutinate human erythrocytes in the presence of D-mannose.	(235, 244, 255)
csgGFED and *csgBAC* operons	CsgBAC operon transcriptional regulatory protein	Synthesis and assemblence of Curli fimbriae.Involved in cellulose synthesis.	(182, 196, 225, 235, 236, 244)
RcsCDB regulator	the RcsC, RcsB, and RcsD proteins	Synthesis of the capsule, regulate the synthesis of the Colanic Acid and the expression of some genes related to the synthesis of the flagella and adhesion structures such as curli and Ag43	(182, 235, 236, 244)
flu	Antigen 43	Adhesin protein that helps in auto-aggregation	(178, 192, 203, 220, 221, 229)
INDIRECT			
tolC	Outer membrane channel (TolC)	Major channel for drug efflux across the outer membrane of E. coli, involved in the transportation of various types of chemicals, leading to bacterial antimicrobial resistance	(182, 235, 236, 246, 264, 280)
luxS	S-ribosylhomocysteine	Synthesises autoinducer substances (furanosyl borate diester). Stimulates biofilm formation and controls the biofilm architecture	(182, 196, 225, 235, 236)
qseBC	Transcriptional regulatory protein QseB; Sensor protein QseC	Response regulator in flagella synthesis as it activates transcription of FlhDC and regulates motility.	(182, 196, 225, 235, 236)
flhDC	Flagellar transcriptional regulator FlhD, FlhC	flagellar master operon. Sigma factor that activates the class 3 flagellum operons. Component of Flagellar Motor Complex	(182, 196, 225, 235, 236)
fliA	RNA polymerase sigma factor FliA	Sigma factor that activates flagella gene transcription	(182, 196, 225, 235, 236, 285)
motA	Motility Protein A	Flagellor stator which regulates rotation	(182, 196, 225, 235, 236, 285)
rpoS	RNA polymerase Sigma factor RpoS	Regulating genes and structural proteins involved in the synthesis and degradation of biofilm, under stress conditions	(182, 196, 225, 226, 234-236)
hfq	RNA-binding protein Hfq	Stabilizes to small regulatory RNA in response to stress and stress responses mediated by the sigma factors RpoS	(196, 225, 244)
BILE RESISTANCE			
emrAB	Multidrug export (emr) proteins	EmrAB-TolC multidrug efflux transport system	(182, 281, 284)
macAB	Macrolide export (mac) proteins	MacAB-TolC macrolide efflux transport system	(281)
mdtAEF	Multidrug export (mdt) proteins	MdtABC-TolC multidrug efflux transport system	(182, 281)
acrDEF	Aminoglycoside efflux pump, multidrug eflux (ecr) proteins	AcrEF-TolC multidrug efflux transport system	(182, 225, 235, 280, 281, 282, 284, 285)
fadHE	reductase and dehydrogenase	involved in fatty acid degradation	(280)
marRAB	Multiple antibiotic resistance (mar) proteins	Multiple antibiotic and bile resistance	(282, 285)
yojI	ABC transporter ATP-binding/permease	An efflux pump for microcin J25, with the help of the outer membrane channel TolC.	(285)
bsh	bile salt hydrolase	Acts as a bile salt hydrolase that catalyzes the deconjugation of glycine- and taurine-linked bile salts	(286)

For the biofilm positive versus negative analysis, all isolates contained the following genes: *csgA*; *csgC*; *csgE*; *csgF*; *csgG*; *fimF*; *fimG*; *flhC*; *fliA*; *hfq*; *hha*; *luxS*; *motA*; *rcsC*; *macA*; *emrA*; *yojI*; *marR*; *marA*; *emrB*; *mdtA*; *mdtE*; *mdtF*; *fadH_1*; *fadE* and none of the isolates contained the *kpsMSTII* and *bsh* genes. Therefore, those genes were not included in the analysis and the heatmaps. All other genes, including gene variants, had presence between 0% and 100% throughout 43 isolates.

Out of 61 identified genes (Table 3.4), 8 (13%) had higher incidence in biofilm positive isolates while 3 (5%) had higher incidence in biofilm negative isolates. Type 1 fimbriae genes, *FimACDFGHI* showed higher incidence in biofilm positive isolates. In addition, *rcsA*_1 and *acrE* had a higher incidence in biofilm positive isolates, while *flu*, *hha_2* and *pgaC* had higher incidence in biofilm negative isolates.

Table 3.4 – Biofilm positive and biofilm negative isolate gene profile comparison.
The pre-existing gene presence/absence table was used to investigate biofilm and bile resistance genes. The first column shows genes associated with biofilm formation or bile resistance. The second and third columns show the percentage and number of isolates, respectively, with the specific gene in biofilm positive isolates. The fourth and fifth columns show the percentage and number of isolates, respectively, with the specific gene in biofilm negative isolates. Gold colour indicates 25% or more higher gene presence percentage in biofilm positive isolates. Aqua colour indicates 25% or more higher gene presence percentage in biofilm negative isolates.

Gene	Biofilm positive, percentage (%) and number of isolates		Biofilm negative, percentage (%) and number of isolates	
afaD	6.70%	1/15	17.90%	5/28
afaD_2	0%	0/15	3.60%	1/28
afaE3	6.70%	1/15	3.60%	1/28
bcsA	66.70%	10/15	82.10%	23/28
bcsB	86.70%	13/15	78.60%	22/28
bcsB_1	0%	0/15	3.60%	1/28
bcsC	93.30%	14/15	92.90%	26/28
bcsF	100%	15/15	96.40%	27/28
bcsG	66.70%	10/15	78.60%	22/28
bcsG_1	0%	0/15	21.40%	6/28
bcsZ	100%	15/15	96.40%	27/28
csgB	100%	15/15	96.40%	27/28
csgD	80%	12/15	89.30%	25/28
fimA_1	26.70%	4/15	21.40%	6/28
fimA_2	86.70%	13/15	92.90%	26/28
fimA_3	13.30%	2/15	0%	0/28
fimB	66.70%	10/15	75%	21/28
fimB_2	86.70%	13/15	85.70%	24/28
fimC_1	80%	12/15	96.40%	27/28
fimC_2	93.30%	14/15	96.40%	27/28
fimC_3	0%	0/15	7.10%	2/28
fimC_4	66.70%	10/15	17.90%	5/28
fimD_1	60%	9/15	67.90%	19/28
fimD_2	86.70%	13/15	85.70%	24/28
fimD_3	66.70%	10/15	25%	7/28
fimE	86.70%	13/15	100%	28/28
fimF_1	6.70%	1/15	7.10%	2/28
fimF_2	60%	9/15	25%	7/28
fimG_2	46.70%	7/15	10.70%	3/28
fimH	93.30%	14/15	96.40%	27/28
fimH_2	53.30%	8/15	14.30%	4/28
fimI	93.30%	14/15	96.40%	27/28
fimI_2	66.70%	10/15	17.90%	5/28
flhD	100%	15/15	96.40%	27/28
fliA_2	20%	3/15	35.70%	10/28
flu	20%	3/15	60.70%	17/28
flu_1	20%	3/15	32.10%	9/28
flu_2	20%	3/15	3.60%	1/28
flu_3	6.70%	1/15	7.10%	2/28
hha_2	6.70%	1/15	35.70%	10/28
motA_2	20%	3/15	35.70%	10/28
pgaA	93.30%	14/15	89.30%	25/28
pgaB	86.70%	13/15	75%	21/28
pgaC	33.30%	5/15	64.30%	18/28
pgaD	100%	15/15	92.90%	26/28
qseC	100%	15/15	96.40%	27/28
rcsA	93.30%	14/15	92.90%	26/28
rcsA_1	66.70%	10/15	35.70%	10/28
rcsB	46.70%	7/15	25%	7/28
rcsD	80%	12/15	92.90%	26/28
rpoS	93.30%	14/15	82.10%	23/28
tolC	66.70%	10/15	75%	21/28
tolC_2	0%	0/15	14.30%	4/28
fadH_2	86.70%	13/15	85.70%	24/28
acrF	93.30%	14/15	100%	28/28
acrD	86.70%	13/15	96.40%	27/28
acrE	80%	12/15	53.60%	15/28
emrB_1	80%	12/15	78.60%	22/28
macB	93.30%	14/15	96.40%	27/28
macA_2	6.70%	1/15	7.10%	2/28
marB	100%	15/15	96.40%	27/28

For the ST73 versus ST131 analysis, all isolates contained the following genes: *csgA*; *csgC*; *csgE*; *csgF*; *csgG*; *fimF*; *fimG*; *flhC*; *fliA*; *hfq*; *hha*; *luxS*; *motA*; *rcsC*; *macA*; *emrA*; *yojI*; *marR*; *marA*; *emrB*; *mdtA*; *mdtE*; *mdtF*; *fadH_1*; *fadE* and none of the isolates contained the *afaD_2*, *afaE3*, *bcsB_1*, *fimC_3, fimF_1*, *tolC_2*, *kpsMSTII* and *bsh* genes. Therefore, those genes were not included in the analysis and the heatmaps. All other genes, including gene variants, had presence between 0% and 100% throughout 26 isolates.

Analysing ST73 and ST131 isolates, 55 genes were identified (Table 3.5) and 11 genes (20%) were found to have higher incidence in ST73 isolates, while 7 genes (13%) had higher incidence in ST131 isolates. *FimCDFGHI* genes had higher incidence in ST73 isolates, while *fimB* had higher incidence in ST131 isolates. Furthermore, the *rcsA_1*, *rcsB* and *acrE* had higher incidence in ST73 isolates, whereas *bcsG_1*, *fliA_2*, *flu/_1*, *motA_2* and *pgaC* showed higher incidence in ST131 isolates. Most importantly, *fimC_4*, *fimD_3*, *fimF_2*, *fimI_2*, *rcsA_1*, *rcsB* and *acrE* genes had extremely higher incidence (80%+ versus 0%) in ST73 compared to ST131, but *pgaC* had an extremely higher incidence in ST131 compared to ST73.

Table 3.5 – ST73 versus ST131 biofilm related and bile resistance gene comparison.
The pre-existing gene presence/absence table was used to investigate biofilm and bile resistance genes. The first column shows genes associated with biofilm formation or bile resistance. The second and third columns show the percentage and number of isolates, respectively, with the specific gene in ST73 isolates. The fourth and fifth columns show the percentage and number of isolates, respectively, with the specific gene in ST131 isolates. Green colour indicates 25% or more higher gene presence percentage in ST73 isolates. Blue colour indicates 25% or more higher gene presence percentage in ST131 isolates.

Gene	ST73, percentage (%) and number of isolates		ST131, percentage (%) and number of isolates	
afaD	0%	0/13	23.10%	3/13
bcsA	92.30%	12/13	100%	13/13
bcsB	84.60%	11/13	92.30%	12/13
bcsC	92.30%	12/13	100%	13/13
bcsF	92.30%	12/13	100%	13/13
bcsG	100%	13/13	92.30%	12/13
bcsG_1	0%	0/13	46.20%	6/13
bcsZ	92.30%	12/13	100%	13/13
csgB	100%	13/13	100%	13/13
csgD	84.60%	11/13	76.90%	10/13
fimA_1	46.20%	6/13	23.10%	3/13
fimA_2	84.60%	11/13	100%	13/13
fimA_3	7.70%	1/13	0%	0/13
fimB	30.70%	4/13	84.60%	11/13
fimB_2	100%	13/13	100%	13/13
fimC_1	92.30%	12/13	100%	13/13
fimC_2	92.30%	12/13	100%	13/13
fimC_4	84.60%	11/13	0%	0/13
fimD_1	92.30%	12/13	38.50%	5/13
fimD_2	100%	13/13	69.20%	9/13
fimD_3	92.30%	12/13	0%	0/13
fimE	92.30%	12/13	92.30%	12/13
fimF_2	84.60%	11/13	0%	0/13
fimG_2	69.20%	9/13	0%	0/13
fimH	84.60%	11/13	100%	13/13
fimH_2	69.20%	9/13	0%	0/13
fimI	84.60%	11/13	100%	13/13
fimI_2	84.60%	11/13	0%	0/13
flhD	92.30%	12/13	100%	13/13
fliA_2	0%	0/13	46.20%	6/13
flu	30.80%	4/13	76.90%	10/13
flu_1	30.80%	4/13	61.50%	8/13
flu_2	15.40%	2/13	7.70%	1/13
flu_3	15.40%	2/13	0%	0/13
hha_2	23.10%	3/13	30.80%	4/13
motA_2	0%	0/13	46.20%	6/13
pgaA	100%	13/13	92.30%	12/13
pgaB	69.20%	9/13	92.30%	12/13
pgaC	0%	0/13	100%	13/13
pgaD	100%	13/13	100%	13/13
qseC	100%	13/13	100%	13/13
rcsA	84.60%	11/13	100%	13/13
rcsA_1	100%	13/13	0%	0/13
rcsB	100%	13/13	0%	0/13
rcsD	100%	13/13	100%	13/13
rpoS	92.30%	12/13	100%	13/13
tolC	69.20%	9/13	76.90%	10/13
fadH_2	100%	13/13	100%	13/13
acrF	100%	13/13	100%	13/13
acrD	100%	13/13	92.30%	12/13
acrE	84.60%	11/13	0%	0/13
emrB_1	100%	13/13	100%	13/13
macB	92.30%	12/13	100%	13/13
macA_2	0%	0/13	7.70%	1/13
marB	100%	13/13	100%	13/13

3.10 CLSM biofilm visualization and data analysis

Live biofilm formation was investigated, and additional analysis were done using CLSM in a subset of chosen strains (Table 3.6). The sample preparation, imaging and analysis were performed as described previously (Section 2.6.2). The biofilm images were studied (Figure 3.13c), and image analysis using COMSTAT tool confirmed biofilm biomass (Figure 3.13a) and biofilm thickness (Figure 3.13b) measurements.

Table 3.6 – Isolates for CLSM biofilm visualisation and analysis.
E. coli isolates (n=7) were grown in LB with bile salt supplementation (0.45% w/v) over 24 hours. For biofilm imaging, the media was removed, samples were treated with 0.5% live/dead stain and imaged using Zeiss LSM980 CLSM with a x63 objective lens under oil immersion. The yellow colour indicates biofilm positive samples, red colour indicates biofilm negative samples. CFT073 was used as control.

Isolate ID	Sequence type	Site of infection
4	73	Intra-abdominal
45	73	Urinary
K12 (lab)	10	Lab strain
94	1205	Water
102	131	Urinary
103	131	Urinary
CFT073	73	Control urosepsis isolate

Biofilm biomass measurements (Figure 3.13a) revealed that K12 (biofilm positive) and isolate 103 (biofilm negative) were significantly higher than CFT073, which was used as a control isolate. Subsequently, biofilm thickness measurements (Figure 3.13b) showed that K12 and isolate 45 (both biofilm positive) were significantly higher than CFT073 control isolate.

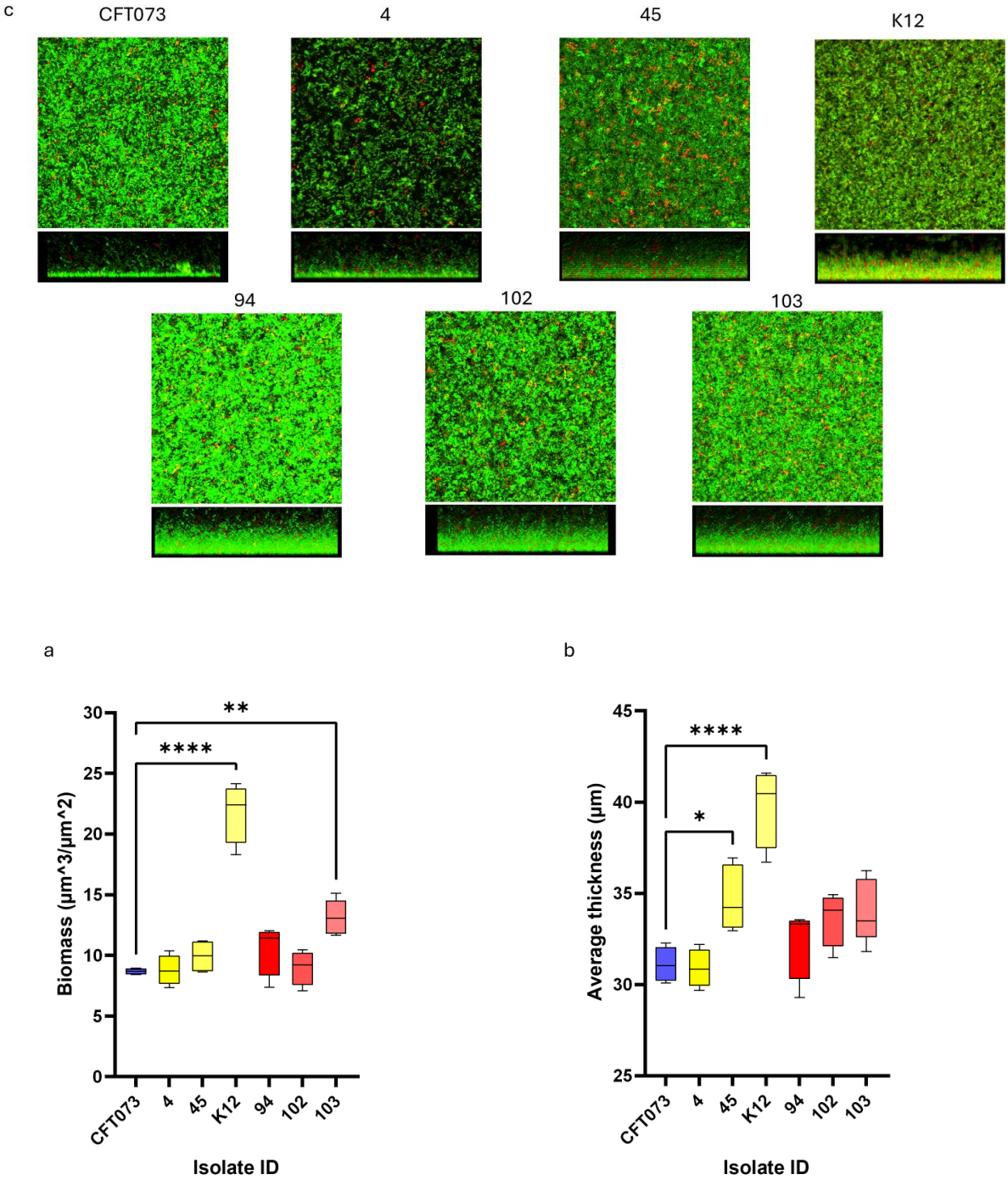

Figure 3.13 – Live biofilm formation and comparison between biofilm positive and biofilm negative isolates.

E. coli samples (n=7) were grown in LB with bile salt supplementation over 24 hours. For biofilm imaging, the media was removed, samples were treated with 0.5% live/dead stain and imaged using Zeiss LSM980 CLSM with a x63 lens under oil immersion (c). Biofilm biomass (a) and thickness (b) measurements were analysed using COMSTAT analysis tool. The results are depicted as box-and-whisker plots, where the boxes represent the median and interquartile ranges, and the whiskers indicate the minimum and maximum values. Statistical analyses were performed using one-way ANOVA with repeated measures, with significance levels indicated as follows: * $p < 0.05$, ** $p < 0.01$, *** $p < 0.001$, **** $p < 0.0001$.

4 Discussion

This project was designed to investigate the optimal conditions for growing biofilms in a collection of clinically relevant ExPEC strains taken from bacteraemia patients in the local Hywel Dda University Health Board. Following the screening of conditions that produced *E. coli* biofilm formation, phenotypic and DNA sequence metadata associated with the isolates was used to group isolates to investigate their role in biofilm formation. Finally, in a subgroup of isolates with defined biofilm properties, CLSM was used to visualise and evaluate their structural properties.

4.1 Growth and biofilm formation utilising different physiological and mechanical parameters

Growth results were consistent with previous literature as LB, TSB+G and EC broths are widely used with *E. coli* and showed strong growth here (270, 287, 288). The PBS+LB, M9 and Leibovitz's results were also higher than all the blank media averages at an OD_{600} = 0.3 value, which is considered sufficient growth for *E. coli* (289). The different parameters used to determine optimal conditions for forming *E. coli* biofilms showed interesting results. In total, 84 different configurations were tested between different parameters (Table 2.3) including the media changes. This produced a significant amount of screening data, although most parameters tested used a limited number of strains (N=6), with only one shown to be biofilm positive (isolate 61). As previous research has reported inconsistencies concerning the benefits of agitation for biofilm development (263, 286, 290), the shaking methods were an important study variable in the current research. The gentle agitation that was used in this project (20 rpm) was not a suitable representation of the shear stress *E. coli* receives in the human body but a good indication to showcase the impact it has in a medical setting, such as simulating hydrodynamic conditions in urinary catheters or different parts of circulatory system around the body (291). Despite that, the impact was fairly limited, as none of the shaking methods showed higher biofilm development and so circular shaking was selected as convenient shaking method (290). Overall, the screening showed that none of the conditions had enough impact to push the average biofilm formation beyond the threshold of OD_{570} = 0.1, but EC broth gave some indication of biofilm in some isolates and the bile salt effect was investigated using this *E. coli* biofilm definition.

Despite decades of studies exploring biofilm formation and development in *E. coli*, the definition for a positive biofilm in the standardised crystal violet assay is not established. This is not surprising given the complex requirements and stresses needed for biofilm formation in *E. coli* and its ability to adhere to tube walls. The majority of *E. coli* studies use $OD_{570}/_{590}$ = 0.2 as a cut-off to determine a biofilm positive strain. This measurement is likely related to *S. aureus* studies, which adhere to the bottom of microtiter plates (251, 292, 293), making it less than a viable comparison. Furthermore, a large number of *E. coli* biofilm studies use ethanol or acetic acid, or a combination of other solvents to solubilise the final fixed biofilm on the sides of the well (265, 268, 270, 294), simplifying the quantification of biofilm and optimising the assay to "standard" microtiter plates for easier comparison. The measurement that was used in this study (OD 0.1) is also consistent with previous work as there are a plethora of studies utilising this measurement (277, 295). Taking the nature of *E. coli* biofilms and the validity of quantification into account, it seemed the best choice for meaningful results. In addition, using 0.01% crystal violet ensured the validity of biofilm formation at OD 0.1 (266) by significantly lowering the concentrations of dye used increasing the stringency of biofilm detection.

4.2 Biofilm formation in *E. coli* and other pathogens, the bile salts effect, and the influence of iron

The bile salt addition to the EC broth as a selective method to inhibit Gram-positives, especially for bacilli and faecal streptococci, led us to significantly higher quantities (296, 297), and the induced biofilms in *E. coli* showcased some interesting results. The strongest biofilms were observed in the highest concentration tested, suggesting that even higher concentrations could potentially induce more biofilm. However, the growth results show that even 0.45% w/v concentration reduced the bacterial population to minimal amounts for survival (289). In addition, despite TSB+G broth with bile salts showing higher biofilm formation at 0.45% w/v concentration (Figure 3.4), the LB broth was selected due to having more literature relevance for usage in *E. coli* (236, 249, 298). Other studies have also identified that bile salts influence biofilm formation in *E. coli*. In a Brazilian study, when 0.015% (w/v) bile salts were added to the media, the average OD values were decreased and only 2 strains managed to form strong to moderate biofilms (299), while other studies showed a very significant biofilm increase in commensal and pathogenic *E. coli* when supplemented with

0.4% (w/v) bile salts ((286, 300). Studies with other bacteria like *Cronobacter malonaticus*, *Shigella spp*. had varying results. Bile salts did not induce biofilm formation in *Cronobacter malonaticus* but biofilm development was significantly increased in a *tolC* gene deletion mutant at 0.02% (w/v) of bile salts, while *Shigella* spp. had a significant increase in biofilm formation with 0.4% (w/v) bile salt supplementation (300, 301).

One of the most fascinating results in this work is the ST73 biofilm formation disparity compared to ST131 isolates. While there has been some discussion about ST131 biofilm formation (260-262), very minimal literature discussed biofilm formation in ST73 isolates. Despite this, the ST73 isolates showed much higher biofilm formation compared to ST131, while growth was equivalent.

Iron has a significant influence in ExPEC growth and pathogenesis (120, 121, 123) but the observed effect on biofilm formation was weak. Despite conflicting literature (269, 270), iron was expected to inhibit biofilm formation due to its reduction of growth, (e.g. LB broth + 5 µM iron, figure 3.5a), or promote biofilm formation to showcase better resistance to environmental stressors (120, 121). Although several isolates managed to reach biofilm positive threshold due to additional iron in bile salts + iron combination, the iron only supplementation did not lead to any differences in growth and biofilm.

The deposition of EPS was significantly different, spatially and synthetically, between *S. epidermidis* (and *S. aureus*) compared to *E. coli* (302-305). Initial laboratory observations following preculture confirmed that *S. epidermidis* generated robust biofilms on the bottom of bijou tubes, whereas *E. coli* generated surface biofilms producing a ring at the surface interface with the tube. Furthermore, when bottom-generated biofilms were compared *S. epidermidis* generated OD570 readings at ~1.0 whereas *E. coli* that did produce biofilm had OD570 readings ~0.2-0.4.

It is clear that there are important differences in the synthetic requirements or stimuli needed for biofilm production in *S. epidermidis* versus *E. coli*. Specifically in *S. epidermidis* 1457, glucose, salt, tricarboxylic acid cycle stress and even low concentrations of ethanol and antibiotics induce biofilm (302-307). In striking contrast, mechanical stress, changes in osmolality, nutrient limitation, and bile salts are vital to biofilm induction in *E. coli* (246, 286, 308, 309).

4.3 *E. coli* genes important for biofilm formation

The results of the gene presence/absence experiments confirm the significant complexity associated with biofilm formation in ExPEC. This study focused on genes known to be associated with biofilm formation (61, 182, 196, 234, 244) and was not an exhaustive list. However, some clear observations were reported. Whilst comparing biofilm positive against biofilm negative phenotypes for relevant genes showed some differences, the significant increase in biofilm formation in ST73 versus ST131 isolates seemed more important. Tables and heatmaps clearly demonstrate the complete absence of *rcsA* and *rcsB* in ST131 isolates compared to a presence in ST73 isolates. This is consistent with a role for capsule and colonic acid production in biofilm formation (182, 244, 259). While not quite as dramatic, increased expression of *fimG*, *fimF*, *fimH* and *fimI* are also increased in ST73 compared to ST131 isolates, confirming a role for adhesins (182, 196, 214, 235, 236, 244, 255). In addition, The ST131 isolates' inability to form biofilms could be attributed to the missing *kpsMSTII* gene, as it was absent in all isolates, while the gene has been identified as a major contributor to successful biofilm formation in ExPEC (260).

The results also yielded some surprising outcomes including the complete absence of *pgaC* in ST73 isolates. Considering that characterisation studies focused on the roles of the *pgaADBC* operon confirm that *pgaA* and *pgaC* are required for biofilm production our observation is compelling (182, 245). One exciting possibility is that ST73 isolates do not form polysaccharide-based biofilm and therefore rely on other mechanisms, such as protein based or DNA products to produce their EPS (241). Another more likely scenario is that *E. coli* might use competing polysaccharide-based mechanisms (*pgaADBC* vs *rcs* / colonic acid / cellulose, polysialic acid) to generate biofilm with the systems substituting for one another if required. To our knowledge there are limited studies on the molecular characterisation of EPS in *E. coli* (310-312).

4.4 Differences in methods to study biofilm formation

The Confocal Laser Scanning Microscopy images showed clear evidence of biofilm stained with live/dead dye. The measurements obtained from CLSM images showed that biofilm negative, ST131 isolate 103 had higher biomass than the biofilm positive, ST73 isolates 4 and 45. Furthermore, average thickness calculations also showed isolate 103 having much higher

thickness than isolate 4. Looking at the gene presence/absence of genes, these differences could be attributed to *bcsG*, *flu* and *pgaC* genes absence in isolates 4 and 45 compared to isolate 103. The *bcsG* and *pgaC* genes are known to promote cellulose synthesis and PGA polymerisation respectively, significantly impacting biofilm formation (182, 196, 235, 236, 244). These results show that live biofilm measurements can contradict the standard biofilm crystal violet assay. The differences identified could be due to crystal violet staining not only the biomass of the cells in the biofilm but also the surrounding EPS as well. Since only live/dead stain without EPS probing was used for CLSM imaging, this could potentially relate to similar biofilm biomass between biofilm negative and biofilm positive isolates. In addition, the lack of variants of *fimACDFGHI* genes in 103 isolate, could influence the low biofilm OD_{570} value in the biofilm assay. The *fim* genes responsible for adhesion to the surface can complicate the robustness of biofilms during the multiple washes in the crystal violet method, resulting in disruption of biofilms (313-315). Another reason for the disparity in results could be the material used to establish the biofilms. For crystal violet assay, plastic based microtiter plates were used, whereas CLSM required glass-bottomed plates. It has been noted, that glass has an impact in cell adhesion and biofilm formation in *E. coli* strains, which could explain isolate 4 showing decreased biofilm due to being more reliant on *fim* gene adhesion mechanisms to form biofilms (316).

The crystal violet assay has been a preferred method of choice for decades in biofilm studies (236, 249). It has a lot of advantages, such as ease of handling, cost-effectiveness, relatively short time requirement, suitability for early-stage biofilm formation, such as screening, and lab-scale research. There are however several drawbacks of using crystal violet assay, such as inconsistencies between samples, showing false-positive results in specific scenarios, inaccurate quantification in multi-species biofilms and for weaker biofilms, the amount of washing can disrupt the biofilms completely, especially since *E. coli* can bind to the sides of the well rather than to the bottom of a 96-well plate so fixation becomes important (249, 313-315). Most of these limitations can be altered by using CLSM live biofilm imaging, which provide real-time visualisations and easy to use quantification tools for measurement analysis (199, 290). However, CLSM microscopes are very expensive as they require some specific equipment, and the quality of the data and images relies heavily on the user being able to correctly perform the required tasks and is very time-consuming (249, 317). In addition, the

crystal violet assay usually stains not just the cellular components of the biofilms but the surrounding EPS as well. This is usually not the case for CLSM, as there aren't any universal EPS staining methods determined, but numerous methods are available to characterise the properties of EPS (236, 318).

4.5 Physiological and clinical relevance, biofilm formation on pathogenesis and host-pathogen interactions

One major strength of this work is the novelty associated with the characterisation of a collection of *E. coli* bacteraemia isolates. The isolates are a novel collection with associated meta data ranging from laboratory data to clinical patient data. This was useful in assigning groups in analysis post biofilm assay measurement although we did not find any differences. A further strength of this work used iron and bile salts in physiological levels of human body. Since iron levels in plasma are maintained in the range of 10 – 30 µM, although most of it is sequestered to other molecules, and the concentration of bile salts in the small intestine ranges from approximately 0.2 to 2% (w/v) (319, 320).

The ability to form biofilms has long been associated with pathogenesis of bacteria, including *E. coli* (174, 321). The exact impact of biofilm formation in ExPEC strains is still unknown but given the beneficial mechanisms it provides in survival and antimicrobial resistance it is fair to conclude that the role is substantial (187, 191-193). A study using biofilm formation as a predictive marker for patient prognosis in sepsis concluded that biofilm forming *E. coli* strains had increased pathogenicity compared to non-formers (271). As the authors mention, this needs to be confirmed with a prospective study, but it provides a glimpse into biofilm forming *E. coli* capabilities. In addition, biofilm contributes to evasion of host immune system subsequently altering host-pathogen interaction (182, 187, 196)

This work did not study the effect of the host on biofilm formation and vice-versa. However, future work should investigate the role of biofilm producing *E. coli* on the host, specifically in epithelial cells or in whole blood. Bacterial infections with *E. coli* are commonly linked with pathogen associated molecular patterns (PAMPs) being recognised by pattern recognition receptors (PRRs) that subsequently induce damage associated molecular patterns (DAMPs), which can activate PRRs and recognise PAMPs, starting a vicious cycle promoting a sustained immune response. (2, 322). These mechanisms trigger signal transduction pathways leading

to pro-inflammatory cytokines, such as tumour necrosis factor (TNF), interleukin-1β (IL-1β), IL-12 and IL-18 (6, 323, 324). Recent studies in our laboratory also show that the host's immune response differs based on bacterial genera, species and even strains (325). Macrophage inflammatory protein 3α (MIP-3α) and IL-6 were significantly increased in response to *E. coli*, compared to Staphylococcus genera, while macrophage inflammatory protein 1α (MIP-1α) was significantly increased compared to *E. coli* control (325) highlighting the importance of host biomarkers in the response to *E. coli* (325).

4.6 Limitations

Despite this work achieving most of its goals, some limitations were encountered. During the parameter testing for optimal biofilm forming conditions, the Leibovitz's medium was used as iron-free media to test the influence of iron supplementation for *E. coli* biofilms. However, due to low nutrient amounts it never produced sufficient biofilm. Similarly, with the human blood serum coating, an extended analysis was planned to investigate the role of and potentially perform quantitative RT-PCR to determine the gene influence on the interaction between isolates and blood serum regarding the biofilm formation. Nevertheless, due to unpredictable results from blood serum coating and time constraints, it was not a priority. Regarding the CLSM imaging, due to equipment and scheduling issues, the imaging was only done once. Repeated attempts would have helped to determine accurate measuring parameters for the isolates used as some of the repeats had migrated to the top layer of biofilm, extending unusually high in the well.

4.7 Future Perspectives

The findings of this thesis suggest numerous avenues for future work, which are described below. Firstly, gene profiling in LB broth + bile salts media would provide a much clearer image of which biofilm formation and bile resistance associated genes' expression impact biofilm formation the most. Subsequently, based on those results, a knockout mutant strain analysis using CFT073 background would be beneficial to pinpoint the exact contribution of each gene in biofilm formation (275). In addition, it would be interesting to investigate the comparison of ST69 and ST95 ExPEC isolates in LB broth + bile salts media, considering the difference found between sequence types in this work (60, 88). Subsequently, expanding the comparison to different pathotypes (Commensal vs IPEC vs ExPEC *E. coli*) could give some valuable insights.

Bile salts are a gut related biofilm induction factor, but since the origin of infection of the isolates used varies from gut to urinary tract, it would be interesting to see the impact on biofilm formation in this collection of isolates using a urinary tract biofilm induction factor (e.g. human urine or synthetic urine) and compare gene expression in LB broth + bile salt media (326-329).

While the genome sequencing was not performed during this project, using the previously acquired genomic data the presence and absence levels of genes related to biofilm or bile resistance were evaluated. The actual quantities of biofilm components could vary drastically between the isolates, even with similar gene profiles. Biofilm component detection methods, such as wheat germ agglutinin for Pga detection or oligothiophene for cellulose detection could provide valuable insights determining the composition of the biofilm matrix (330, 331).

Lastly, analysis of the previously acquired genomic data revealed a notable number of gene variants that show different presence and absence levels depending on the sequence type of the isolate, as well as between biofilm-positive and biofilm-negative isolates. Investigating the molecular differences between these variants, using *in vitro* transcription or quantitative RT-PCR, might give further information on the mechanisms underlying biofilm formation in *E. coli*.

5 Conclusion

This thesis aimed to investigate the optimal parameters for biofilm formation in ExPEC *E. coli* isolates, then use these conditions to compare isolates based on phenotypic and gene data and visualise the biofilms using CLSM. This thesis found:

- The most important biofilm assay parameters for biofilm formation were LB, TSB+G or EC broth, 24-hour pre-culture and bile salt addition, while iron supplementation and blood serum coating had little to no effect.
- The majority of biofilm positive isolates were ST73 isolates, which had significantly higher biofilm formation when directly compared to ST131 isolates.
- The genes *fimACDFGHI*, *rcsAB* and *acrE* were associated with biofilm formation in biofilm positive ExPEC strains.
- CLSM live biofilm imaging showed significant biomass and thickness detection in biofilm positive and negative isolates.

6 References

1. Singer M, Deutschman CS, Seymour CW, Shankar-Hari M, Annane D, Bauer M, et al. The Third International Consensus Definitions for Sepsis and Septic Shock (Sepsis-3). Jama. 2016;315(8):801-10.
2. van der Poll T, van de Veerdonk FL, Scicluna BP, Netea MG. The immunopathology of sepsis and potential therapeutic targets. Nature Reviews Immunology. 2017;17(7):407-20.
3. Coburn B, Morris AM, Tomlinson G, Detsky AS. Does This Adult Patient With Suspected Bacteremia Require Blood Cultures? JAMA. 2012;308(5).
4. Sweeney TE, Liesenfeld O, May L. Diagnosis of bacterial sepsis: why are tests for bacteremia not sufficient? Expert Review of Molecular Diagnostics. 2019;19(11):959-62.
5. Funk DJ, Parrillo JE, Kumar A. Sepsis and Septic Shock: A History. Critical Care Clinics. 2009;25(1):83-101.
6. van der Poll T, Shankar-Hari M, Wiersinga WJ. The immunology of sepsis. Immunity. 2021;54(11):2450-64.
7. Bone RC, Sibbald WJ, Sprung CL. The ACCP-SCCM Consensus Conference on Sepsis and Organ Failure. Chest. 1992;101(6):1481-3.
8. Rudd KE, Seymour CW, Aluisio AR, Augustin ME, Bagenda DS, Beane A, et al. Association of the Quick Sequential (Sepsis-Related) Organ Failure Assessment (qSOFA) Score With Excess Hospital Mortality in Adults With Suspected Infection in Low- and Middle-Income Countries. Jama. 2018;319(21):2202-11.
9. Evans L, Rhodes A, Alhazzani W, Antonelli M, Coopersmith CM, French C, et al. Surviving sepsis campaign: international guidelines for management of sepsis and septic shock 2021. Intensive Care Med. 2021;47(11):1181-247.
10. Guarino M, Perna B, Cesaro AE, Maritati M, Spampinato MD, Contini C, et al. 2023 Update on Sepsis and Septic Shock in Adult Patients: Management in the Emergency Department. J Clin Med. 2023;12(9).
11. Gotts JE, Matthay MA. Sepsis: pathophysiology and clinical management. BMJ. 2016;353:i1585.
12. Kumar A, Roberts D, Wood KE, Light B, Parrillo JE, Sharma S, et al. Duration of hypotension before initiation of effective antimicrobial therapy is the critical determinant of survival in human septic shock. Crit Care Med. 2006;34(6):1589-96.
13. Ferrer R, Martin-Loeches I, Phillips G, Osborn TM, Townsend S, Dellinger RP, et al. Empiric antibiotic treatment reduces mortality in severe sepsis and septic shock from the first hour: results from a guideline-based performance improvement program. Crit Care Med. 2014;42(8):1749-55.
14. Kuttab HI, Lykins JD, Hughes MD, Wroblewski K, Keast EP, Kukoyi O, et al. Evaluation and Predictors of Fluid Resuscitation in Patients With Severe Sepsis and Septic Shock. Crit Care Med. 2019;47(11):1582-90.
15. Permpikul C, Tongyoo S, Viarasilpa T, Trainarongsakul T, Chakorn T, Udompanturak S. Early Use of Norepinephrine in Septic Shock Resuscitation (CENSER). A Randomized Trial. Am J Respir Crit Care Med. 2019;199(9):1097-105.
16. Ammar MA, Ammar AA, Wieruszewski PM, Bissell BD, M TL, Albert L, et al. Timing of vasoactive agents and corticosteroid initiation in septic shock. Ann Intensive Care. 2022;12(1):47.
17. Biorender.com. The biofilm life cycle [Available from: https://BioRender.com.

18. Rudd KE, Johnson SC, Agesa KM, Shackelford KA, Tsoi D, Kievlan DR, et al. Global, regional, and national sepsis incidence and mortality, 1990-2017: analysis for the Global Burden of Disease Study. Lancet. 2020;395(10219):200-11.
19. Kempker JA, Martin GS. A global accounting of sepsis. The Lancet. 2020;395(10219):168-70.
20. Fleischmann-Struzek C, Goldfarb DM, Schlattmann P, Schlapbach LJ, Reinhart K, Kissoon N. The global burden of paediatric and neonatal sepsis: a systematic review. The Lancet Respiratory Medicine. 2018;6(3):223-30.
21. Weiss SL, Peters MJ, Alhazzani W, Agus MSD, Flori HR, Inwald DP, et al. Surviving sepsis campaign international guidelines for the management of septic shock and sepsis-associated organ dysfunction in children. Intensive Care Med. 2020;46(Suppl 1):10-67.
22. Sakr Y, Jaschinski U, Wittebole X, Szakmany T, Lipman J, Ñamendys-Silva SA, et al. Sepsis in Intensive Care Unit Patients: Worldwide Data From the Intensive Care over Nations Audit. Open Forum Infect Dis. 2018;5(12):ofy313.
23. Rhee C, Dantes R, Epstein L, Murphy DJ, Seymour CW, Iwashyna TJ, et al. Incidence and Trends of Sepsis in US Hospitals Using Clinical vs Claims Data, 2009-2014. Jama. 2017;318(13):1241-9.
24. Angus DC, Linde-Zwirble WT, Lidicker J, Clermont G, Carcillo J, Pinsky MR. Epidemiology of severe sepsis in the United States: analysis of incidence, outcome, and associated costs of care. Crit Care Med. 2001;29(7):1303-10.
25. Mellhammar L, Wullt S, Lindberg Å, Lanbeck P, Christensson B, Linder A. Sepsis Incidence: A Population-Based Study. Open Forum Infect Dis. 2016;3(4):ofw207.
26. Bion J BG, Boyle A, Carlson G, Carrol E, Christian W, Crossland S, Faust S, Gabbay F, Gent N, Gibbs P, Harden J, Howard P, Inada-Kim M, Lanzman M, Leanord A, Lees N, Noursadeghi M, Rajesh P, Shrestha S, Sriskandan S, Stockley S, Waldmann C, Walsh T, Wilson P, Singer M. Statement on the Initial Antimicrobial Treatment of Sepsis. aomrc.org.uk: Academy of Medical Royal Colleges; 2022 2022. Contract No.: Version 2.0.
27. Prescott HC, Angus DC. Enhancing Recovery From Sepsis: A Review. Jama. 2018;319(1):62-75.
28. Shahin J, Harrison DA, Rowan KM. Relation between volume and outcome for patients with severe sepsis in United Kingdom: retrospective cohort study. BMJ : British Medical Journal. 2012;344:e3394.
29. The-UK-SEPSIS-TRUST. The Sepsis Manual. 2024.
30. Cancer-research-UK. Cancer Statistics For The UK 2019 [Available from: https://www.cancerresearchuk.org/health-professional/cancer-statistics-for-the-uk.
31. Kopczynska M, Sharif B, Cleaver S, Spencer N, Kurani A, Lee C, et al. Red-flag sepsis and SOFA identifies different patient population at risk of sepsis-related deaths on the general ward. Medicine (Baltimore). 2018;97(49):e13238.
32. Kopczynska M, Unwin H, Pugh RJ, Sharif B, Chandy T, Davies DJ, et al. Four consecutive yearly point-prevalence studies in Wales indicate lack of improvement in sepsis care on the wards. Sci Rep. 2021;11(1):16222.
33. Szakmany T, Lundin RM, Sharif B, Ellis G, Morgan P, Kopczynska M, et al. Sepsis Prevalence and Outcome on the General Wards and Emergency Departments in Wales: Results of a Multi-Centre, Observational, Point Prevalence Study. PLoS One. 2016;11(12):e0167230.

34. Szakmany T, Pugh R, Kopczynska M, Lundin RM, Sharif B, Morgan P, et al. Defining sepsis on the wards: results of a multi-centre point-prevalence study comparing two sepsis definitions. Anaesthesia. 2018;73(2):195-204.
35. Arefian H, Heublein S, Scherag A, Brunkhorst FM, Younis MZ, Moerer O, et al. Hospital-related cost of sepsis: A systematic review. Journal of Infection. 2017;74(2):107-17.
36. Torio CM AR. National Inpatient Hospital Costs: The Most Expensive Conditions by Payer, 2011. Rockville (MD): Agency for Healthcare Research and Quality (US); 2013. Contract No.: 160.
37. York-Health-Economics-Consortium. The cost of sepsis care in the UK. University of York; 2017.
38. Umemura Y, Ogura H, Takuma K, Fujishima S, Abe T, Kushimoto S, et al. Current spectrum of causative pathogens in sepsis: A prospective nationwide cohort study in Japan. International Journal of Infectious Diseases. 2021;103:343-51.
39. Reinhart K, Daniels R, Kissoon N, Machado FR, Schachter RD, Finfer S. Recognizing Sepsis as a Global Health Priority - A WHO Resolution. N Engl J Med. 2017;377(5):414-7.
40. Montrucchio G, Sales G, Catozzi G, Bosso S, Scanu M, Vignola TV, et al. Effectiveness of an Active and Continuous Surveillance Program for Intensive Care Units Infections Based on the EPIC III (Extended Prevalence of Infection in Intensive Care) Approach. J Clin Med. 2022;11(9).
41. Markwart R, Saito H, Harder T, Tomczyk S, Cassini A, Fleischmann-Struzek C, et al. Epidemiology and burden of sepsis acquired in hospitals and intensive care units: a systematic review and meta-analysis. Intensive Care Med. 2020;46(8):1536-51.
42. World-Health-Organization. Report on the Burden of Endemic Health Care-Associated Infection Worldwide. World-Health-Organization; 2011.
43. Walraven CJ, North MS, Marr-Lyon L, Deming P, Sakoulas G, Mercier R-C. Site of infection rather than vancomycin MIC predicts vancomycin treatment failure in methicillin-resistant Staphylococcus aureus bacteraemia. Journal of Antimicrobial Chemotherapy. 2011;66(10):2386-92.
44. Bukh AS, Schønheyder HC, Emmersen JMG, Søgaard M, Bastholm S, Roslev P. Escherichia coli phylogenetic groups are associated with site of infection and level of antibiotic resistance in community-acquired bacteraemia: a 10 year population-based study in Denmark. Journal of Antimicrobial Chemotherapy. 2009;64(1):163-8.
45. Mayr FB, Yende S, Angus DC. Epidemiology of severe sepsis. Virulence. 2014;5(1):4-11.
46. Dolin HH, Papadimos TJ, Chen X, Pan ZK. Characterization of Pathogenic Sepsis Etiologies and Patient Profiles: A Novel Approach to Triage and Treatment. Microbiol Insights. 2019;12:1178636118825081.
47. De Santis V, Gresoiu M, Corona A, Wilson APR, Singer M. Bacteraemia incidence, causative organisms and resistance patterns, antibiotic strategies and outcomes in a single university hospital ICU: continuing improvement between 2000 and 2013. Journal of Antimicrobial Chemotherapy. 2014;70(1):273-8.
48. Cross A, Levine MM. Patterns of bacteraemia aetiology. The Lancet Infectious Diseases. 2017;17(10):1005-6.
49. Opota O, Croxatto A, Prod'hom G, Greub G. Blood culture-based diagnosis of bacteraemia: state of the art. Clinical Microbiology and Infection. 2015;21(4):313-22.
50. Public-Health-Wales. Antimicrobial Resistance Programme. Public Health Wales; 2013.

51. Health-And-Care-Research-Wales. Identifying host and bacterial biomarkers to predict sepsis 2022 [Available from: https://healthandcareresearchwales.org/researchers/our-funded-projects/identifying-host-and-bacterial-biomarkers-predict-sepsis.
52. Public-Health-Wales. Wales HCAI Surveillance Monthly Dashboard: Public-Health-Wales; 2024 [Available from: https://public.tableau.com/shared/C8Q525QPH?:display_count=n&:origin=viz_share_link.
53. Tenaillon O, Skurnik D, Picard B, Denamur E. The population genetics of commensal Escherichia coli. Nat Rev Microbiol. 2010;8(3):207-17.
54. Kaper JB, Nataro JP, Mobley HLT. Pathogenic Escherichia coli. Nature Reviews Microbiology. 2004;2(2):123-40.
55. Leimbach A, Hacker J, Dobrindt U. E. coli as an All-Rounder: The Thin Line Between Commensalism and Pathogenicity. In: Dobrindt U, Hacker JH, Svanborg C, editors. Between Pathogenicity and Commensalism. Berlin, Heidelberg: Springer Berlin Heidelberg; 2013. p. 3-32.
56. Köhler C-D, Dobrindt U. What defines extraintestinal pathogenic Escherichia coli? International Journal of Medical Microbiology. 2011;301(8):642-7.
57. Lindstedt BA, Finton MD, Porcellato D, Brandal LT. High frequency of hybrid Escherichia coli strains with combined Intestinal Pathogenic Escherichia coli (IPEC) and Extraintestinal Pathogenic Escherichia coli (ExPEC) virulence factors isolated from human faecal samples. BMC Infect Dis. 2018;18(1):544.
58. Ochman H, Selander RK. Standard reference strains of Escherichia coli from natural populations. J Bacteriol. 1984;157(2):690-3.
59. Beghain J, Bridier-Nahmias A, Le Nagard H, Denamur E, Clermont O. ClermonTyping: an easy-to-use and accurate in silico method for Escherichia genus strain phylotyping. Microb Genom. 2018;4(7).
60. Maldonado N, López-Hernández I, García-Montaner A, López-Cortés LE, Pérez-Crespo PMM, Retamar-Gentil P, et al. Whole-genome characterisation of Escherichia coli isolates from patients with bacteraemia presenting with sepsis or septic shock in Spain: a multicentre cross-sectional study. The Lancet Microbe. 2024;5(4):e390-e9.
61. Sarowska J, Futoma-Koloch B, Jama-Kmiecik A, Frej-Madrzak M, Ksiazczyk M, Bugla-Ploskonska G, et al. Virulence factors, prevalence and potential transmission of extraintestinal pathogenic Escherichia coli isolated from different sources: recent reports. Gut Pathog. 2019;11:10.
62. Fratamico PM, DebRoy C, Liu Y, Needleman DS, Baranzoni GM, Feng P. Advances in Molecular Serotyping and Subtyping of Escherichia coli†. Frontiers in Microbiology. 2016;7.
63. Kunduru BR, Nair SA, Rathinavelan T. EK3D: an E. coli K antigen 3-dimensional structure database. Nucleic Acids Res. 2016;44(D1):D675-81.
64. Johnson JR, Owens KL, Clabots CR, Weissman SJ, Cannon SB. Phylogenetic relationships among clonal groups of extraintestinal pathogenic Escherichia coli as assessed by multi-locus sequence analysis. Microbes Infect. 2006;8(7):1702-13.
65. Baldy-Chudzik K, Bok E, Mazurek J. [Well-known and new variants of pathogenic Escherichia coli as a consequence of the plastic genome]. Postepy Hig Med Dosw (Online). 2015;69:345-61.
66. Manges AR, Geum HM, Guo A, Edens TJ, Fibke CD, Pitout JDD. Global Extraintestinal Pathogenic Escherichia coli (ExPEC) Lineages. Clin Microbiol Rev. 2019;32(3).

67. Maiden MCJ, Bygraves JA, Feil E, Morelli G, Russell JE, Urwin R, et al. Multilocus sequence typing: A portable approach to the identification of clones within populations of pathogenic microorganisms. Proceedings of the National Academy of Sciences. 1998;95(6):3140-5.
68. Johnson JR, Owens K, Gajewski A, Clabots C. Escherichia coli Colonization Patterns among Human Household Members and Pets, with Attention to Acute Urinary Tract Infection. The Journal of Infectious Diseases. 2008;197(2):218-24.
69. Flores-Mireles AL, Walker JN, Caparon M, Hultgren SJ. Urinary tract infections: epidemiology, mechanisms of infection and treatment options. Nat Rev Microbiol. 2015;13(5):269-84.
70. Stamm WE, Norrby SR. Urinary tract infections: disease panorama and challenges. J Infect Dis. 2001;183 Suppl 1:S1-4.
71. Tan CW, Chlebicki MP. Urinary tract infections in adults. Singapore Med J. 2016;57(9):485-90.
72. Conceição RA, Ludovico MS, Andrade CG, Yano T. Human sepsis-associated Escherichia coli (SEPEC) is able to adhere to and invade kidney epithelial cells in culture. Braz J Med Biol Res. 2012;45(5):417-24.
73. Kemmett K, Williams NJ, Chaloner G, Humphrey S, Wigley P, Humphrey T. The contribution of systemic Escherichia coli infection to the early mortalities of commercial broiler chickens. Avian Pathol. 2014;43(1):37-42.
74. Kathayat D, Lokesh D, Ranjit S, Rajashekara G. Avian Pathogenic Escherichia coli (APEC): An Overview of Virulence and Pathogenesis Factors, Zoonotic Potential, and Control Strategies. Pathogens. 2021;10(4).
75. Woll C, Neuman MI, Pruitt CM, Wang ME, Shapiro ED, Shah SS, et al. Epidemiology and Etiology of Invasive Bacterial Infection in Infants ≤60 Days Old Treated in Emergency Departments. J Pediatr. 2018;200:210-7.e1.
76. Ku LC, Boggess KA, Cohen-Wolkowiez M. Bacterial meningitis in infants. Clin Perinatol. 2015;42(1):29-45, vii-viii.
77. Chambers CA, Lacey CA, Brown DC, Skyberg JA. Nitric oxide inhibits interleukin-1-mediated protection against Escherichia coli K1-induced sepsis and meningitis in a neonatal murine model. Immunology & Cell Biology. 2021;99(6):596-610.
78. Alshammari MK, Alsanad AH, Alnusayri RJ, Alanazi AS, Shamakhi FQ, Alshahrani KM, et al. Risk and diagnostic factors and therapy outcome of neonatal early onset sepsis in ICU patients of Saudi Arabia: a systematic review and meta analysis. Front Pediatr. 2023;11:1206389.
79. Shao Q, Chen D, Chen S, Ru X, Ye Q. Escherichia coli Infection Sepsis: An Analysis of Specifically Expressed Genes and Clinical Indicators. Diagnostics. 2023;13(23):3542.
80. Croxen MA, Finlay BB. Molecular mechanisms of Escherichia coli pathogenicity. Nat Rev Microbiol. 2010;8(1):26-38.
81. Bonten M, Johnson JR, van den Biggelaar AHJ, Georgalis L, Geurtsen J, de Palacios PI, et al. Epidemiology of Escherichia coli Bacteremia: A Systematic Literature Review. Clin Infect Dis. 2021;72(7):1211-9.
82. de Lastours V, Laouénan C, Royer G, Carbonnelle E, Lepeule R, Esposito-Farèse M, et al. Mortality in Escherichia coli bloodstream infections: antibiotic resistance still does not make it. J Antimicrob Chemother. 2020;75(8):2334-43.

83. Abernethy JK, Johnson AP, Guy R, Hinton N, Sheridan EA, Hope RJ. Thirty day all-cause mortality in patients with Escherichia coli bacteraemia in England. Clinical Microbiology and Infection. 2015;21(3):251.e1-.e8.
84. Kocsis B, Gulyás D, Szabó D. Emergence and Dissemination of Extraintestinal Pathogenic High-Risk International Clones of Escherichia coli. Life (Basel). 2022;12(12).
85. Lindblom A, Kiszakiewicz C, Kristiansson E, Yazdanshenas S, Kamenska N, Karami N, et al. The impact of the ST131 clone on recurrent ESBL-producing E. coli urinary tract infection: a prospective comparative study. Sci Rep. 2022;12(1):10048.
86. Yardena S-I, Boaz F, Ruth O-W, Yoav G, Aliza N, David S, et al. Reappraisal of Community-Acquired Bacteremia: A Proposal of a New Classification for the Spectrum of Acquisition of Bacteremia. Clinical Infectious Diseases. 2002;34(11):1431-9.
87. Phetsouvanh R, Phongmany S, Soukaloun D, Rasachak B, Soukhaseum V, Soukhaseum S, et al. Causes of community-acquired bacteremia and patterns of antimicrobial resistance in Vientiane, Laos. Am J Trop Med Hyg. 2006;75(5):978-85.
88. Maldonado N, López-Hernández I, López-Cortés LE, Martínez Pérez-Crespo PM, Retamar-Gentil P, García-Montaner A, et al. Association of microbiological factors with mortality in Escherichia coli bacteraemia presenting with sepsis/septic shock: a prospective cohort study. Clin Microbiol Infect. 2024;30(8):1035-41.
89. Sora VM, Meroni G, Martino PA, Soggiu A, Bonizzi L, Zecconi A. Extraintestinal Pathogenic Escherichia coli: Virulence Factors and Antibiotic Resistance. Pathogens. 2021;10(11):1355.
90. Hacker J, Hentschel U, Dobrindt U. Prokaryotic chromosomes and disease. Science. 2003;301(5634):790-3.
91. Proença JT, Barral DC, Gordo I. Commensal-to-pathogen transition: One-single transposon insertion results in two pathoadaptive traits in Escherichia coli -macrophage interaction. Scientific Reports. 2017;7(1):4504.
92. Oshima K, Toh H, Ogura Y, Sasamoto H, Morita H, Park SH, et al. Complete genome sequence and comparative analysis of the wild-type commensal Escherichia coli strain SE11 isolated from a healthy adult. DNA Res. 2008;15(6):375-86.
93. Toh H, Oshima K, Toyoda A, Ogura Y, Ooka T, Sasamoto H, et al. Complete genome sequence of the wild-type commensal Escherichia coli strain SE15, belonging to phylogenetic group B2. J Bacteriol. 2010;192(4):1165-6.
94. Johnson JR, Gajewski A, Lesse AJ, Russo TA. Extraintestinal pathogenic Escherichia coli as a cause of invasive nonurinary infections. J Clin Microbiol. 2003;41(12):5798-802.
95. Johnson JR, Kuskowski MA, Owens K, Gajewski A, Winokur PL. Phylogenetic Origin and Virulence Genotype in Relation to Resistance to Fluoroquinolones and/or Extended-Spectrum Cephalosporins and Cephamycins among Escherichia coli Isolates from Animals and Humans. The Journal of Infectious Diseases. 2003;188(5):759-68.
96. Muhammad A Khan UoM, Minneapolis, MN; Timothy, O'Bryan NK, Minneapolis VAMC, Minneapolis, MN; Fran Lebahn,, James R Johnson UoM, Minneapolis, MN. Abstracts of the IDSA 37th Annual Meeting; (193) Pap And Other Virulence Factors (Vfs) In Escherichiacoli Bacteremia (B)

In Veterans: A Case-Control Study. Clinical Infectious Diseases. 1999;29(4):959-1088.
97. Johnson JR, Delavari P, Kuskowski M, Stell AL. Phylogenetic distribution of extraintestinal virulence-associated traits in Escherichia coli. J Infect Dis. 2001;183(1):78-88.
98. Johnson JR, Kuskowski M. Clonal origin, virulence factors, and virulence. Infect Immun. 2000;68(1):424-5.

99. Picard B, Garcia JS, Gouriou S, Duriez P, Brahimi N, Bingen E, et al. The link between phylogeny and virulence in Escherichia coli extraintestinal infection. Infect Immun. 1999;67(2):546-53.
100. Lindberg S, Xia Y, Sondén B, Göransson M, Hacker J, Uhlin BE. Regulatory Interactions among adhesin gene systems of uropathogenic Escherichia coli. Infect Immun. 2008;76(2):771-80.
101. Bouguénec CL, Lalioui L, Merle Ld, Jouve M, Courcoux P, Bouzari S, et al. Characterization of AfaE Adhesins Produced by Extraintestinal and Intestinal Human Escherichia coliIsolates: PCR Assays for Detection of Afa Adhesins That Do or Do Not Recognize Dr Blood Group Antigens. Journal of Clinical Microbiology. 2001;39(5):1738-45.
102. Mulvey MA, Lopez-Boado YS, Wilson CL, Roth R, Parks WC, Heuser J, et al. Induction and Evasion of Host Defenses by Type 1-Piliated Uropathogenic Escherichia coli. Science. 1998;282(5393):1494-7.
103. Connell I, Agace W, Klemm P, Schembri M, Mărild S, Svanborg C. Type 1 fimbrial expression enhances Escherichia coli virulence for the urinary tract. Proceedings of the National Academy of Sciences. 1996;93(18):9827-32.
104. Bahrani-Mougeot FK, Buckles EL, Lockatell CV, Hebel JR, Johnson DE, Tang CM, et al. Type 1 fimbriae and extracellular polysaccharides are preeminent uropathogenic Escherichia coli virulence determinants in the murine urinary tract. Mol Microbiol. 2002;45(4):1079-93.
105. Bonacorsi S, Bingen E. Molecular epidemiology of Escherichia coli causing neonatal meningitis. International Journal of Medical Microbiology. 2005;295(6):373-81.
106. Qin X, Hu F, Wu S, Ye X, Zhu D, Zhang Y, et al. Comparison of adhesin genes and antimicrobial susceptibilities between uropathogenic and intestinal commensal Escherichia coli strains. PLoS One. 2013;8(4):e61169.
107. Tarchouna M, Ferjani A, Ben-Selma W, Boukadida J. Distribution of uropathogenic virulence genes in Escherichia coli isolated from patients with urinary tract infection. International Journal of Infectious Diseases. 2013;17(6):e450-e3.
108. Valle J, Mabbett AN, Ulett GC, Toledo-Arana A, Wecker K, Totsika M, et al. UpaG, a New Member of the Trimeric Autotransporter Family of Adhesins in Uropathogenic Escherichia coli. Journal of Bacteriology. 2008;190(12):4147-61.
109. Frömmel U, Lehmann W, Rödiger S, Böhm A, Nitschke J, Weinreich J, et al. Adhesion of Human and Animal Escherichia coli Strains in Association with Their Virulence-Associated Genes and Phylogenetic Origins. Applied and Environmental Microbiology. 2013;79(19):5814-29.
110. Wullt B, Bergsten G, Connell H, Röllano P, Gebratsedik N, Hang L, et al. P-fimbriae trigger mucosal responses to Escherichia coli in the human urinary tract. Cellular Microbiology. 2001;3(4):255-64.
111. Wallecha A, Oreh H, Woude MWvd, deHaseth PL. Control of Gene Expression at a Bacterial Leader RNA, the agn43 Gene Encoding Outer Membrane Protein Ag43 of Escherichia coli. Journal of Bacteriology. 2014;196(15):2728-35.
112. Brandt S, Shafikhani S, Balachandran P, Jin S, Hartig R, König W, et al. Use of a novel coinfection system reveals a role for Rac1, H-Ras, and CrkII phosphorylation in Helicobacter pylori-induced host cell actin cytoskeletal rearrangements. FEMS Immunology & Medical Microbiology. 2007;50(2):190-205.
113. Shin S, Kim KS. RhoA and Rac1 contribute to type III group B streptococcal invasion of human brain microvascular endothelial cells. Biochemical and Biophysical Research Communications. 2006;345(1):538-42.

114. Kim KS. Mechanisms of microbial traversal of the blood–brain barrier. Nature Reviews Microbiology. 2008;6(8):625-34.
115. Maruvada R, Kim KS. IbeA and OmpA of Escherichia coli K1 Exploit Rac1 Activation for Invasion of Human Brain Microvascular Endothelial Cells. Infection and Immunity. 2012;80(6):2035-41.
116. Sáez-López E, Bosch J, Salvia MD, Fernández-Orth D, Cepas V, Ferrer-Navarro M, et al. Outbreak Caused by Escherichia coli O18:K1:H7 Sequence Type 95 in a Neonatal Intensive Care Unit in Barcelona, Spain. The Pediatric Infectious Disease Journal. 2017;36(11):1079-86.
117. Cieza RJ, Hu J, Ross BN, Sbrana E, Torres AG. The IbeA Invasin of Adherent-Invasive Escherichia coli Mediates Interaction with Intestinal Epithelia and Macrophages. Infection and Immunity. 2015;83(5):1904-18.
118. Huang S-H, Wan Z-S, Chen Y-H, Jong AY, Kim KS. Further Characterization of Escherichia coli Brain Microvascular Endothelial Cell Invasion Gene ibeA by Deletion, Complementation, and Protein Expression. The Journal of Infectious Diseases. 2001;183(7):1071-8.
119. Huang SH, Wass C, Fu Q, Prasadarao NV, Stins M, Kim KS. Escherichia coli invasion of brain microvascular endothelial cells in vitro and in vivo: molecular cloning and characterization of invasion gene ibe10. Infection and Immunity. 1995;63(11):4470-5.
120. Zhang Y, Sen S, Giedroc DP. Iron Acquisition by Bacterial Pathogens: Beyond Tris-Catecholate Complexes. ChemBioChem. 2020;21(14):1955-67.
121. Frawley ER, Fang FC. The ins and outs of bacterial iron metabolism. Molecular Microbiology. 2014;93(4):609-16.
122. Ghssein G, Ezzeddine Z. The Key Element Role of Metallophores in the Pathogenicity and Virulence of Staphylococcus aureus: A Review. Biology. 2022;11(10):1525.
123. Lau CKY, Krewulak KD, Vogel HJ. Bacterial ferrous iron transport: the Feo system. FEMS Microbiology Reviews. 2015;40(2):273-98.
124. Weinberg ED. Nutritional immunity. Host's attempt to withold iron from microbial invaders. Jama. 1975;231(1):39-41.
125. Su Q, Guan T, Lv H. Siderophore biosynthesis coordinately modulated the virulence-associated interactive metabolome of uropathogenic Escherichia coli and human urine. Scientific Reports. 2016;6(1):24099.
126. Ratledge C, Dover LG. Iron Metabolism in Pathogenic Bacteria. Annual Review of Microbiology. 2000;54(Volume 54, 2000):881-941.
127. Garénaux A, Caza M, Dozois CM. The Ins and Outs of siderophore mediated iron uptake by extra-intestinal pathogenic Escherichia coli. Veterinary Microbiology. 2011;153(1):89-98.
128. Bister B, Bischoff D, Nicholson GJ, Valdebenito M, Schneider K, Winkelmann G, et al. The structure of salmochelins: C-glucosylated enterobactins of Salmonella enterica§. Biometals. 2004;17(4):471-81.
129. Lin H, Fischbach MA, Liu DR, Walsh CT. In Vitro Characterization of Salmochelin and Enterobactin Trilactone Hydrolases IroD, IroE, and Fes. Journal of the American Chemical Society. 2005;127(31):11075-84.
130. Caza M, Lépine F, Milot S, Dozois CM. Specific Roles of the iroBCDEN Genes in Virulence of an Avian Pathogenic Escherichia coli O78 Strain and in Production of Salmochelins. Infection and Immunity. 2008;76(8):3539-49.

131. Garcia EC, Brumbaugh AR, Mobley HLT. Redundancy and Specificity of Escherichia coli Iron Acquisition Systems during Urinary Tract Infection. Infection and Immunity. 2011;79(3):1225-35.
132. Dozois CM, Daigle F, Curtiss R. Identification of pathogen-specific and conserved genes expressed in vivo by an avian pathogenic Escherichia coli strain. Proceedings of the National Academy of Sciences. 2003;100(1):247-52.
133. Konopka K, Neilands JB. Effect of serum albumin on siderophore-mediated utilization of transferrin iron. Biochemistry. 1984;23(10):2122-7.
134. Williams PH, Carbonetti NH. Iron, siderophores, and the pursuit of virulence: independence of the aerobactin and enterochelin iron uptake systems in Escherichia coli. Infection and Immunity. 1986;51(3):942-7.
135. Caza M, Lépine F, Dozois CM. Secretion, but not overall synthesis, of catecholate siderophores contributes to virulence of extraintestinal pathogenic Escherichia coli. Molecular Microbiology. 2011;80(1):266-82.
136. Fetherston JD, Kirillina O, Bobrov AG, Paulley JT, Perry RD. The yersiniabactin transport system is critical for the pathogenesis of bubonic and pneumonic plague. Infect Immun. 2010;78(5):2045-52.
137. Paauw A, Leverstein-van Hall MA, van Kessel KPM, Verhoef J, Fluit AC. Yersiniabactin Reduces the Respiratory Oxidative Stress Response of Innate Immune Cells. PLOS ONE. 2010;4(12):e8240.
138. Sabri M, Caza M, Proulx J, Lymberopoulos MH, Brée A, Moulin-Schouleur M, et al. Contribution of the SitABCD, MntH, and FeoB Metal Transporters to the Virulence of Avian Pathogenic Escherichia coli O78 Strain χ7122. Infection and Immunity. 2008;76(2):601-11.
139. Stromberg ZR, Johnson JR, Fairbrother JM, Kilbourne J, Van Goor A, Curtiss RR, et al. Evaluation of Escherichia coli isolates from healthy chickens to determine their potential risk to poultry and human health. PLoS One. 2017;12(7):e0180599.
140. Sukupolvi S, O'Connor CD. TraT lipoprotein, a plasmid-specified mediator of interactions between gram-negative bacteria and their environment. Microbiological Reviews. 1990;54(4):331-41.
141. Agüero ME, Aron L, DeLuca AG, Timmis KN, Cabello FC. A plasmid-encoded outer membrane protein, TraT, enhances resistance of Escherichia coli to phagocytosis. Infection and Immunity. 1984;46(3):740-6.
142. Khalid S, Bond PJ, Carpenter T, Sansom MSP. OmpA: Gating and dynamics via molecular dynamics simulations. Biochimica et Biophysica Acta (BBA) - Biomembranes. 2008;1778(9):1871-80.
143. Dabo SM, Confer A, Montelongo M, York P, Wyckoff JH. Vaccination with Pasteurella multocida recombinant OmpA induces strong but non-protective and deleterious Th2-type immune response in mice. Vaccine. 2008;26(34):4345-51.
144. Kim SW, Choi CH, Moon DC, Jin JS, Lee JH, Shin J-H, et al. Serum resistance of Acinetobacter baumannii through the binding of factor H to outer membrane proteins. FEMS Microbiology Letters. 2009;301(2):224-31.
145. Sukumaran SK, Selvaraj SK, Prasadarao NV. Inhibition of Apoptosis by Escherichia coli K1 Is Accompanied by Increased Expression of Bcl_{XL} and Blockade of Mitochondrial Cytochrome c Release in Macrophages. Infection and Immunity. 2004;72(10):6012-22.

146. Kröncke KD, Golecki JR, Jann K. Further electron microscopic studies on the expression of Escherichia coli group II capsules. Journal of Bacteriology. 1990;172(6):3469-72.
147. Willis LM, Whitfield C. Structure, biosynthesis, and function of bacterial capsular polysaccharides synthesized by ABC transporter-dependent pathways. Carbohydrate Research. 2013;378:35-44.
148. Kim KS, Itabashi H, Gemski P, Sadoff J, Warren RL, Cross AS. The K1 capsule is the critical determinant in the development of Escherichia coli meningitis in the rat. The Journal of Clinical Investigation. 1992;90(3):897-905.
149. Buckles EL, Wang X, Lane MC, Lockatell CV, Johnson DE, Rasko DA, et al. Role of the K2 Capsule in Escherichia coli Urinary Tract Infection and Serum Resistance. The Journal of Infectious Diseases. 2009;199(11):1689-97.
150. Brooks HJL, O'Grady F, McSherry MA, Cattell WR. UROPATHOGENIC PROPERTIES OF ESCHERICHIA COLI IN RECURRENT URINARY-TRACT INFECTION. Journal of Medical Microbiology. 1980;13(1):57-68.
151. Opal S, Cross A, Gemski P. K antigen and serum sensitivity of rough Escherichia coli. Infection and Immunity. 1982;37(3):956-60.
152. Svanborg-Edén C, Hagberg L, Hull R, Hull S, Magnusson KE, Ohman L. Bacterial virulence versus host resistance in the urinary tracts of mice. Infection and Immunity. 1987;55(5):1224-32.
153. Johnson JR. Virulence factors in Escherichia coli urinary tract infection. Clinical Microbiology Reviews. 1991;4(1):80-128.
154. Bien J, Sokolova O, Bozko P. Role of Uropathogenic Escherichia coli Virulence Factors in Development of Urinary Tract Infection and Kidney Damage. International Journal of Nephrology. 2012;2012(1):681473.
155. Van Dijk WC, Verbrugh HA, van der Tol ME, Peters R, Verhoef J. Role of Escherichia coli K capsular antigens during complement activation, C3 fixation, and opsonization. Infect Immun. 1979;25(2):603-9.
156. Leying H, Suerbaum S, Kroll HP, Stahl D, Opferkuch W. The capsular polysaccharide is a major determinant of serum resistance in K-1-positive blood culture isolates of Escherichia coli. Infection and Immunity. 1990;58(1):222-7.
157. Mellata M, Dho-Moulin M, Dozois CM, Curtiss R, Brown PK, Arné P, et al. Role of Virulence Factors in Resistance of Avian Pathogenic Escherichia coli to Serum and in Pathogenicity. Infection and Immunity. 2003;71(1):536-40.
158. Li G, Tivendale KA, Liu P, Feng Y, Wannemuehler Y, Cai W, et al. Transcriptome Analysis of Avian Pathogenic Escherichia coli O1 in Chicken Serum Reveals Adaptive Responses to Systemic Infection. Infection and Immunity. 2011;79(5):1951-60.
159. Ghazaei C. Advances in the Study of Bacterial Toxins, Their Roles and Mechanisms in Pathogenesis. Malays J Med Sci. 2022;29(1):4-17.
160. Johnson JR, Russo TA. Extraintestinal pathogenic Escherichia coli : “The other bad E coli &#x201d. The Journal of Laboratory and Clinical Medicine. 2002;139(3):155-62.
161. Ombarak RA, Hinenoya A, Awasthi SP, Iguchi A, Shima A, Elbagory A-RM, et al. Prevalence and pathogenic potential of Escherichia coli isolates from raw milk and raw milk cheese in Egypt. International Journal of Food Microbiology. 2016;221:69-76.
162. Skals M, Jensen UB, Ousingsawat J, Kunzelmann K, Leipziger J, Praetorius HA. Escherichia coli α-Hemolysin Triggers Shrinkage of Erythrocytes via

K_{Ca}3.1 and TMEM16A Channels with Subsequent Phosphatidylserine Exposure *. Journal of Biological Chemistry. 2010;285(20):15557-65.
163. Jorgensen SE, Mulcahy PF, Wu GK, Louis CF. Calcium accumulation in human and sheep erythrocytes that is induced by Escherichia coli hemolysin. Toxicon. 1983;21(5):717-27.
164. Flatau G, Lemichez E, Gauthier M, Chardin P, Paris S, Fiorentini C, et al. Toxin-induced activation of the G protein p21 Rho by deamidation of glutamine. Nature. 1997;387(6634):729-33.
165. Munro P, Flatau G, Doye A, Boyer L, Oregioni O, Mege J-L, et al. Activation and Proteasomal Degradation of Rho GTPases by Cytotoxic Necrotizing Factor-1 Elicit a Controlled Inflammatory Response *. Journal of Biological Chemistry. 2004;279(34):35849-57.
166. Schmidt G, Sehr P, Wilm M, Selzer J, Mann M, Aktories K. Gln 63 of Rho is deamidated by Escherichia coli cytotoxic necrotizing factor-1. Nature. 1997;387(6634):725-9.
167. Andreu A, Stapleton AE, Fennell C, Lockman HA, Xercavins M, Fernandez F, et al. Urovirulence Determinants in Escherichia coli Strains Causing Prostatitis. The Journal of Infectious Diseases. 1997;176(2):464-9.
168. Welch RA. Uropathogenic Escherichia coli-Associated Exotoxins. Microbiology Spectrum. 2016;4(3):10.1128/microbiolspec.uti-0011-2012.
169. Maroncle NM, Sivick KE, Brady R, Stokes FE, Mobley HL. Protease activity, secretion, cell entry, cytotoxicity, and cellular targets of secreted autotransporter toxin of uropathogenic Escherichia coli. Infect Immun. 2006;74(11):6124-34.
170. Guyer DM, Radulovic S, Jones F-E, Mobley HLT. Sat, the Secreted Autotransporter Toxin of Uropathogenic Escherichia coli, Is a Vacuolating Cytotoxin for Bladder and Kidney Epithelial Cells. Infection and Immunity. 2002;70(8):4539-46.
171. Ruiz-Perez F, Wahid R, Faherty CS, Kolappaswamy K, Rodriguez L, Santiago A, et al. Serine protease autotransporters from Shigella flexneri and pathogenic Escherichia coli target a broad range of leukocyte glycoproteins. Proceedings of the National Academy of Sciences. 2011;108(31):12881-6.
172. Parham NJ, Pollard SJ, Desvaux M, Scott-Tucker A, Liu C, Fivian A, et al. Distribution of the Serine Protease Autotransporters of the Enterobacteriaceae among Extraintestinal Clinical Isolates of Escherichia coli. Journal of Clinical Microbiology. 2005;43(8):4076-82.
173. Costerton JW, Stewart PS, Greenberg EP. Bacterial Biofilms: A Common Cause of Persistent Infections. Science. 1999;284(5418):1318-22.
174. Vestby LK, Grønseth T, Simm R, Nesse LL. Bacterial Biofilm and its Role in the Pathogenesis of Disease. Antibiotics. 2020;9(2):59.
175. Høiby N. A short history of microbial biofilms and biofilm infections. APMIS. 2017;125(4):272-5.
176. Bjarnsholt T. The role of bacterial biofilms in chronic infections. APMIS Suppl. 2013(136):1-51.
177. Whittaker CJ, Klier CM, Kolenbrander PE. MECHANISMS OF ADHESION BY ORAL BACTERIA. Annual Review of Microbiology. 1996;50(Volume 50, 1996):513-52.
178. Gristina AG. Biomaterial-centered infection: microbial adhesion versus tissue integration. Science. 1987;237(4822):1588-95.
179. Davies D. Understanding biofilm resistance to antibacterial agents. Nat Rev Drug Discov. 2003;2(2):114-22.

180. Khatoon Z, McTiernan CD, Suuronen EJ, Mah TF, Alarcon EI. Bacterial biofilm formation on implantable devices and approaches to its treatment and prevention. Heliyon. 2018;4(12):e01067.
181. Veerachamy S, Yarlagadda T, Manivasagam G, Yarlagadda PK. Bacterial adherence and biofilm formation on medical implants: a review. Proc Inst Mech Eng H. 2014;228(10):1083-99.
182. Ballén V, Cepas V, Ratia C, Gabasa Y, Soto SM. Clinical Escherichia coli: From Biofilm Formation to New Antibiofilm Strategies. Microorganisms. 2022;10(6).
183. Donlan RM, Costerton JW. Biofilms: survival mechanisms of clinically relevant microorganisms. Clin Microbiol Rev. 2002;15(2):167-93.
184. Fux CA, Stoodley P, Hall-Stoodley L, Costerton JW. Bacterial biofilms: a diagnostic and therapeutic challenge. Expert Rev Anti Infect Ther. 2003;1(4):667-83.
185. Hall-Stoodley L, Stoodley P. Evolving concepts in biofilm infections. Cell Microbiol. 2009;11(7):1034-43.
186. Flemming HC, Wingender J, Szewzyk U, Steinberg P, Rice SA, Kjelleberg S. Biofilms: an emergent form of bacterial life. Nat Rev Microbiol. 2016;14(9):563-75.
187. Harrell JE, Hahn MM, D'Souza SJ, Vasicek EM, Sandala JL, Gunn JS, et al. Salmonella Biofilm Formation, Chronic Infection, and Immunity Within the Intestine and Hepatobiliary Tract. Front Cell Infect Microbiol. 2020;10:624622.
188. Costerton JW, Lewandowski Z, Caldwell DE, Korber DR, Lappin-Scott HM. Microbial biofilms. 1995.
189. O'Toole G, Kaplan HB, Kolter R. Biofilm formation as microbial development. Annu Rev Microbiol. 2000;54:49-79.
190. O'Toole GA, Kolter R. Initiation of biofilm formation in Pseudomonas fluorescens WCS365 proceeds via multiple, convergent signalling pathways: a genetic analysis. Mol Microbiol. 1998;28(3):449-61.
191. Espeland EM, Wetzel RG. Complexation, Stabilization, and UV Photolysis of Extracellular and Surface-Bound Glucosidase and Alkaline Phosphatase: Implications for Biofilm Microbiota. Microb Ecol. 2001;42(4):572-85.
192. Mah TF, O'Toole GA. Mechanisms of biofilm resistance to antimicrobial agents. Trends Microbiol. 2001;9(1):34-9.
193. Stewart PS, Costerton JW. Antibiotic resistance of bacteria in biofilms. Lancet. 2001;358(9276):135-8.
194. Hall-Stoodley L, Costerton JW, Stoodley P. Bacterial biofilms: from the natural environment to infectious diseases. Nat Rev Microbiol. 2004;2(2):95-108.
195. Stoodley P, Sauer K, Davies DG, Costerton JW. Biofilms as complex differentiated communities. Annu Rev Microbiol. 2002;56:187-209.
196. Sharma G, Sharma S, Sharma P, Chandola D, Dang S, Gupta S, et al. Escherichia coli biofilm: development and therapeutic strategies. J Appl Microbiol. 2016;121(2):309-19.
197. Dalton HM, Goodman AE, Marshall KC. Diversity in surface colonization behavior in marine bacteria. Journal of Industrial Microbiology and Biotechnology. 1996;17(3-4):228-34.
198. Korber DR, Lawrence JR, Lappin-Scott HM, Costerton JW. Growth of Microorganisms on Surfaces. In: Lappin-Scott HM, Costerton JW, editors. Microbial Biofilms. Biotechnology Research. Cambridge: Cambridge University Press; 1995. p. 15-45.
199. Heydorn A, Nielsen AT, Hentzer M, Sternberg C, Givskov M, Ersbøll BK, et al. Quantification of biofilm structures by the novel computer program COMSTAT. Microbiology (Reading). 2000;146 (Pt 10):2395-407.

200. Tolker-Nielsen T, Brinch UC, Ragas PC, Andersen JB, Jacobsen CS, Molin S. Development and dynamics of Pseudomonas sp. biofilms. J Bacteriol. 2000;182(22):6482-9.
201. Flemming HC, Wingender J. The biofilm matrix. Nat Rev Microbiol. 2010;8(9):623-33.
202. O'Toole GA, Kolter R. Flagellar and twitching motility are necessary for Pseudomonas aeruginosa biofilm development. Mol Microbiol. 1998;30(2):295-304.
203. Marshall KC, Stout R, Mitchell R. Mechanism of the Initial Events in the Sorption of Marine Bacteria to Surfaces. Microbiology. 1970;68:337-48.
204. Di Martino P. Extracellular polymeric substances, a key element in understanding biofilm phenotype. AIMS Microbiol. 2018;4(2):274-88.
205. Lichtenberg M, Coenye T, Parsek MR, Bjarnsholt T, Jakobsen TH. What's in a name? Characteristics of clinical biofilms. FEMS Microbiol Rev. 2023;47(5).
206. Brözel VS, Strydom GM, Cloete TE. A method for the study of de novo protein synthesis in pseudomonas aeruginosa after attachment. Biofouling. 1995;8(3):195-201.
207. Prigent-Combaret C, Vidal O, Dorel C, Lejeune P. Abiotic surface sensing and biofilm-dependent regulation of gene expression in Escherichia coli. J Bacteriol. 1999;181(19):5993-6002.
208. Sauer K, Camper AK. Characterization of phenotypic changes in Pseudomonas putida in response to surface-associated growth. J Bacteriol. 2001;183(22):6579-89.
209. Clark ME, He Z, Redding AM, Joachimiak MP, Keasling JD, Zhou JZ, et al. Transcriptomic and proteomic analyses of Desulfovibrio vulgaris biofilms: carbon and energy flow contribute to the distinct biofilm growth state. BMC Genomics. 2012;13:138.
210. Thöming JG, Tomasch J, Preusse M, Koska M, Grahl N, Pohl S, et al. Parallel evolutionary paths to produce more than one Pseudomonas aeruginosa biofilm phenotype. NPJ Biofilms Microbiomes. 2020;6:2.
211. Gerke C, Kraft A, Süßmuth R, Schweitzer O, Götz F. Characterization of theN-Acetylglucosaminyltransferase Activity Involved in the Biosynthesis of the Staphylococcus epidermidisPolysaccharide Intercellular Adhesin *. Journal of Biological Chemistry. 1998;273(29):18586-93.
212. Olsén A, Jonsson A, Normark S. Fibronectin binding mediated by a novel class of surface organelles on Escherichia coll. Nature. 1989;338(6217):652-5.
213. Ben Nasr A, Olsén A, Sjöbring U, Müller-Esterl W, Björck L. Assembly of human contact phase proteins and release of bradykinin at the surface of curli-expressing Escherichia coli. Molecular Microbiology. 1996;20(5):927-35.
214. Wood TK. Insights on Escherichia coli biofilm formation and inhibition from whole-transcriptome profiling. Environ Microbiol. 2009;11(1):1-15.
215. Beloin C, Roux A, Ghigo JM. Escherichia coli biofilms. Curr Top Microbiol Immunol. 2008;322:249-89.
216. Davies DG, Parsek MR, Pearson JP, Iglewski BH, Costerton JW, Greenberg EP. The involvement of cell-to-cell signals in the development of a bacterial biofilm. Science. 1998;280(5361):295-8.
217. Sauer K, Camper AK, Ehrlich GD, Costerton JW, Davies DG. Pseudomonas aeruginosa displays multiple phenotypes during development as a biofilm. J Bacteriol. 2002;184(4):1140-54.
218. Whiteley M, Bangera MG, Bumgarner RE, Parsek MR, Teitzel GM, Lory S, et al. Gene expression in Pseudomonas aeruginosa biofilms. Nature. 2001;413(6858):860-4.

219. Vogeleer P, Tremblay YDN, Mafu AA, Jacques M, Harel J. Life on the outside: role of biofilms in environmental persistence of Shiga-toxin producing Escherichia coli. Frontiers in Microbiology. 2014;5.
220. Daniels R, Vanderleyden J, Michiels J. Quorum sensing and swarming migration in bacteria. FEMS Microbiol Rev. 2004;28(3):261-89.
221. De Kievit TR, Gillis R, Marx S, Brown C, Iglewski BH. Quorum-sensing genes in Pseudomonas aeruginosa biofilms: their role and expression patterns. Appl Environ Microbiol. 2001;67(4):1865-73.
222. Fuqua WC, Winans SC, Greenberg EP. Quorum sensing in bacteria: the LuxR-LuxI family of cell density-responsive transcriptional regulators. J Bacteriol. 1994;176(2):269-75.
223. Kim CS, Gatsios A, Cuesta S, Lam YC, Wei Z, Chen H, et al. Characterization of Autoinducer-3 Structure and Biosynthesis in E. coli. ACS Cent Sci. 2020;6(2):197-206.
224. Miller MB, Bassler BL. Quorum Sensing in Bacteria. Annual Review of Microbiology. 2001;55(Volume 55, 2001):165-99.
225. Serra DO, Hengge R. Stress responses go three dimensional - the spatial order of physiological differentiation in bacterial macrocolony biofilms. Environ Microbiol. 2014;16(6):1455-71.
226. Hengge-Aronis R. Survival of hunger and stress: the role of rpoS in early stationary phase gene regulation in E. coli. Cell. 1993;72(2):165-8.
227. Allison DG, Ruiz B, SanJose C, Jaspe A, Gilbert P. Extracellular products as mediators of the formation and detachment of Pseudomonas fluorescens biofilms. FEMS Microbiol Lett. 1998;167(2):179-84.
228. Sara MS, Francesc M, Elisabet G, Jordi V. Biofilm Formation in Uropathogenic Escherichia coli Strains: Relationship with Urovirulence Factors and Antimicrobial Resistance. In: Ahmad N, editor. Clinical Management of Complicated Urinary Tract Infection. Rijeka: IntechOpen; 2011. p. Ch. 10.
229. Lee SF, Li YH, Bowden GH. Detachment of Streptococcus mutans biofilm cells by an endogenous enzymatic activity. Infect Immun. 1996;64(3):1035-8.
230. Puskas A, Greenberg EP, Kaplan S, Schaefer AL. A quorum-sensing system in the free-living photosynthetic bacterium Rhodobacter sphaeroides. J Bacteriol. 1997;179(23):7530-7.
231. Rumbaugh KP, Sauer K. Biofilm dispersion. Nature Reviews Microbiology. 2020;18(10):571-86.
232. Høiby N, Bjarnsholt T, Givskov M, Molin S, Ciofu O. Antibiotic resistance of bacterial biofilms. Int J Antimicrob Agents. 2010;35(4):322-32.
233. González JF, Hahn MM, Gunn JS. Chronic biofilm-based infections: skewing of the immune response. Pathog Dis. 2018;76(3).
234. Adnan M, Morton G, Singh J, Hadi S. Contribution of rpoS and bolA genes in biofilm formation in Escherichia coli K-12 MG1655. Mol Cell Biochem. 2010;342(1-2):207-13.
235. Rossi E, Cimdins A, Lüthje P, Brauner A, Sjöling Å, Landini P, et al. "It's a gut feeling" - Escherichia coli biofilm formation in the gastrointestinal tract environment. Crit Rev Microbiol. 2018;44(1):1-30.
236. Öztürk FY, Darcan C, Kariptaş E. The Determination, Monitoring, Molecular Mechanisms and Formation of Biofilm in E. coli. Braz J Microbiol. 2023;54(1):259-77.
237. Whiteley CG, Lee D-J. Bacterial diguanylate cyclases: Structure, function and mechanism in exopolysaccharide biofilm development. Biotechnology Advances. 2015;33(1):124-41.

238. Römling U, Galperin MY, Gomelsky M. Cyclic di-GMP: the first 25 years of a universal bacterial second messenger. Microbiol Mol Biol Rev. 2013;77(1):1-52.
239. Pescaretti MdlM, López FE, Morero RD, Delgado MA. Transcriptional autoregulation of the RcsCDB phosphorelay system in Salmonella enterica serovar Typhimurium. Microbiology. 2010;156(12):3513-21.
240. Majdalani N, Gottesman S. The Rcs phosphorelay: a complex signal transduction system. Annu Rev Microbiol. 2005;59:379-405.
241. Navasa N, Rodríguez-Aparicio L, Martínez-Blanco H, Arcos M, Ferrero MA. Temperature has reciprocal effects on colanic acid and polysialic acid biosynthesis in E. coli K92. Appl Microbiol Biotechnol. 2009;82(4):721-9.
242. Gualdi L, Tagliabue L, Bertagnoli S, Ieranò T, De Castro C, Landini P. Cellulose modulates biofilm formation by counteracting curli-mediated colonization of solid surfaces in Escherichia coli. Microbiology (Reading). 2008;154(Pt 7):2017-24.
243. Acheson JF, Ho R, Goularte NF, Cegelski L, Zimmer J. Molecular organization of the E. coli cellulose synthase macrocomplex. Nat Struct Mol Biol. 2021;28(3):310-8.
244. Ageorges V, Monteiro R, Leroy S, Burgess C, Pizza M, Chaucheyras-Durand F, et al. Molecular Determinants of Surface Colonisation in Diarrhoeagenic Escherichia coli (DEC): from Bacterial Adhesion to Biofilm Formation. FEMS Microbiology Reviews. 2020;175:105996.
245. Itoh Y, Rice JD, Goller C, Pannuri A, Taylor J, Meisner J, et al. Roles of pgaABCD genes in synthesis, modification, and export of the Escherichia coli biofilm adhesin poly-beta-1,6-N-acetyl-D-glucosamine. J Bacteriol. 2008;190(10):3670-80.
246. Hou B, Meng XR, Zhang LY, Tan C, Jin H, Zhou R, et al. TolC promotes ExPEC biofilm formation and curli production in response to medium osmolarity. Biomed Res Int. 2014;2014:574274.
247. Soto SM. Role of efflux pumps in the antibiotic resistance of bacteria embedded in a biofilm. Virulence. 2013;4(3):223-9.
248. Pereira CS, Thompson JA, Xavier KB. AI-2-mediated signalling in bacteria. FEMS Microbiol Rev. 2013;37(2):156-81.
249. Han A, Lee SY. An overview of various methods for in vitro biofilm formation: a review. Food Sci Biotechnol. 2023;32(12):1617-29.
250. Fletcher M. The effects of culture concentration and age, time, and temperature on bacterial attachment to polystyrene. Canadian Journal of Microbiology. 1977;23(1):1-6.
251. Christensen GD, Simpson WA, Bisno AL, Beachey EH. Adherence of slime-producing strains of Staphylococcus epidermidis to smooth surfaces. Infect Immun. 1982;37(1):318-26.
252. Reichhardt C, Ferreira JA, Joubert LM, Clemons KV, Stevens DA, Cegelski L. Analysis of the Aspergillus fumigatus Biofilm Extracellular Matrix by Solid-State Nuclear Magnetic Resonance Spectroscopy. Eukaryot Cell. 2015;14(11):1064-72.
253. Ceri H, Olson ME, Stremick C, Read RR, Morck D, Buret A. The Calgary Biofilm Device: new technology for rapid determination of antibiotic susceptibilities of bacterial biofilms. J Clin Microbiol. 1999;37(6):1771-6.
254. Crémet L, Corvec S, Batard E, Auger M, Lopez I, Pagniez F, et al. Comparison of three methods to study biofilm formation by clinical strains of Escherichia coli. Diagn Microbiol Infect Dis. 2013;75(3):252-5.
255. Mirzahosseini HK, Najmeddin F, Najafi A, Ahmadi A, Sharifnia H, Khaledi A, et al. Correlation of biofilm formation, virulence factors, and phylogenetic groups among

Escherichia coli strains causing urinary tract infection: A global systematic review and meta-analysis. J Res Med Sci. 2023;28:66.
256. Alshaikh SA, El-Banna T, Sonbol F, Farghali MH. Correlation between antimicrobial resistance, biofilm formation, and virulence determinants in uropathogenic Escherichia coli from Egyptian hospital. Ann Clin Microbiol Antimicrob. 2024;23(1):20.
257. Talieh M, Pournajaf A, Bijani A, Mohammadi M, Rajabnia M, Halaji M. Phylogenetic analysis, biofilm formation, antimicrobial resistance and relationship between these characteristics in Uropathogenic Escherichia coli. Mol Biol Rep. 2024;51(1):327.
258. Novais Â, Vuotto C, Pires J, Montenegro C, Donelli G, Coque TM, et al. Diversity and biofilm-production ability among isolates of Escherichia coli phylogroup D belonging to ST69, ST393 and ST405 clonal groups. BMC Microbiol. 2013;13:144.
259. Mostafavi SKS, Najar-Peerayeh S, Mobarez AM, Parizi MK. Characterization of uropathogenic E. coli O25b-B2-ST131, O15:K52:H1, and CGA: Neutrophils apoptosis, serum bactericidal assay, biofilm formation, and virulence typing. J Cell Physiol. 2019;234(10):18272-82.
260. Ebrahimi MT, Hedayati MA, Pirlar RF, Mortazavi N, Nazari M, Ahmadi A, et al. Investigation of the biofilm formation in extra-intestinal pathogenic Escherichia coli ST131 strains and its correlation with the presence of fimH, afa, and kpsMSTII genes. Journal of Applied Genetics. 2023;64(2):367-73.
261. Hassuna NA, Rabea EM, Mahdi WKM, Abdelraheem WM. Biofilm formation and antimicrobial resistance pattern of uropathogenic E. coli ST131 isolated from children with malignant tumors. J Antibiot (Tokyo). 2024;77(5):324-30.
262. Aydın E, Kocaaga M, Temel A. Association of antibiotic resistance and biofilm formation in Escherichia coli ST131/O25b. Acta Microbiologica et Immunologica Hungarica. 2024;71(3):197-205.
263. Magistro G, Hoffmann C, Schubert S. The salmochelin receptor IroN itself, but not salmochelin-mediated iron uptake promotes biofilm formation in extraintestinal pathogenic Escherichia coli (ExPEC). International Journal of Medical Microbiology. 2015;305(4):435-45.
264. Li B, Huang Q, Cui A, Liu X, Hou B, Zhang L, et al. Overexpression of Outer Membrane Protein X (OmpX) Compensates for the Effect of TolC Inactivation on Biofilm Formation and Curli Production in Extraintestinal Pathogenic Escherichia coli (ExPEC). Front Cell Infect Microbiol. 2018;8:208.
265. Naves P, del Prado G, Huelves L, Gracia M, Ruiz V, Blanco J, et al. Measurement of biofilm formation by clinical isolates of Escherichia coli is method-dependent. J Appl Microbiol. 2008;105(2):585-90.
266. Xu Z, Liang Y, Lin S, Chen D, Li B, Li L, et al. Crystal Violet and XTT Assays on Staphylococcus aureus Biofilm Quantification. Current Microbiology. 2016;73(4):474-82.
267. Tremblay YDN, Vogeleer P, Jacques M, Harel J. High-Throughput Microfluidic Method To Study Biofilm Formation and Host-Pathogen Interactions in Pathogenic Escherichia coli. Applied and Environmental Microbiology. 2015;81(8):2827-40.
268. Wu C, Labrie J, Tremblay YD, Haine D, Mourez M, Jacques M. Zinc as an agent for the prevention of biofilm formation by pathogenic bacteria. J Appl Microbiol. 2013;115(1):30-40.
269. Rowe MC, Withers HL, Swift S. Uropathogenic Escherichia coli forms biofilm aggregates under iron restriction that disperse upon the supply of iron. FEMS Microbiol Lett. 2010;307(1):102-9.

270. Alves JR, Pereira AC, Souza MC, Costa SB, Pinto AS, Mattos-Guaraldi AL, et al. Iron-limited condition modulates biofilm formation and interaction with human epithelial cells of enteroaggregative Escherichia coli (EAEC). J Appl Microbiol. 2010;108(1):246-55.
271. Kermit Zhang DS, Rakesh Biswas, Mariana Gomez de la Espriella, Jayasimha Rao, Anthony Baffoe-Bonnie. 2603. Biofilm Formation as a Predictive Marker of Prognosis for Escherichia coli Sepsis. Open Forum Infect Dis. 2019;6(Suppl 2):S904-5. doi: 10.1093/ofid/ofz360.2281. eCollection 019 Oct.
272. Lewis ML. Identifying Host and Bacterial Biomarkers to Predict Sepsis: Swansea University; 2023.
273. Bachmann BJ. Pedigrees of some mutant strains of Escherichia coli K-12. Bacteriol Rev. 1972;36(4):525-57.
274. Collection ATC. Escherichia coli (Migula) Castellani and Chalmers 1969 [Escherichia coli strain K12 is a whole-genome sequenced bacterium that was isolated in 1969 from Basel, Switzerland.]. Available from: https://www.atcc.org/products/29425.
275. Shea AE, Marzoa J, Himpsl SD, Smith SN, Zhao L, Tran L, et al. Escherichia coli CFT073 Fitness Factors during Urinary Tract Infection: Identification Using an Ordered Transposon Library. Appl Environ Microbiol. 2020;86(13).
276. Mobley HL, Green DM, Trifillis AL, Johnson DE, Chippendale GR, Lockatell CV, et al. Pyelonephritogenic Escherichia coli and killing of cultured human renal proximal tubular epithelial cells: role of hemolysin in some strains. Infect Immun. 1990;58(5):1281-9.
277. Mack D, Siemssen N, Laufs R. Parallel induction by glucose of adherence and a polysaccharide antigen specific for plastic-adherent Staphylococcus epidermidis: evidence for functional relation to intercellular adhesion. Infect Immun. 1992;60(5):2048-57.
278. Harris LG, Dudley E, Rohde H, Frommelt L, Siemssen N, Wilkinson TS, et al. Limitations in the use of PSMγ, agr, RNAIII, and biofilm formation as biomarkers to define invasive Staphylococcus epidermidis from chronic biomedical device-associated infections. Int J Med Microbiol. 2017;307(7):382-7.
279. Sambrook J. Molecular cloning: a laboratory manual. Cold Spring Habor Laboratory. 1989.
280. Joffre E, Nicklasson M, Álvarez-Carretero S, Xiao X, Sun L, Nookaew I, et al. The bile salt glycocholate induces global changes in gene and protein expression and activates virulence in enterotoxigenic Escherichia coli. Scientific Reports. 2019;9(1):108.
281. Le VVH, Biggs PJ, Wheeler D, Davies IG, Rakonjac J. Novel mechanisms of TolC-independent decreased bile-salt susceptibility in Escherichia coli. FEMS Microbiology Letters. 2020;367(10).
282. Doranga S, Conway T. OmpC-Dependent Bile Tolerance Contributes to E. coli Colonization of the Mammalian Intestine. Microbiology Spectrum. 2023;11(3):e05241-22.
283. Bernstein C, Bernstein H, Payne CM, Beard SE, Schneider J. Bile salt activation of stress response promoters in Escherichia coli. Curr Microbiol. 1999;39(2):68-72.
284. Thanassi DG, Cheng LW, Nikaido H. Active efflux of bile salts by Escherichia coli. J Bacteriol. 1997;179(8):2512-8.
285. Hamner S, McInnerney K, Williamson K, Franklin MJ, Ford TE. Bile salts affect expression of Escherichia coli O157:H7 genes for virulence and iron acquisition, and promote growth under iron limiting conditions. PLoS One. 2013;8(9):e74647.
286. Nickerson KP, Faherty CS. Bile Salt-induced Biofilm Formation in Enteric Pathogens: Techniques for Identification and Quantification: 1940-087X; 2018. e57322 p.

287. Baev MV, Baev D, Radek AJ, Campbell JW. Growth of Escherichia coli MG1655 on LB medium: monitoring utilization of sugars, alcohols, and organic acids with transcriptional microarrays. Applied Microbiology and Biotechnology. 2006;71(3):310-6.
288. Gullian-Klanian M, Sánchez-Solis MJ. Growth kinetics of Escherichia coli O157:H7 on the epicarp of fresh vegetables and fruits. Brazilian Journal of Microbiology. 2018;49(1):104-11.
289. Sezonov G, Joseleau-Petit D, D'Ari R. Escherichia coli Physiology in Luria-Bertani Broth. Journal of Bacteriology. 2007;189(23):8746-9.
290. Powell LC, Pritchard MF, Ferguson EL, Powell KA, Patel SU, Rye PD, et al. Targeted disruption of the extracellular polymeric network of Pseudomonas aeruginosa biofilms by alginate oligosaccharides. NPJ Biofilms Microbiomes [Internet]. 2018 2018; 4:[13 p.].
291. Moreira JMR, Gomes LC, Araújo JDP, Miranda JM, Simões M, Melo LF, et al. The effect of glucose concentration and shaking conditions on Escherichia coli biofilm formation in microtiter plates. Chemical Engineering Science. 2013;94:192-9.
292. Davenport DS, Massanari RM, Pfaller MA, Bale MJ, Streed SA, Hierholzer WJ, Jr. Usefulness of a test for slime production as a marker for clinically significant infections with coagulase-negative staphylococci. J Infect Dis. 1986;153(2):332-9.
293. Deighton MA, Balkau B. Adherence measured by microtiter assay as a virulence marker for Staphylococcus epidermidis infections. J Clin Microbiol. 1990;28(11):2442-7.
294. Charbonneau ME, Berthiaume F, Mourez M. Proteolytic processing is not essential for multiple functions of the Escherichia coli autotransporter adhesin involved in diffuse adherence (AIDA-I). J Bacteriol. 2006;188(24):8504-12.
295. Mack D, Haeder M, Siemssen N, Laufs R. Association of Biofilm Production of Coagulase-Negative Staphylococci with Expression of a Specific Polysaccharide Intercellular Adhesin. The Journal of Infectious Diseases. 1996;174(4):881-3.
296. Hajna AA, Perry CA. Comparative Study of Presumptive and Confirmative Media for Bacteria of the Coliform Group and for Fecal Streptococci. Am J Public Health Nations Health. 1943;33(5):550-6.
297. Begley M, Gahan CG, Hill C. The interaction between bacteria and bile. FEMS Microbiol Rev. 2005;29(4):625-51.
298. Tuttle AR, Trahan ND, Son MS. Growth and Maintenance of Escherichia coli Laboratory Strains. Curr Protoc. 2021;1(1):e20.
299. Machado MAM, Chapartegui-González I, Castro VS, Figueiredo EEdS, Conte-Junior CA, Torres AG. Biofilm-producing Escherichia coli O104:H4 overcomes bile salts toxicity by expressing virulence and resistance proteins. Letters in Applied Microbiology. 2024;77(4).
300. Nickerson KP, Chanin RB, Sistrunk JR, Rasko DA, Fink PJ, Barry EM, et al. Analysis of Shigella flexneri Resistance, Biofilm Formation, and Transcriptional Profile in Response to Bile Salts. Infect Immun. 2017;85(6).
301. Wang X, Wang Y, Ling N, Shen Y, Zhang D, Liu D, et al. Effects of tolC on tolerance to bile salts and biofilm formation in Cronobacter malonaticus. Journal of Dairy Science. 2021;104(9):9521-31.
302. Vuong C, Kidder JB, Jacobson ER, Otto M, Proctor RA, Somerville GA. Staphylococcus epidermidis polysaccharide intercellular adhesin production significantly increases during tricarboxylic acid cycle stress. J Bacteriol. 2005;187(9):2967-73.
303. Dobinsky S, Kiel K, Rohde H, Bartscht K, Knobloch JK, Horstkotte MA, et al. Glucose-related dissociation between icaADBC transcription and biofilm expression by

Staphylococcus epidermidis: evidence for an additional factor required for polysaccharide intercellular adhesin synthesis. J Bacteriol. 2003;185(9):2879-86.
304. Lim Y, Jana M, Luong TT, Lee CY. Control of glucose- and NaCl-induced biofilm formation by rbf in Staphylococcus aureus. J Bacteriol. 2004;186(3):722-9.
305. Knobloch JK, Bartscht K, Sabottke A, Rohde H, Feucht HH, Mack D. Biofilm formation by Staphylococcus epidermidis depends on functional RsbU, an activator of the sigB operon: differential activation mechanisms due to ethanol and salt stress. J Bacteriol. 2001;183(8):2624-33.
306. Knobloch JK, Horstkotte MA, Rohde H, Kaulfers PM, Mack D. Alcoholic ingredients in skin disinfectants increase biofilm expression of Staphylococcus epidermidis. J Antimicrob Chemother. 2002;49(4):683-7.
307. Weiser J, Henke HA, Hector N, Both A, Christner M, Büttner H, et al. Sub-inhibitory tigecycline concentrations induce extracellular matrix binding protein Embp dependent Staphylococcus epidermidis biofilm formation and immune evasion. Int J Med Microbiol. 2016;306(6):471-8.
308. Teodósio JS, Simões M, Melo LF, Mergulhão FJ. Flow cell hydrodynamics and their effects on E. coli biofilm formation under different nutrient conditions and turbulent flow. Biofouling. 2011;27(1):1-11.
309. Skyberg JA, Siek KE, Doetkott C, Nolan LK. Biofilm formation by avian Escherichia coli in relation to media, source and phylogeny. J Appl Microbiol. 2007;102(2):548-54.
310. Danese PN, Pratt LA, Kolter R. Exopolysaccharide production is required for development of Escherichia coli K-12 biofilm architecture. J Bacteriol. 2000;182(12):3593-6.
311. Eboigbodin KE, Biggs CA. Characterization of the extracellular polymeric substances produced by Escherichia coli using infrared spectroscopic, proteomic, and aggregation studies. Biomacromolecules. 2008;9(2):686-95.
312. Gupta A, Guptasarma P. E. coli cells advance into phase-separated (biofilm-simulating) extracellular polymeric substance containing DNA, HU, and lipopolysaccharide. J Bacteriol. 2024;206(11):e0030924.
313. Castro J, Lima Â, Sousa LGV, Rosca AS, Muzny CA, Cerca N. Crystal Violet Staining Alone Is Not Adequate to Assess Synergism or Antagonism in Multi-Species Biofilms of Bacteria Associated With Bacterial Vaginosis. Front Cell Infect Microbiol. 2021;11:795797.
314. Latka A, Drulis-Kawa Z. Advantages and limitations of microtiter biofilm assays in the model of antibiofilm activity of Klebsiella phage KP34 and its depolymerase. Scientific Reports. 2020;10(1):20338.
315. Peeters E, Nelis HJ, Coenye T. Comparison of multiple methods for quantification of microbial biofilms grown in microtiter plates. Journal of Microbiological Methods. 2008;72(2):157-65.
316. Gomes LC, Silva LN, Simões M, Melo LF, Mergulhão FJ. Escherichia coli adhesion, biofilm development and antibiotic susceptibility on biomedical materials. Journal of Biomedical Materials Research Part A. 2015;103(4):1414-23.
317. Elliott AD. Confocal Microscopy: Principles and Modern Practices. Curr Protoc Cytom. 2020;92(1):e68.
318. Pan M, Zhu L, Chen L, Qiu Y, Wang J. Detection Techniques for Extracellular Polymeric Substances in Biofilms: A Review. BioResources. 2016;11.
319. Ganz T, Nemeth E. Hepcidin and Disorders of Iron Metabolism. Annual Review of Medicine. 2011;62(Volume 62, 2011):347-60.

320. Kristoffersen SM, Ravnum S, Tourasse NJ, Økstad OA, Kolstø AB, Davies W. Low concentrations of bile salts induce stress responses and reduce motility in Bacillus cereus ATCC 14579 [corrected]. J Bacteriol. 2007;189(14):5302-13.
321. Milton AAP, Srinivas K, Lyngdoh V, Momin AG, Lapang N, Priya GB, et al. Biofilm-forming antimicrobial-resistant pathogenic Escherichia coli: A one health challenge in Northeast India. Heliyon. 2023;9(9):e20059.
322. Deutschman Clifford S, Tracey Kevin J. Sepsis: Current Dogma and New Perspectives. Immunity. 2014;40(4):463-75.
323. Tang BM, Huang SJ, McLean AS. Genome-wide transcription profiling of human sepsis: a systematic review. Critical Care. 2010;14(6):R237.
324. Jarczak D, Kluge S, Nierhaus A. Sepsis—Pathophysiology and Therapeutic Concepts. Frontiers in Medicine. 2021;8.
325. Chick HM, Rees ME, Lewis ML, Williams LK, Bodger O, Harris LG, et al. Using the Traditional Ex Vivo Whole Blood Model to Discriminate Bacteria by Their Inducible Host Responses. Biomedicines. 2024;12(4).
326. Hancock V, Ferrières L, Klemm P. The ferric yersiniabactin uptake receptor FyuA is required for efficient biofilm formation by urinary tract infectious Escherichia coli in human urine. Microbiology (Reading). 2008;154(Pt 1):167-75.
327. Hancock V, Klemm P. Global gene expression profiling of asymptomatic bacteriuria Escherichia coli during biofilm growth in human urine. Infect Immun. 2007;75(2):966-76.
328. Cerqueira L, Oliveira JA, Nicolau A, Azevedo NF, Vieira MJ. Biofilm formation with mixed cultures of Pseudomonas aeruginosa/Escherichia coli on silicone using artificial urine to mimic urinary catheters. Biofouling. 2013;29(7):829-40.
329. Wurpel DJ, Totsika M, Allsopp LP, Webb RI, Moriel DG, Schembri MA. Comparative proteomics of uropathogenic Escherichia coli during growth in human urine identify UCA-like (UCL) fimbriae as an adherence factor involved in biofilm formation and binding to uroepithelial cells. J Proteomics. 2016;131:177-89.
330. Vogeleer P, Tremblay YDN, Jubelin G, Jacques M, Harel J. Biofilm-Forming Abilities of Shiga Toxin-Producing Escherichia coli Isolates Associated with Human Infections. Appl Environ Microbiol. 2015;82(5):1448-58.
331. Antypas H, Choong FX, Libberton B, Brauner A, Richter-Dahlfors A. Rapid diagnostic assay for detection of cellulose in urine as biomarker for biofilm-related urinary tract infections. NPJ Biofilms Microbiomes. 2018;4:26.

7 Appendices

Biofilm formation at two incubation temperatures (30°C vs. 37°C) in LB, circular shaking. (Graph a, n=15)	
30°C	37°C
0.0280	0.0221
0.0113	0.0522
0.0055	0.0440
0.0047	0.0367
0.0272	0.0500
0.0235	0.0493
0.0085	0.0477
0.0030	0.0128
0.0045	0.0344
0.0390	0.0507
0.0050	0.0163
0.0000	0.0188
0.0000	0.0218
0.0000	0.0258
0.0000	0.0162

Biofilm formation at two incubation temperatures (30°C vs. 37°C) in TSB-G, circular shaking. (Graph b, n=5)	
30°C	37°C
0.0135	0.0537
0.0278	0.0850
0.0128	0.0563
0.0127	0.0380
0.0130	0.0497

Comparison of different shaking methods during incubation in LB at 37°C. (Graph c, n=6)		
No shaking	Circular shaking	Orbital shaking
0.0000	0.0221	0.0063
0.0037	0.0522	0.0120
0.0000	0.0440	0.0132
0.0000	0.0367	0.0130
0.0000	0.0500	0.0200
0.0047	0.0522	0.0165

Comparison of different shaking methods during incubation in TSB-G at 37°C. (Graph d, n=6)		
No shaking	Circular shaking	Orbital shaking
0.0050	0.0537	0.0310
0.0060	0.0850	0.0417
0.0013	0.0563	0.0405
0.0013	0.0380	0.0400
0.0097	0.0497	0.0500
0.0040	0.0753	0.0250

Comparison of different pre-culture times in TSB+G, Orbital shaking at 37°C. Graph e, n=5)	
20 min	3600 min
0.0030	0.0230
0.0127	0.0312
0.0033	0.0217
0.0060	0.0312
0.0110	0.0207

Influence of serum presence (+) or absence (–) on biofilm formation in EC, Circular shaking at 30°C. (Graph f, n=20)	
+	-
0.0000	0.0105
0.0185	0.0175
0.0000	0.1020
0.1005	0.0440
0.0145	0.0030
0.0130	0.1115
0.0580	0.0715
0.0000	0.0300
0.0655	0.0125
0.0470	0.2545
0.0000	0.0105
0.1310	0.0760
0.0000	0.3035
0.0055	0.0270
0.0935	0.0785
0.0040	0.0080
0.0000	0.0010
0.0000	0.0055
0.0000	0.0360
0.0000	0.0155

Appendix 1.1 – Figure 3.2 data values of each comparison in the graphs.
The data values have been normalised by subtracting the blank value from the value of each replicate.

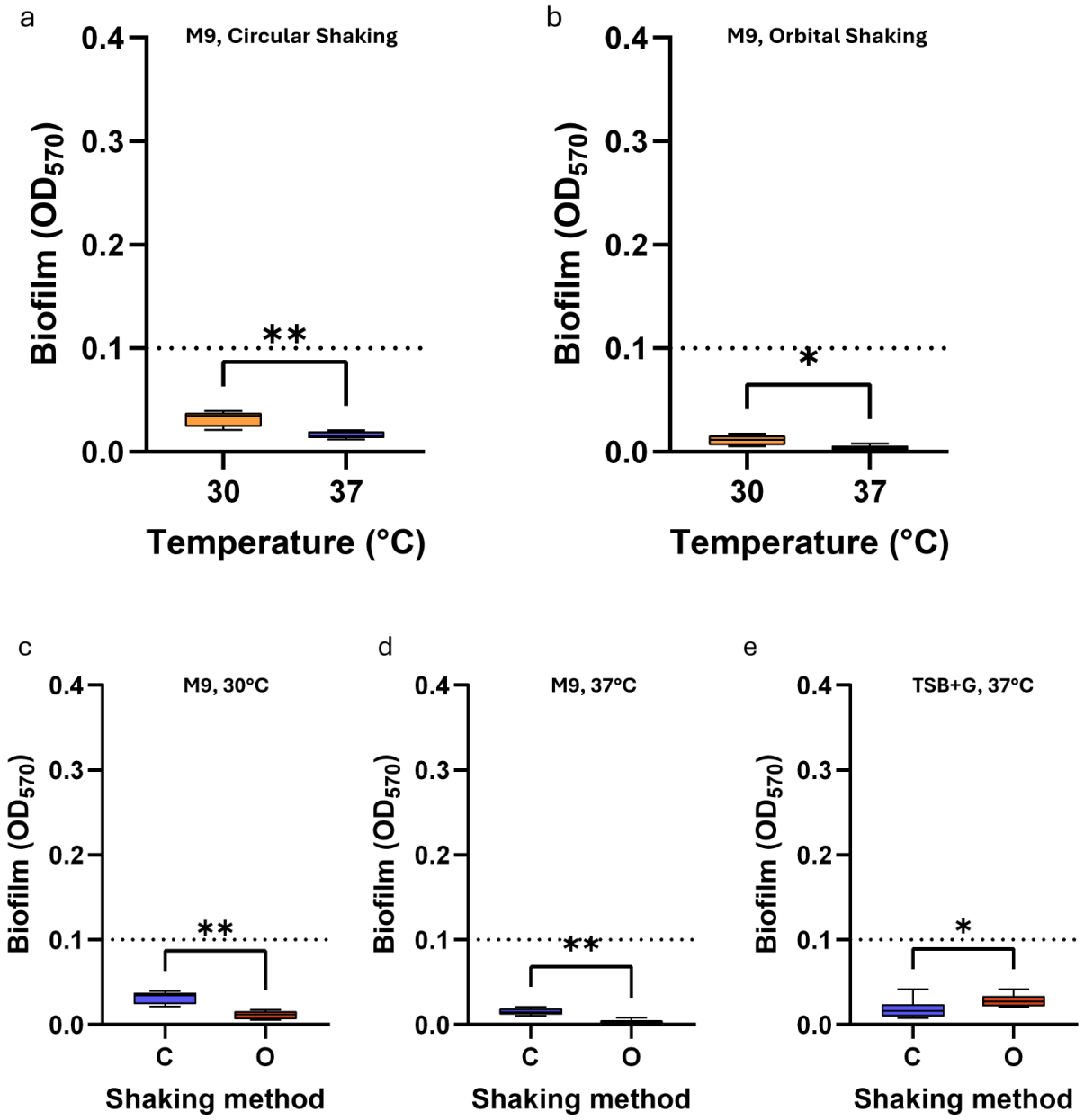

Appendix 1.2 – Biofilm deposition of *E. coli* isolates under different physiological and mechanical conditions; additional graphs.

Biofilms were grown on 96 well plates for up to 24 hours. Then, *E. coli* biofilms were washed with PBS, dried overnight, and stained with 0.01% crystal violet. Following staining, the samples were rinsed, and optical density was measured at OD_{570}. The results are presented as box-and-whisker plots, where the boxes represent the median and interquartile ranges, and the whiskers indicate the minimum and maximum values. The dotted line represents the threshold of 0.1 showing a significant biofilm formation. **Graphs a, b**: Biofilm formation at two incubation temperatures (30°C vs. 37°C). **Graphs c ,d, e:** Comparison of different shaking methods during incubation (C = Circular, O = Orbital). Statistical analyses were performed using Mann-Whitney non-parametric test. Statistical significance is indicated as follows: * $p < 0.05$, ** $p < 0.01$. The positive control (*S. epidermidis* 1457) consistently showed biofilm and growth values within the range of 0.8–1.2.

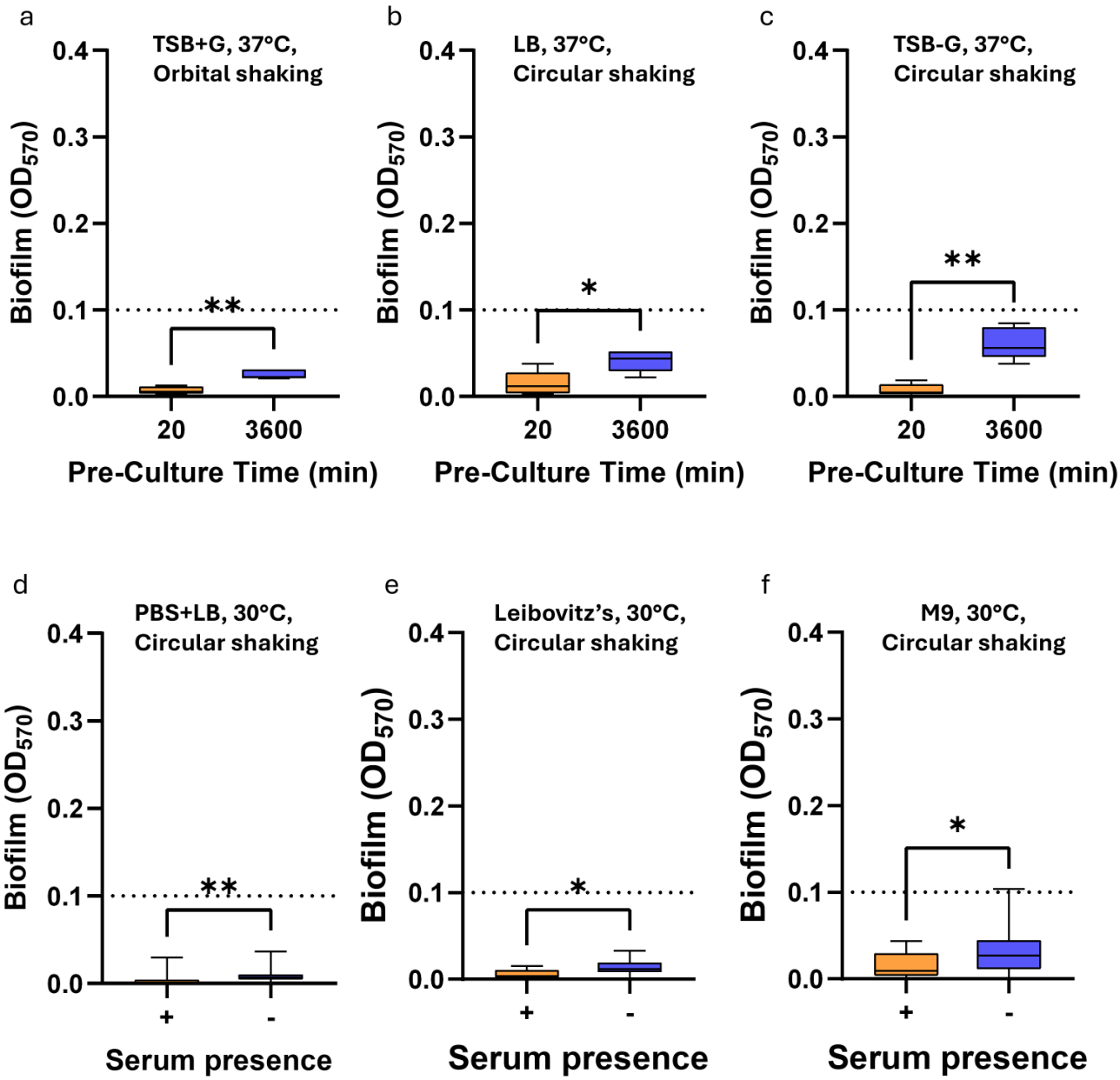

Appendix 1.3 – Biofilm deposition of *E. coli* isolates under different physiological and mechanical conditions; additional graphs 2.

Biofilms were grown on 96 well plates for up to 24 hours. Then, *E. coli* biofilms were washed with PBS, dried overnight, and stained with 0.01% crystal violet. Following staining, the samples were rinsed, and optical density was measured at OD_{570}. The results are presented as box-and-whisker plots, where the boxes represent the median and interquartile ranges, and the whiskers indicate the minimum and maximum values. The dotted line represents the threshold of 0.1 showing a significant biofilm formation. **Graphs a, b, c:** comparison of different pre-culture times (20 minutes vs. 3600 minutes). **Graphs d, e, f**: Influence of serum presence (+) or absence (–) on biofilm formation. Statistical analyses were performed using Mann-Whitney non-parametric tests. Statistical significance is indicated as follows: * $p < 0.05$, ** $p < 0.01$. The positive control (*S. epidermidis* 1457) consistently showed biofilm and growth values within the range of 0.8–1.2.

Appendix 1.4 – Biofilm direct, indirect and bile resistance gene presence/absence heatmap of biofilm positive versus biofilm negative isolates.

A pre-existing presence-absence table of genomic data was used (272). Selected genes, as described previously (Table 3.3), were analysed for presence/absence and heatmap were generated using R version 4.4.2 with ggplot2 package.

Appendix 1.5 – Biofilm direct, indirect and bile resistance gene presence/absence heatmap of ST73 versus ST131 isolates.
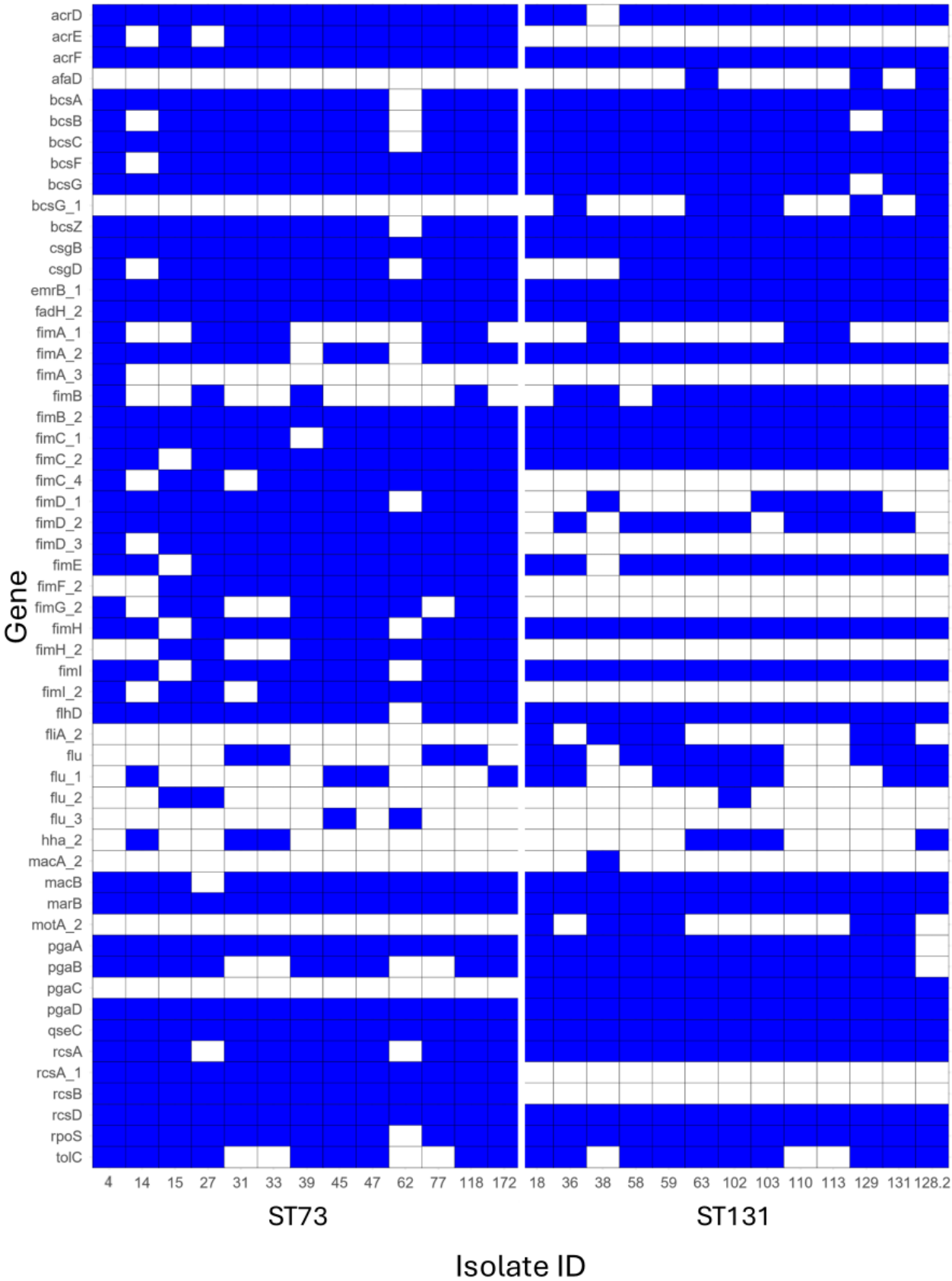
A pre-existing presence-absence table of genomic data was used (272). Selected genes, as described previously (Table 3.3), were analysed for presence/absence and heatmap were generated using R version 4.4.2 with ggplot2 package.